Planetary and Space Science ∎ (∎∎∎∎) ∎∎∎–∎∎∎

Contents lists available at ScienceDirect

Planetary and Space Science

journal homepage: www.elsevier.com/locate/pss

Photoionization and photodissociation rates in solar and blackbody radiation fields

W.F. Huebner *, J. Mukherjee

Southwest Research Institute, P. O. Drawer 28510, San Antonio, TX 78228-0510, USA

ARTICLE INFO

Article history:
Received 22 August 2014
Received in revised form
12 November 2014
Accepted 19 November 2014

Keywords:
Atoms
Ions
Molecules
Molecular ions
Photodissociation
Photoionization
Dissociative photoionization
Excess energy
Solar radiation
Blackbody radiation

ABSTRACT

Rate coefficients for ionization and dissociation have been calculated for over 140 atomic, molecular, and ionic species in the radiation fields of (1) the quiet and the active Sun at 1 AU heliocentric distance and (2) blackbodies at four selected temperatures in the range from $T=1000$ K to 1,000,000 K without factors for radiation dilution with distance from the source. The rate coefficients in units of transitions per second (s^{-1}) and associated excess energies of the photo products in eV are tabulated for about 265 ionization, dissociation, and dissociative ionization branches. Users can interactively access this information and plot and download cross sections and wavelength-binned results for various solar activities and blackbody temperatures on our website http://phidrates.space.swri.edu.

1. Introduction

Our database for photoionization of atoms, ions, and molecules and for photodissociation and dissociative photoionization of molecules of relevance to investigations of the planetary system has historic origins. It was originally developed for modeling comet comae and for interpreting observational data of comets (Huebner and Carpenter, 1979; Huebner et al., 1992). The new database has entries for over 140 mother species resulting in about 265 branches of products and has been expanded to include temperature-dependent blackbody radiation fields. Replacing old cross section data and thresholds with newer experimental and theoretical data and adding new species to our database have not only improved and expanded it, but also guaranteed that all photo rate coefficients are calculated consistently and uniformly with the same solar and blackbody sources for the radiation fields. Except for diatomic and many triatomic molecules, the products of photodissociation are not always well known and can vary strongly with dissociation channel, i.e., wavelength. We have improved on this situation whenever possible.

The unattenuated rate coefficient for the wavelength interval between λ_i and $\lambda_i+\Delta\lambda_i$ is

$$k_i = \int_{\lambda_i}^{\lambda_i+\Delta\lambda_i} \sigma(\lambda)\Phi(\lambda)\, d\lambda. \quad (1)$$

The integration is approximated by a sum

$$k = \sum_i k_i, \quad (2)$$

where

$$k_i = \sigma_i \Phi_i, \quad (3)$$

σ_i is the wavelength-averaged photo cross section in bin i of width $\Delta\lambda_i$, and, for the solar radiation field (SRF), Φ_i is the wavelength-integrated spectral photon flux at 1 AU heliocentric distance in the same bin. The spectral photon flux for the solar radiation field and its ratio for the active Sun to that of the quiet Sun, as used here, is the same as presented by Huebner et al. (1992).

For the blackbody radiation field (BBRF) the spectral photon flux (as opposed to the spectral energy flux) as a function of wavelength, without geometric dilution factor, is

$$\Phi(\lambda) = \frac{2\pi c}{4\lambda^4[\exp(hc/\lambda kT)-1]}, \quad (4)$$

* Corresponding author.
E-mail address: WFHuebner@cs.com (J. Mukherjee).

http://dx.doi.org/10.1016/j.pss.2014.11.022
0032-0633/

where c is the speed of light, h is the Planck constant, k is the Boltzmann constant, and λ is the wavelength of the radiation. For blackbody radiation we use the same wavelength grid as for the solar radiation field, but have added a few bins at long wavelengths for better resolution.

Rate coefficients for blackbody radiation are of interest in some models of planetary atmospheres, but in particular in laboratory experiments. Although the temperature range covers $T=100$ K to more than 1,000,000 K, at the lower temperatures, in particular for $T<1000$ K, the unattenuated and distance undiluted rate coefficients, k, for some species are so small that they are of little interest. Thus, we do not present values for $T<1000$ K. Even at $T\approx 1000$ K some rate coefficients depend strongly on the cross sections at threshold and on the precise values of the threshold energies themselves. In these cases the rate coefficients are not very reliable; examples include Sc, Ti, V, Fe, Co, Xe, P^+, and Ca^+. In a few cases the wavelengths of the ionization thresholds are so short, e.g., $\lambda=163.91$ Å for Li^+, 227.84 Å for He^+, and 262.20 Å for Na^+ that the photo rate coefficients for blackbody radiation are essentially zero even at $T=2000$ K. Indeed, some lifetimes, $1/k$, are longer than the age of the solar system, which is about 10^{17} s. If a rate coefficient is less than $1\times 10^{-99}\,s^{-1}$ the entry in the tables has been left blank.

Because of some steep gradients with respect to wavelength, we used more significant digits in all calculations. This brought about some small differences when comparing with our older results for solar radiation. These differences are mostly in the range of rounding errors and we will not dwell on them further. For the blackbody spectral photon flux see Fig. 1.

Fig. 2 compares the solar spectral photon flux (number of photons per square centimeter per second per angstrom) at 1 AU heliocentric distance for the quiet Sun with that of the active Sun. The binned values of the spectral flux for the quiet Sun and the binned spectral flux ratios for the active Sun to that of the quiet Sun have already been presented by Huebner et al. (1992). Also shown is the blackbody spectral photon flux at $T=5770$ K, which simulates the solar spectral flux above $\lambda=4000$ Å when diluted by the square of the ratio of the radius of the Sun ($R=6.955\times 10^5$ km) to that of the Earth's mean orbital radius ($r=1$ AU $=1.496\times 10^8$ km): $(R/r)^2=2.16\times 10^{-5}$. However, the blackbody flux deviates markedly from that of the Sun below $\lambda=4000$ Å and becomes negligibly small, which is not surprising because that is the region where most of the strong atomic and molecular emission lines are in hot plasmas such as in the Sun or other stars. This is an important fact to keep in mind when simulating stellar or interstellar radiation fields by blackbody radiation.

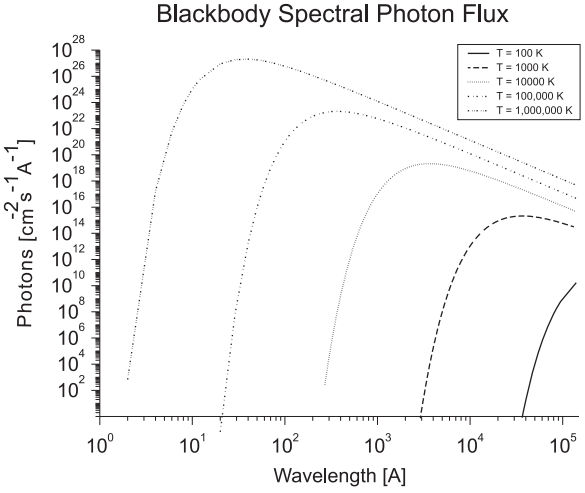

Fig. 1. Comparison of blackbody spectral fluxes (without radiation dilution factor) vs. wavelength of radiation and as a function of blackbody temperatures from $T=10^2$ K (far right) to $T=10^6$ K (far left). Note that for low temperatures the blackbody flux is very small in the wavelength range below dissociation or ionization thresholds of most atoms and molecules.

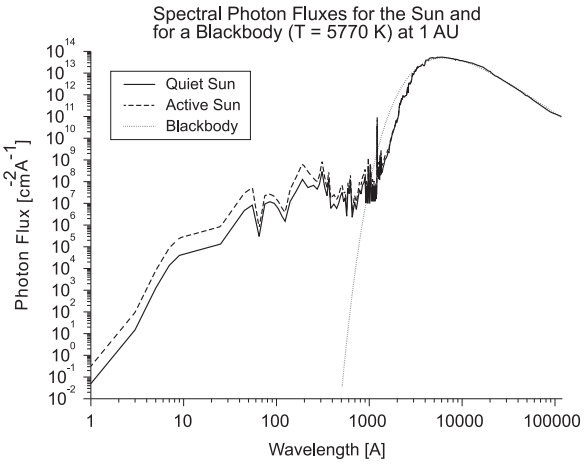

Fig. 2. A comparison of the spectral photon fluxes from the quiet Sun (full curve), active Sun (dashed curve), and a blackbody source at $T=5770$ K (dotted curve) using the same radiation dilution factor as for the Sun at 1 AU. Note the significant contribution to the spectral photon flux of the Sun below $\lambda\approx 1000$ Å.

Rate coefficients for ionization, dissociation, and dissociative ionization and the corresponding excess energies of the photo products can be calculated interactively on our website, http://phidrates.space.swri.edu, for various conditions ranging from the quiet to the active Sun and for various temperatures of the blackbody radiation field (BBRF). We have improved the website to make it consistent with modern web standards and to make it easier to download cross section data by including a download link after each cross section display. Rate coefficients for photoionization, photodissociation, and dissociative photoionization in units of s^{-1} and associated average excess energies in eV can be obtained for various levels of solar activity, ranging from the quiet Sun (activity=0) to the active Sun (activity=1), or blackbody temperatures in the range from about 100 K to over 10^6 K. The rate coefficients can also be viewed and downloaded in preset wavelength or photon energy bins. When temperature-dependent blackbody radiation fields are considered, the list allows the user to cross compare rate coefficients under various conditions.

The excess energy is the photon energy above the dissociation or ionization threshold (i.e., binding energy) that is converted into kinetic energy of the given photo products. The mean excess energy of photolysis products for a particular bound state j is

$$E^j=\frac{\int_0^{\lambda^j_{th}} hc\left(\frac{1}{\lambda}-\frac{1}{\lambda^j_{th}}\right)\sigma^j(\lambda)\Phi(\lambda)\,d\lambda}{\int_0^{\lambda^j_{th}}\sigma^j(\lambda)\Phi(\lambda)\,d\lambda},\quad(\lambda\le\lambda^j_{th})$$
$$\approx\sum_i hc\left[\frac{\lambda_i+\Delta\lambda_i/2}{\lambda_i(\lambda_i+\Delta\lambda_i)}-\frac{1}{\lambda^j_{th}}\right]\frac{k^j_i}{k^j},\qquad(5)$$

where $\sigma^j(\lambda)$ is the partial photodissociation or photoionization cross section for bound state j having a threshold wavelength $\lambda^j_{(th)}=hc/E^j$, where h is Planck's constant, c is the speed of light, and k^j is the rate coefficient as given in Eq. (2). The mean value of the excess energy is then

$$E=\sum_i E^j.\qquad(6)$$

The summation over i in Eq. (5) is over all wavelength bins. Thus, the most tightly bound components of a molecule or

Please cite this article as: Huebner, W.F., Mukherjee, J., Photoionization and photodissociation rates in solar and blackbody radiation fields. Planetary and Space Science (2015), http://dx.doi.org/10.1016/j.pss.2014.11.022

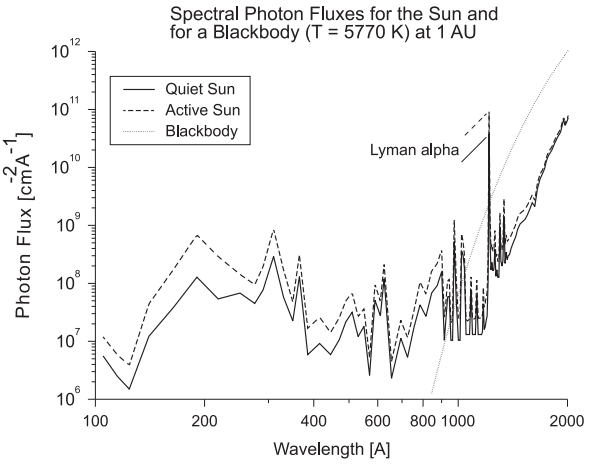

Fig. 3. Details of the spectral photon flux in the $\lambda = 200$ to 2000 Å region. Solid curve: quiet Sun; dashed curve: active Sun; dotted curve: a blackbody source the size of the Sun at $T = 5770$ K and diluted to 1 AU heliocentric distance. The Ly-α line is at 1215.7 Å.

electrons of an atom contribute mostly only to the low energy spectrum of the photolysis products. For ionization, the excess energy is almost entirely in the form of kinetic energy of the photoelectrons, yielding the photoelectron energy spectrum. This can be important for secondary (electron impact) excitation, dissociation, and ionization.

Details around the Lyman alpha line at $\lambda = 1215.7$ Å are shown in Fig. 3. Any coincidence of a predissociation or an autoionization line of a mother species with the solar Lα line could strongly influence the rate coefficient that then could drastically change with Doppler shifts caused by changes in the velocity distribution of that species. Such a coincidence occurs for N_2 with the solar Lγ line at $\lambda = 972.5$ Å as reported earlier by Huebner et al. (1992).

2. Rate coefficients and excess energies

In the following discussions and tables species are listed according to increasing complexity: Monatomic neutrals, followed by monatomic ions, diatomics, triatomics, etc., and within each group they are listed according to increasing atomic number of the heaviest element in the molecule. We will not discuss details of species published in our earlier publication (Huebner et al., 1992), but refer to them when making comparisons. We will also not present plots of binned rate coefficients and binned excess energies since they are readily available on our website.

The database also contains some branching ratios for photo excitation of atoms and molecules, but this part has in general not been developed. It would be easy to add additional excitation branches if this becomes desirable. Two very general examples of excitation are given for the case of SO_2 and C_2H_2, but the transitions are not described in detail.

In a number of cases we have used several sources of cross section data. This allows users to assess uncertainties and variances in their model calculations and data analyses.

2.1. Neutral atoms

We have supplemented our earlier list of monatomic neutral species (Huebner et al., 1992) with the atoms for all missing elements up to atomic number $Z = 30$. The new photoionization cross sections are taken from two related databases: (1) TOPbase and NORAD that contain results from close-coupling approximations using the R-matrix method and (2) analytic fits to partial photoionization cross sections including subshells made by Verner et al. (1993, 1996) and Verner and Yakovlev (1995) [we will refer to them collectively as Verner and co-workers]. TOPbase originated with the opacity project (Seaton, 1995) and NORAD [Nahar Ohio (State University) Radiative Atomic Data] is a follow-on to TOPbase, maintained by Nahar (2013). Both not only include autoionization resonances but also contain power law extensions of the calculated cross sections [mostly a hydrogenic approximation $(h\nu)^{-3}$] at the high energy end of the calculations. These power law extensions become unrealistic with increasing atomic number, Z, and are a direct contradiction to the high-quality close-coupling calculations. Also, neither TOPbase nor NORAD includes cross section data for inner shell ionizations. The analytic fits made by Verner and co-workers for the partial photoionization cross sections are based on TOPbase R-matrix methods supplemented with results from Hartree–Dirac–Slater calculations. They smoothed the autoionization resonances in the cross sections and thus are not as detailed, but they contain inner shell ionization cross sections. The fitted cross sections are computationally easy to use. Thus, for the purposes intended here, we use TOPbase and NORAD data that include the autoionization structures, but replace the unrealistic power law extensions with the appropriate fitted photoionization cross sections from Verner and co-workers. Although TOPbase claims to contain cross section data for all elements and their ions up to atomic number $Z = 30$, many elements and their ions are missing.

Autoionizing line transitions can be important for chance coincidences with solar spectrum lines. In such cases the Doppler shift of a narrow autoinizing line with respect to the solar emission line should be taken into account. However, such details are beyond present objectives and we average the cross sections of spectral structures with spacing less than about 0.01 Å.

We will not quote all the above references in each case discussed here, but only when needed for comparisons with other data. References to the TOPbase or NORAD databases will simply be referred to as TOP-base or NORAD, respectively. We have replaced in all cases the ionization threshold values (wave-lengths) by the most widely accepted values listed in the Handbook of Basic Atomic Spectroscopic Data [in the following simply referred to as NIST (http://www.nist.gov/pml/data/handbook/index.cfm) where each element can be accessed either by its name or its atomic number], but we quote the original references as given in the NIST webpage for these data. When rate coefficients and excess energies are insignificantly different from our earlier results, we do not discuss the details of the changes. In general, when two or more different sets of cross section data are compared for an atom the corresponding rate coefficients and excess energies are discussed in the appropriate subsection about that atom and are not listed separately in the tables. The user is referred to details in the appropriate references. Rate coefficients for blackbody radiation fields (BBRFs) without dilution factors for four temperatures from $T = 10^3$ K to $T = 10^6$ K and associated average excess energies are summarized in Table 1.

In the following discussions of rate coefficients and excess energies, "TOPbase; Verner and co-workers" shall mean that the combined data from TOPbase and the fitted cross section data from Verner and co-workers were used for the extension beyond the TOPbase results. "Verner and co-workers" shall mean that only the fitted cross section from Verner and co-workers were used. Any additional entries will be clear from the quoted references. "QS" and "AS" mean quiet Sun and active Sun, respectively.

2.1.1. Atomic hydrogen, H

Cross section: The new photoionization cross section data are based on fits made by Verner et al. (1993, 1996) and Verner and Yakovlev (1995) to close-coupling R-matrix calculations of Seaton (1995). These cross sections are in excellent agreement with the earlier data of Stobbe (1930), Sauter (1931a,b), and Bethe and

Please cite this article as: Huebner, W.F., Mukherjee, J., Photoionization and photodissociation rates in solar and blackbody radiation fields. Planetary and Space Science (2015), http://dx.doi.org/10.1016/j.pss.2014.11.022

Salpeter (1957). They can barely be resolved when plotted on the same graph.

Threshold: The ionization threshold $\lambda_{th} = 911.75$ Å as given by Mohr and Kotochigova (2000) compares very well with the value 911.76 Å used in our earlier calculations (Huebner et al., 1992).

Rate coefficient: We compare results in units of s^{-1} for the new cross sections with those obtained earlier by Huebner et al. (1992):

Solar activity	QS	AS
Huebner et al. (1992)	7.26×10^{-8}	1.72×10^{-7}
Verner and co-workers	7.30×10^{-8}	1.73×10^{-7}

Agreement is within 1%. Our recommendations based on our earlier calculations for the best solar rate coefficients for the quiet Sun (7.26×10^{-8}) and the active Sun (1.72×10^{-7}) remain unchanged. For blackbody radiation the rate coefficients are presented in Table 1.

Excess energy: We compare results in units of eV from the new, fitted cross sections with those obtained earlier by Huebner et al. (1992):

Solar activity	QS	AS
Huebner et al. (1992)	3.54	3.97
Verner and co-workers	3.53	3.95

Agreement is within 1%. Our recommended values (Huebner et al., 1992) for the excess energies remain the same. For blackbody radiation the excess energies are presented in Table 1.

2.1.2. Atomic helium, He

Cross section: Shown in Fig. 4 (labeled as TOPbase; Verner and co-workers) is the combined cross section from TOPbase extended with the cross section of Verner and co-workers for $\lambda < 22$ Å . Also shown is the cross section from Verner and co-workers without the TOPbase contribution. It tracks the TOPbase contribution (except for the autoionization lines) extremely well. We also show the photoionization cross section from Barfield et al. (1972) as used earlier by Huebner et al. (1992). The first two of these cross sections are almost 50% higher than the results quoted by Barfield et al. (1972) in the wavelength region for $\lambda \approx 170$ Å and about 25% lower near threshold.

Threshold: The new ionization threshold $\lambda_{th} = 504.26$ Å as given by Martin (2002) is in excellent agreement with the earlier value of $\lambda_{th} = 504.27$ Å.

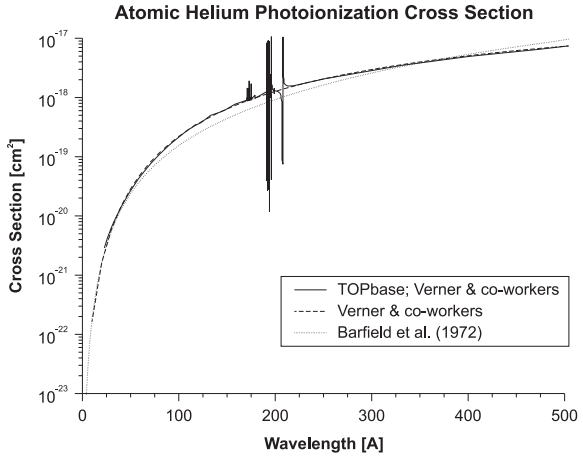

Fig. 4. Comparison of the photoionization cross section for He from three different sources: (1) a combination of TOPbase with extension by fits from Verner and co-workers for $\lambda < 22$ Å , (2) fits from Verner and co-workers without TOPbase results, and (3) calculations from Barfield et al. (1972).

Rate coefficient: We compare results in units of s^{-1} from the new cross sections with those obtained earlier by Huebner et al. (1992) using the cross sections of Barfield et al. (1972):

Solar activity	QS	AS
TOPbase, Verner and co-workers	5.64×10^{-8}	1.68×10^{-7}
Verner and co-workers	5.71×10^{-8}	1.69×10^{-7}
Huebner et al. (1992)	5.25×10^{-8}	1.51×10^{-7}

The results of Huebner et al. (1992) used the cross section data from Barfield et al. (1972). Agreement between the first two results is within 2% and for all three results within about 10%. For blackbody radiation the rate coefficients at $T = 1000$ K are less than 1×10^{-100} and differ by about 20% from the three cross section sources in the temperature range $T = 10{,}000$–$1{,}000{,}000$ K.

Excess energies: The excess energies in units of eV are compared as follows:

Solar activity	QS	AS
TOPbase, Verner and co-workers	17.3	20.0
Verner and co-workers	17.0	19.6
Huebner et al. (1992)	15.5	17.8

Agreement between the first two results is within 2% and for all three results within about 10%. Excess energies for the blackbody radiation fields are presented in Table 1.

2.1.3. Atomic lithium, Li

Cross section: TOPbase cross sections show no autoionization resonances. We use the cross section from the fits by Verner and co-workers.

Threshold: The ionization threshold $\lambda_{th} = 2299.53$ Å is given by Kelly (1987).

Rate coefficient: The rate coefficient is $1.97 \times 10^{-4}\ s^{-1}$ for the quiet Sun and $2.07 \times 10^{-4}\ s^{-1}$ for the active Sun. Rate coefficients for blackbody radiation are given in Table 1.

Excess energy: The excess energy is 0.351 eV for the quiet Sun and 0.389 eV for the active Sun. Excess energies for blackbody radiation are given in Table 1.

2.1.4. Atomic beryllium, Be

Cross section: The cross section from TOPbase is extended with the fitted cross section of Verner and co-workers to wavelengths $\lambda < 850$ Å (Fig. 5).

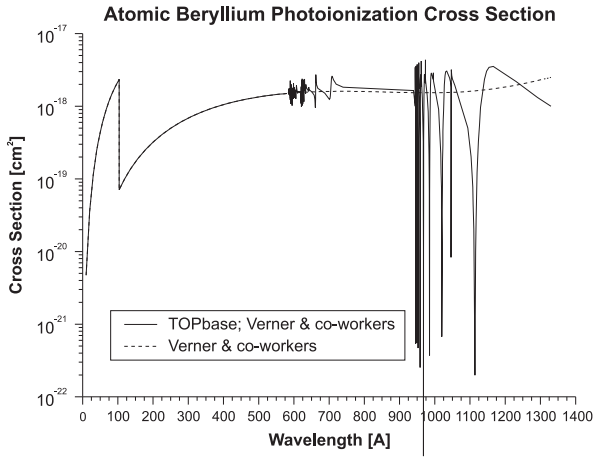

Fig. 5. Comparison of the photoionization cross section for Be from two different sources: (1) a combination of TOPbase and fits from Verner and co-workers and (2) fits from Verner and co-workers without TOPbase.

Please cite this article as: Huebner, W.F., Mukherjee, J., Photoionization and photodissociation rates in solar and blackbody radiation fields. Planetary and Space Science (2015), http://dx.doi.org/10.1016/j.pss.2014.11.022

Threshold: The ionization threshold $\lambda_{th} = 1329.92$ Å is given by Kramida and Martin (1997). TOPbase gives a value of 1337.35 Å. There is a similar discrepancy for the inner shell ionization energy. The fitted cross sections of Verner and co-workers do not have these discrepancies. This helps us to define the point for extending the TOPbase cross section with the fits from Verner and co-workers.

Rate coefficient: The rate coefficients in s^{-1} are

Solar activity	QS	AS
TOPbase, Verner and co-workers	8.91×10^{-7}	2.23×10^{-6}
Verner and co-workers	7.06×10^{-7}	1.75×10^{-6}

Excess energy: The excess energies in eV are

Solar activity	QS	AS
TOPbase, Verner and co-workers	1.67	1.80
Verner and co-workers	1.85	2.03

2.1.5. Atomic boron, B

Cross section: The cross section from TOPbase is extended with the fitted cross section of Verner and co-workers to wavelengths $\lambda < 850$ Å (Fig. 6).

Threshold: The ionization threshold $\lambda_{th} = 1494.1$ Å is given by Ryabtsev (2002).

Rate coefficient: The rate coefficients in units of s^{-1} are

Solar activity	QS	AS
TOPbase; Verner and co-workers	6.76×10^{-6}	1.51×10^{-5}
Verner and co-workers	6.17×10^{-6}	1.41×10^{-5}

Excess energy: The excess energies in eV are

Solar activity	QS	AS
TOPbase; Verner and co-workers	1.66	1.86
Verner and co-workers	1.76	1.94

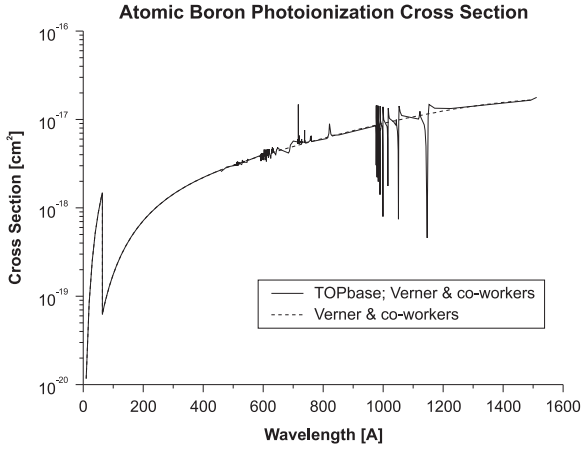

Fig. 6. Comparison of the photoionization cross section for B from two different sources: (1) TOPbase with an extension of the cross section using fits from Verner and co-workers and (2) fits from Verner and co-workers without TOPbase.

2.1.6. Atomic carbon, C

Cross section: In Figs. 7–9 we compare the cross sections of the C(^{3}P) ground state and the C(^{1}D) and C(^{1}S) metastable states

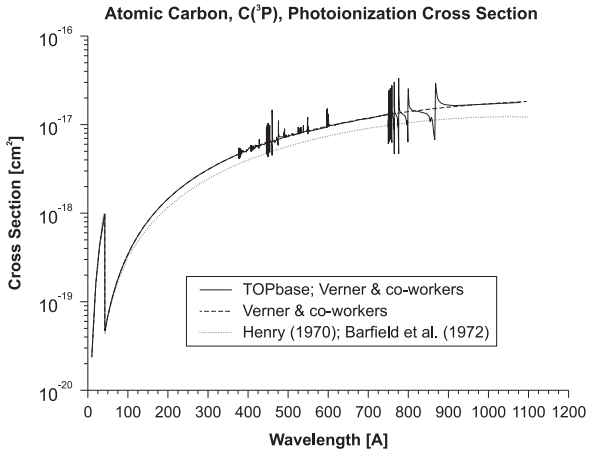

Fig. 7. Comparison of the photoionization cross section from (1) TOPbase ($\lambda > 375.8$ Å) with extension ($\lambda < 370.0$ Å) from fits by Verner and co-workers: Solid curve; (2) cross section from fits only (Verner and co-workers): dashed curve; and (3) calculations of Henry (1970) with modifications from Barfield et al. (1972): dotted curve for the C(^{3}P) ground state of carbon.

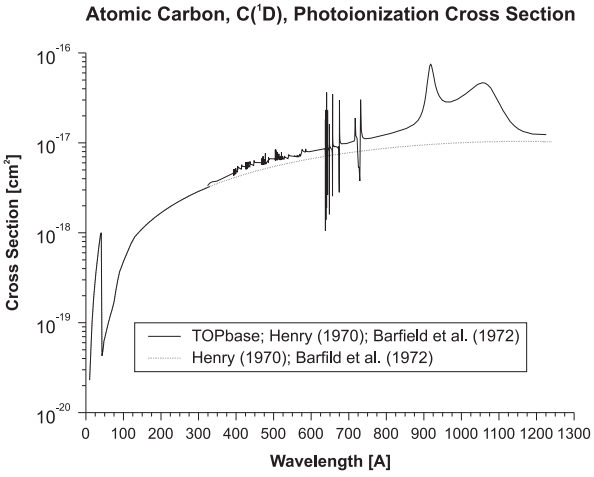

Fig. 8. Comparison of the photoionization cross section for the C(^{1}D) state based on (1) results from TOPbase with extension by Henry (1970) as modified by Barfield et al. (1972) and (2) calculations by Henry (1970) with extension of the cross section by Barfield et al. (1972).

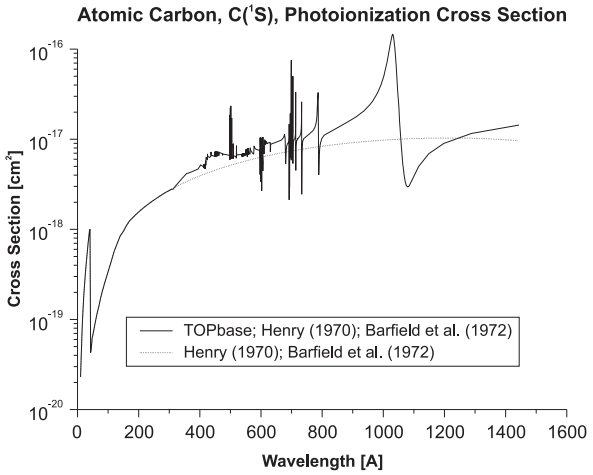

Fig. 9. Comparison of the photoionization cross section for the C(^{1}S) state based on (1) results from TOPbase with cross section extension by Henry (1970) as supplemented by Barfield et al. (1972) and (2) calculations by Henry (1970) with modification by Barfield et al. (1972).

Please cite this article as: Huebner, W.F., Mukherjee, J., Photoionization and photodissociation rates in solar and blackbody radiation fields. Planetary and Space Science (2015), http://dx.doi.org/10.1016/j.pss.2014.11.022

of carbon from various sources. For C(^{3}P) we have replaced the hydrogenic approximation for the extension of the TOPbase cross section for $\lambda < 370$ Å with the cross section using the fit parameters of Verner and co-workers. Except for the resonances, the cross section from the fit data of Verner and co-workers traces the general behavior of the TOPbase cross section for the ^{3}P state well. However, there are significant deviations between the cross sections from TOPbase and the calculations from Henry (1970) for the ^{1}D and the ^{1}S states. For C(^{1}D) we supplement the TOPbase data with the cross section of Barfield et al. (1972) for wavelengths $\lambda < 120$ Å and with the cross section of Henry (1970) between 120 Å and 310 Å. For C(^{1}S) we supplement the TOPbase data with the cross section of Barfield et al. (1972) for wavelengths $\lambda < 140$ Å and with the cross section of Henry (1970) between 140 Å and 310 Å.

Thresholds: According to NIST, the ionization threshold for C(^{3}P) is at a wavenumber of 90820.45 cm^{-1}, equivalent to $\lambda_{th} =$ 1101.07 Å as given by Johansson (1966); see also Moore (1970). Since the $2s^22p^2$ C(^{1}D) is 10,192.66 cm^{-1} above the ground state (Kaufman and Ward, 1966), the ionization potential is 80,627.79 cm^{-1}, equivalent to $\lambda_{th} = 1240.27$ Å. Similarly, the $2s^22p^2$ C(^{1}S) state is 21,648.02 cm^{-1} above the ground state (Kaufman and Ward, 1966) and therefore the ionization potential is 69,172.43 cm^{-1}, equivalent to $\lambda_{th} = 1445.66$ Å.

Rate coefficient: The rate coefficients in s^{-1} for the quiet and the active Sun are

for C(^{3}P):

Solar activity	QS	AS
TOPbase, Verner and co-workers	5.63×10^{-7}	1.26×10^{-6}
Verner and co-workers	5.62×10^{-7}	1.26×10^{-6}
Henry (1970)	4.10×10^{-7}	9.20×10^{-7}

for C(^{1}D):

Solar activity	QS	AS
TOPbase, Henry (1970)	4.80×10^{-6}	1.18×10^{-5}
Henry (1970)	3.58×10^{-6}	9.00×10^{-6}

for C(^{1}S):

Solar activity	QS	AS
TOPbase, Henry (1970)	5.36×10^{-6}	1.22×10^{-5}
Henry (1970)	4.34×10^{-6}	1.04×10^{-5}

Here Henry (1970) refers to rate coefficients based on the cross sections of Henry (1970) with the Barfield et al. (1972) extension of the cross section. The rate coefficients are almost 30% smaller than the ones based on the fit parameters of Verner and co-workers. Rate coefficients for blackbody radiation fields (BBRFs) without dilution factors for four temperatures from $T = 10^3$ K to $T = 10^6$ K are presented in Table 1.

Excess energy: The excess energies in eV for the quiet and the active Sun are

for C(^{3}P):

Solar activity	QS	AS
TOPbase, Verner and co-workers	5.55	6.99
Verner and co-workers	5.55	6.99
Henry (1970)	5.86	7.41

for C(^{1}D):

Solar activity	QS	AS
TOPbase, Henry (1970)	1.14	1.21
Henry (1970)	1.04	1.17

for C(^{1}S):

Solar activity	QS	AS
TOPbase, Henry (1970)	2.38	2.52
Henry (1970)	2.08	2.27

Excess energies for carbon atoms in blackbody radiation fields (BBRFs) without dilution factors are presented for four temperatures from $T = 10^3$ K to $T = 10^6$ K in Table 1.

2.1.7. Atomic nitrogen, N

Cross section: Fig. 10 displays the photoionization cross sections from TOPbase as extended by the cross section from fits produced by Verner and co-workers for $\lambda < 255$ Å. Also shown is the cross section from fit parameters of Verner and co-workers without the TOPbase results and the cross section from Henry (1970) with extension for $\lambda < 110$ Å from Barfield et al. (1972). The fits from Verner and co-workers track the Topbase results extremely well for $\lambda > 255$ Å.

Threshold: The ionization threshold $\lambda_{th} = 853.06$ Å is given by Moore (1975).

Rate coefficient: The rate coefficients in s^{-1} for the quiet and the active Sun are

Solar activity	QS	AS
TOPbase, Verner and co-workers	2.31×10^{-7}	5.90×10^{-7}
Verner and co-workers	2.30×10^{-7}	5.89×10^{-7}
Henry (1970)	1.85×10^{-7}	4.72×10^{-7}

The corresponding rate coefficients for the quiet and the active Sun using the fitted cross section agree to better than 1% with those from TOPbase, but those from Henry (1970) with the Barfield et al. (1972) cross section extension are about 15–20% smaller than the values obtained from the TOPbase or fitted cross sections. The

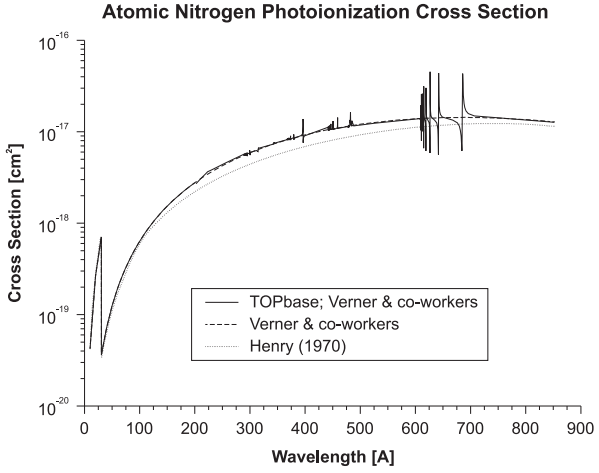

Fig. 10. Comparison of the photoionization cross section for nitrogen from (1) TOPbase including extensions from fits of Verner and co-workers with (2) fits of Verner and co-workers without TOPbase results and with (3) Henry (1970) with extension by Barfield et al. (1972).

Please cite this article as: Huebner, W.F., Mukherjee, J., Photoionization and photodissociation rates in solar and blackbody radiation fields. Planetary and Space Science (2015), http://dx.doi.org/10.1016/j.pss.2014.11.022

rate coefficients for four temperatures in a blackbody radiation field without dilution factors are given in Table 1.

Excess energy: The excess energies in eV for the quiet and the active Sun are

Solar activity	QS	AS
TOPbase, Verner and co-workers	15.5	19.0
Verner and co-workers	15.5	18.9
Henry (1970), Barfield et al. (1972)	14.9	18.4

Here Henry (1970) refers to rate coefficients and excess energies based on the cross section calculations of Henry (1970) with the Barfield et al. (1972) extension of the cross section. Excess energies based on TOPbase cross sections for atomic nitrogen in blackbody radiation fields (BBRFs) without dilution factors are presented for four temperatures from $T=10^3$ K to $T=10^6$ K in Table 1.

2.1.8. Atomic oxygen, O

Cross section: Figs. 11–13 display the photoionization cross sections of the O(^{3}P) ground state and the O(^{1}D) and O(^{1}S) metastable states from various sources. For O(^{3}P) results from TOPbase as modified and extended by fits from Verner and co-workers for $\lambda<235$ Å are compared with the cross section obtained from fit parameters of Verner and co-workers without the TOPbase results and also with the cross section from Henry (1970) extended with the cross section from Barfield et al. (1972). The fits from Verner and co-workers track the TOPbase results for O(^{3}P) extremely well for $\lambda>255$ Å. As can be seen in Figs. 12 and 13, there are significant differences in the cross sections between TOPbase results and the calculations of Henry as modified by Barfield et al. for O(^{1}D) and O(^{1}S).

Threshold: According to NIST, the ionization threshold for O(^{3}P) is at a wavenumber of 109,837.02 cm^{-1}, equivalent to $\lambda_{th}=$ 910.44 Å as given by Moore (1993). The $2s^22p^4$ O(^{1}D) is 15,867.862 cm^{-1} above the ^{3}P ground state and the $2s^22p^4$ O(^{1}S) is 33,792.583 cm^{-1} above the ^{3}P ground state. Unlike the carbon ionization limits, for oxygen, O(^{1}D) and O(^{1}S) the ionization limits are different than that for the O(^{3}P). For O(^{1}D) the series limit is the $2s^22p^3$ $^2D^o$ state of singly ionized oxygen. This state is 26,810.55 cm^{-1} above the ground state of the ion. Thus, the ionization potential is 109,837.02 − 15,867.86 + 26,810.55 = 120,779.70 cm^{-1}, equivalent

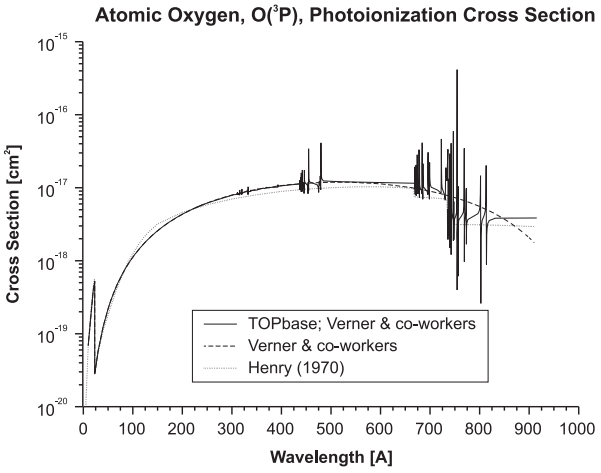

Fig. 11. Comparison of the photoionization cross section of the O(^{3}P) ground state from TOPbase data as extended by the cross section from fits made by Verner and co-workers (solid curve) with the cross section from fits (Verner and co-workers) without TOPbase data (dashed curve), and with the cross section calculated by Henry (1970) as extended by Barfield et al. (1972) (dotted curve).

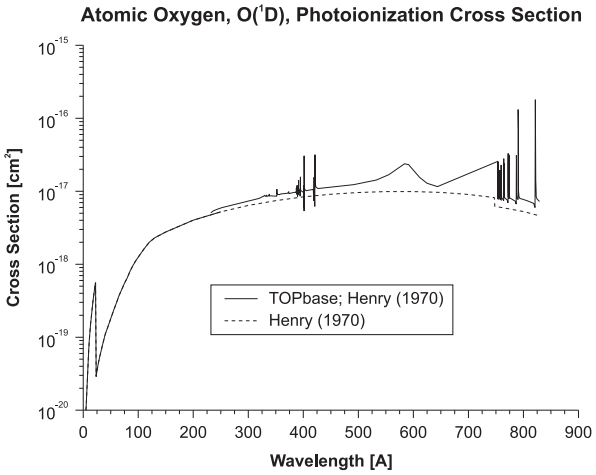

Fig. 12. Comparison of the photoionization cross section of the O(^{1}D) metastable state from TOPbase data as extended by the cross section from Henry (1970) for $130<\lambda<220$ Å and the cross section from Barfield et al. (1972) for $\lambda<130$ Å (solid curve) with the cross section from Henry (1970) as extended by Barfield et al. (1972) without TOPbase data (dashed curve). We used threshold values from the NIST database.

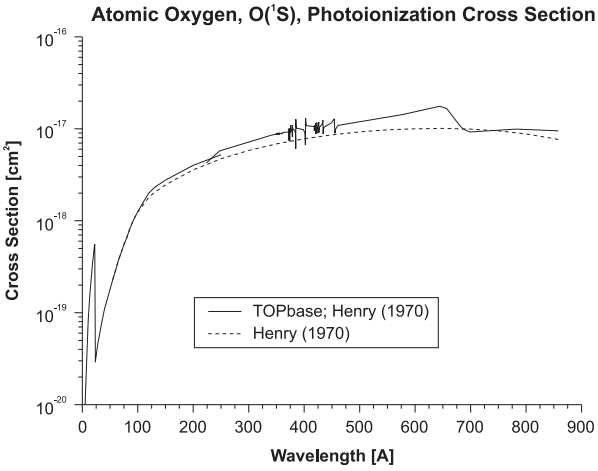

Fig. 13. Comparison of the photoionization cross section of the O(^{1}S) metastable state from TOPbase data as extended by the cross section from Henry (1970) for $130<\lambda<220$ Å and the cross section from Barfield et al. (1972) for $\lambda<130$ Å (solid curve) with the cross section from Henry (1970) as extended by Barfield et al. (1972) without TOPbase data (dashed curve). We used threshold values from the NIST database.

to $\lambda_{th}=827.90$ Å (Moore, 1993). Similarly, the series limit of O(^{1}S) is the $2s^22p^3$ $^2P^o$ state of singly ionized oxygen. It is 40,468.01 cm^{-1} above the ground state of the ion (Moore, 1993). Thus the ionization potential for O(^{1}S) is 109,837.02 − 33,792.58 + 40,468.01 = 116,512.45 cm^{-1}, equivalent to $\lambda_{th}=858.28$ Å. For comparison, TOPbase gives the ionization threshold for the O(^{3}P) state as 110,122.49 cm^{-1}, for the O(^{1}D) state as 121,414.4 cm^{-1}, and for the O(^{1}S) state as 116,909.4 cm^{-1}. These TOPbase values differ from the NIST values by about 0.5% or less. However, the onset of the TOPbase cross section for the O(^{1}S) state is about 14% below their presumably consistently calculated threshold energy. This means that most of the autoionization resonances of the O(^{1}S) state are energetically below the ionization threshold. The onset of the TOPbase cross section for the O(^{1}S) state gives nearly the same discrepancy with respect to the NIST threshold value that we use. Discrepancies for the O(^{1}D) state are much smaller and are negligible for the O(^{3}P) ground state.

Please cite this article as: Huebner, W.F., Mukherjee, J., Photoionization and photodissociation rates in solar and blackbody radiation fields. Planetary and Space Science (2015), http://dx.doi.org/10.1016/j.pss.2014.11.022

Rate coefficient: The rate coefficients in units of s^{-1} for the quiet and the active Sun for the O(^{3}P) state are

Solar activity	QS	AS
TOPbase, Verner and co-workers	2.44×10^{-7}	6.59×10^{-7}
Verner and co-workers	2.37×10^{-7}	6.43×10^{-7}
Henry (1970)	2.12×10^{-7}	5.88×10^{-7}

Here Henry (1970) refers to rate coefficients based on the cross sections of Henry (1970) with the Barfield et al. (1972) extension of the cross section. Rate coefficients for O(^{1}D) and O(^{1}S) in s^{-1} based on data from Henry (1970) and Barfield et al. (1972) are

for O(^{1}D):

Solar activity	QS	AS
TOPbase, Henry (1970)	2.38×10^{-7}	6.25×10^{-7}
Henry (1970)	1.82×10^{-7}	5.04×10^{-7}

and for O(^{1}S):

Solar activity	QS	AS
TOPbase, Henry (1970)	2.47×10^{-7}	6.45×10^{-7}
Henry (1970)	1.96×10^{-7}	5.28×10^{-7}

Here Henry (1970) again refers to rate coefficients based on the cross sections of Henry (1970) with the Barfield et al. (1972) extension of the cross section. Rate coefficients for blackbody radiation fields (BBRFs) without dilution factors for four temperatures from $T = 10^3$ K to $T = 10^6$ K are presented in Table 1.

Excess energy: The excess energies in eV for the quiet and the active Sun for the O(^{3}P) state are

Solar activity	QS	AS
TOPbase, Verner and co-workers	20.1	24.1
Verner and co-workers	20.7	24.7
Henry (1970)	21.6	26.1

Here Henry (1970) refers to rate coefficients based on the cross sections of Henry (1970) with the Barfield et al. (1972) extension of the cross section. Rate coefficients for O(^{1}D) and O(^{1}S) in eV based on data from Henry (1970) and Barfield et al. (1972) are

for O(^{1}D):

Solar activity	QS	AS
TOPbase, Henry (1970)	19.0	23.3
Henry (1970)	21.6	26.1

and for O(^{1}S):

Solar activity	QS	AS
TOPbase, Henry (1970)	17.9	21.7
Henry (1970)	18.9	23.1

Here Henry (1970) again refers to excess energies based on the cross sections of Henry (1970) with the Barfield et al. (1972) extension of the cross section. Excess energies for blackbody radiation fields (BBRFs) without dilution factors for four temperatures from $T = 10^3$ K to $T = 10^6$ K are presented in Table 1.

2.1.9. Atomic fluorine, F

Cross section: In Fig. 14 we compare the cross section from (1) TOPbase containing an extension for $\lambda < 260$ Å from Verner and co-workers with (2) the cross section made from fits by Verner and co-workers and (3) the cross section calculated by Barfield et al. (1972) up to $\lambda = 130$ Å and by Manson et al. (1979) above this wavelength up to threshold. The cross sections from these sources agree well for wavelengths $\lambda < 620$ Å, but the cross section of Manson et al. is up to about 35% smaller above that wavelength.

Threshold: The ionization threshold $\lambda_{th} = 711.62$ Å is given by Liden (1949). This value is smaller than the previously adopted value of $\lambda_{th} = 759.44$ Å (Moore, 1970).

Rate coefficient: The rate coefficients in s^{-1} for the quiet and the active Sun are

Solar activity	QS	AS
TOPbase, Verner and co-workers	2.10×10^{-7}	6.10×10^{-7}
Verner and co-workers	2.08×10^{-7}	6.10×10^{-7}
Manson et al. (1979)	2.10×10^{-7}	6.19×10^{-7}

Here Manson et al. (1979) refers to rate coefficients based on the cross section of Manson et al. (1979) with the Barfield et al. (1972) extension of the cross section. The rate coefficients associated with the different sources for the cross sections and the threshold energies agree very well in the solar radiation field. Rate coefficients for the blackbody radiation fields at four temperatures between $T = 10^3$ K and $T = 10^6$ K are given in Table 1.

Excess energy: The excess energies in eV for the quiet and the active Sun are

Solar activity	QS	AS
TOPbase, Verner and co-workers	22.9	27.2
Verner and co-workers	23.4	27.5
Manson et al. (1979)	24.7	28.9

Here again Manson et al. (1979) refers to the cross section of Manson et al. (1979) with the Barfield et al. (1972) extension of the cross section. Excess energies based on TOPbase cross sections for atomic fluorine in blackbody radiation fields (BBRFs) without

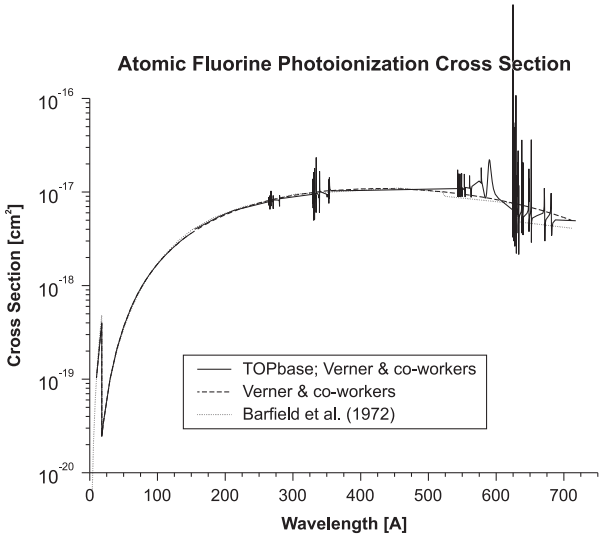

Fig. 14. Comparison of the photoionization cross section for fluorine from (1) TOPbase, (2) fitted data from Verner and co-workers, and (3) data from Barfield et al. (1972) and Manson et al. (1979).

Please cite this article as: Huebner, W.F., Mukherjee, J., Photoionization and photodissociation rates in solar and blackbody radiation fields. Planetary and Space Science (2015), http://dx.doi.org/10.1016/j.pss.2014.11.022

dilution factors are presented for four temperatures from $T = 10^3$ K to $T = 10^6$ K in Table 1.

2.1.10. Atomic neon, Ne

Cross section: In Fig. 15 we compare the cross section from TOPbase at wavelengths $\lambda > 240$ Å with those made from fits by Verner and co-workers. The cross sections from these two sources agree extremely well.

Threshold: As quoted by NIST, the ionization threshold $\lambda_{th} = 574.94$ Å is given by Kaufman and Minnhagen (1972).

Rate coefficient: The rate coefficients in s^{-1} for the quiet and the active Sun are

Solar activity	QS	AS
TOPbase, Verner and co-workers	1.84×10^{-7}	5.87×10^{-7}
Verner and co-workers	1.85×10^{-7}	5.92×10^{-7}

The rate coefficients associated with the two different sources for the cross sections and threshold energies are within 1% the same in the solar radiation field. Rate coefficients for the blackbody radiation fields at four temperatures ranging from $T = 10^3$ K to $T = 10^6$ K are given in Table 1.

Excess energy: The excess energies in eV for the quiet and the active Sun are

Solar activity	QS	AS
TOPbase, Verner and co-workers	24.3	27.8
Verner and co-workers	24.2	27.7

The excess energies associated with the two different sources for the cross sections and threshold energies are within 1% the same in the solar radiation field. Excess energies based on TOPbase cross sections for atomic neon in blackbody radiation fields (BBRFs) without dilution factors are presented for four temperatures from $T = 10^3$ K to $T = 10^6$ K in Table 1.

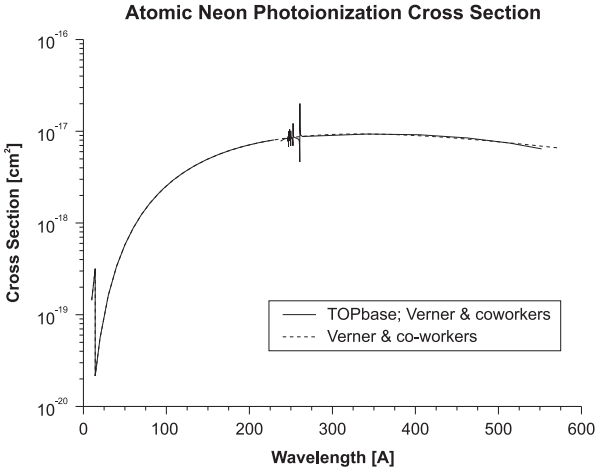

Fig. 15. The photoionization cross section for monatomic neutral neon (Ne) vs. wavelength (Å). The solid curve represents the cross section from TOPbase with extension from fits by Verner and co-workers. Also shown is the cross section from fits of Verner and co-workers without TOPbase data.

2.1.11. Atomic sodium, Na

Cross section: A comparison of photoionization cross sections is presented in Fig. 16. The improved resolution of the Cooper minimum in the cross sections makes the TOPbase data and the

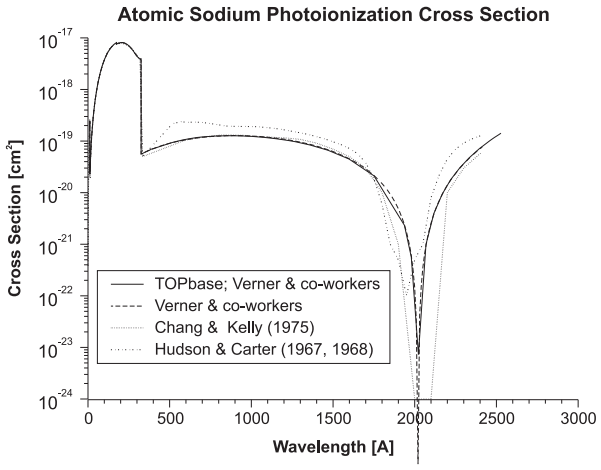

Fig. 16. The photoionization cross section (cm^2) for monatomic neutral sodium (Na) vs. wavelength (Å). The solid curve represents the cross section from TOPbase with extension from fits by Verner and co-workers. Also shown are the cross sections from fits (Verner and co-workers), cross sections from older calculations by Chang and Kelly (1975), and experimental cross sections from Hudson and Carter (1967, 1968).

data from the cross section fits by Verner and co-workers preferable over the older values.

Threshold: The ionization threshold $\lambda_{th} = 2412.58$ Å is given by Baugh et al. (1998). This is virtually unchanged from the previous value (see Huebner et al., 1992).

Rate coefficient: The rate coefficients in s^{-1} for the quiet and the active Sun are

Solar activity	QS	AS
TOPbase, Verner and co-workers	7.26×10^{-6}	7.91×10^{-6}
Verner and co-workers	7.26×10^{-6}	7.91×10^{-6}

Rate coefficients for the blackbody radiation fields at four temperatures ranging from $T = 10^3$ K to $T = 10^6$ K are given in Table 1.

The rate coefficients for the quiet and the active Sun reported previously (Huebner et al., 1992) using the theoretical cross section of Chang and Kelly (1975) were 5.92×10^{-6} s^{-1} and 6.52×10^{-6} s^{-1}, respectively. The rate coefficients are sensitive to the accidental cancellation of wave functions causing the Cooper minimum at $\lambda \approx 2010$ Å. As reported earlier, the rate coefficients based on experimental cross sections from Hudson and Carter (1967, 1968) are 1.62×10^{-5} s^{-1} and 1.72×10^{-5} s^{-1}, and are probably not correct (Samson, 1982).

Excess energy: The preferred values for the excess energies in eV for the quiet and the active Sun are

Solar activity	QS	AS
TOPbase, Verner and co-workers	0.972	2.98
Verner and co-workers	0.972	2.98

The excess energies for four BBRFs at $T = 10^3$, $T = 10^4$, $T = 10^5$, and $T = 10^6$ K are given in Table 1.

The previously reported excess energies for the quiet and the active Sun based on the cross section of Chang and Kelly (1975) were 1.13 eV and 3.52 eV, respectively, while those based on the experimental cross sections of Hudson and Carter (1967, 1968) were 0.57 eV and 1.49 eV.

Please cite this article as: Huebner, W.F., Mukherjee, J., Photoionization and photodissociation rates in solar and blackbody radiation fields. Planetary and Space Science (2015), http://dx.doi.org/10.1016/j.pss.2014.11.022

2.1.12. Atomic magnesium, Mg

Cross section: A comparison of the photoionization cross section from TOPbase and from the cross section fits by Verner and co-workers is presented in Fig. 17.

Threshold: The ionization threshold $\lambda_{th} = 1621.51$ Å is given by Kaufman and Martin (1991a). The threshold is nearly the same as the one used in our earlier calculations (Huebner et al., 1992).

Rate coefficient: The rate coefficients in s^{-1} for the quiet and the active Sun are

Solar activity	QS	AS
TOPbase, Verner and co-workers	6.49×10^{-7}	1.17×10^{-6}
Verner and co-workers	5.69×10^{-7}	1.08×10^{-6}

Rate coefficients for the blackbody radiation fields at four temperatures ranging from $T = 10^3$ K to $T = 10^6$ K are given in Table 1.

Excess energy: The excess energies in eV for the quiet and the active Sun are

Solar activity	QS	AS
TOPbase, Verner and co-workers	4.09	9.51
Verner and co-workers	4.75	10.4

The excess energies for four BBRFs at $T = 10^3$, $T = 10^4$, $T = 10^5$, and $T = 10^6$ K are given in Table 1.

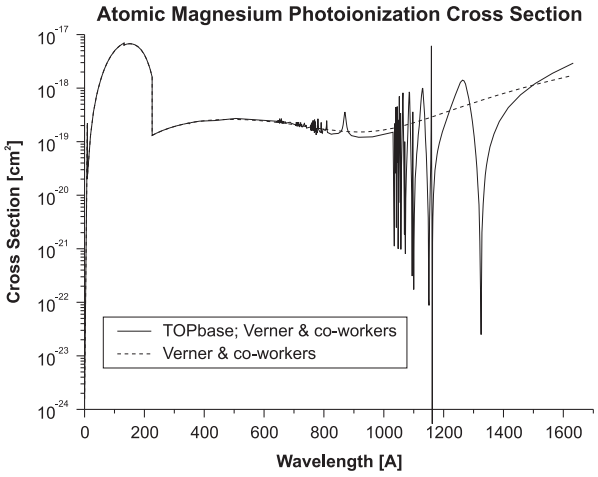

Fig. 17. Photoionization cross section of monatomic neutral magnesium (Mg) vs. wavelength. The solid curve represents the cross section from TOPbase with extension for $\lambda < 630.00$ Å from fits by Verner and co-workers. Also shown is the cross section (dashed curve) from fits (Verner and co-workers) for the entire wavelength range.

2.1.13. Atomic aluminum, Al

Cross section: A comparison of the photoionization cross section from TOPbase and from the cross section fits by Verner and co-workers is presented in Fig. 18.

Threshold: The ionization threshold $\lambda_{th} = 2071.32$ Å is given by Kaufman and Martin (1991b). The threshold is almost the same as the one used in our earlier calculations (Huebner et al., 1992).

Rate coefficient: The rate coefficients in units of s^{-1} for the quiet and the active Sun are

Solar activity	QS	AS
TOPbase, Verner and co-workers	1.20×10^{-3}	1.30×10^{-3}
Verner and co-workers	6.94×10^{-4}	7.65×10^{-4}

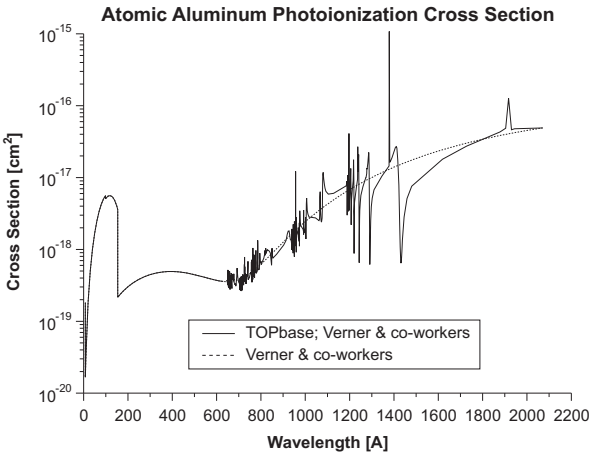

Fig. 18. Photoionization cross section of monatomic neutral aluminum (Al) vs. wavelength. The solid curve represents the cross section from TOPbase with extension for $\lambda < 630.00$ Å from fits by Verner and co-workers. Also shown is the cross section (dashed curve) from fits (Verner and co-workers) for the entire wavelength range.

Rate coefficients for the blackbody radiation fields at four temperatures ranging from $T = 10^3$ K to $T = 10^6$ K are given in Table 1.

Excess energy: The excess energies in eV for the quiet and the active Sun are

Solar activity	QS	AS
TOPbase, Verner and co-workers	0.253	0.281
Verner and co-workers	0.380	0.416

The excess energies for four BBRFs at $T = 10^3$, $T = 10^4$, $T = 10^5$, and $T = 10^6$ K are given in Table 1.

2.1.14. Atomic silicon, Si

Cross section: A comparison of the photoionization cross section from TOPbase and from the cross section fits by Verner and co-workers is presented in Fig. 19.

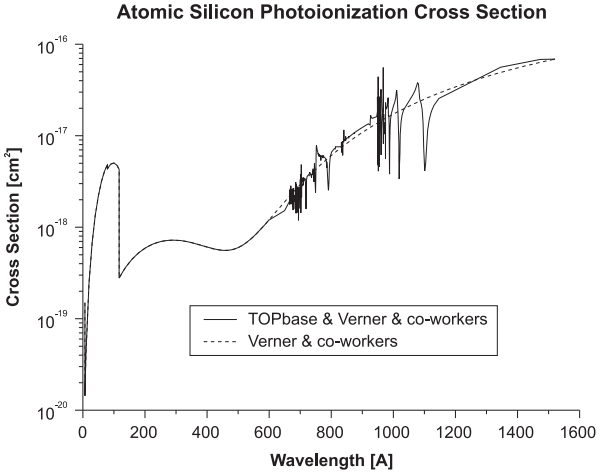

Fig. 19. Photoionization cross section of monatomic neutral silicon (Si) vs. wavelength. The solid curve represents the cross section from TOPbase with extension for $\lambda < 600.00$ Å from fits by Verner and co-workers. Also shown is the cross section (dashed curve) from fits (Verner and co-workers) for the entire wavelength range.

Please cite this article as: Huebner, W.F., Mukherjee, J., Photoionization and photodissociation rates in solar and blackbody radiation fields. Planetary and Space Science (2015), http://dx.doi.org/10.1016/j.pss.2014.11.022

Threshold: The ionization threshold $\lambda_{th} = 1520.96$ Å is given by Martin et al. (1994).

Rate coefficient: The rate coefficients in s^{-1} for the quiet and the active Sun are

Solar activity	QS	AS
TOPbase, Verner and co-workers	2.29×10^{-5}	4.81×10^{-5}
Verner and co-workers	2.06×10^{-5}	4.43×10^{-5}

Rate coefficients for blackbody radiation fields at four temperatures ranging from $T = 10^3$ K to $T = 10^6$ K are given in Table 1.

Excess energy: The excess energies in eV for the quiet and the active Sun are

Solar activity	QS	AS
TOPbase, Verner and co-workers	1.36	1.57
Verner and co-workers	1.47	1.66

The excess energies for four BBRFs at $T = 10^3$, $T = 10^4$, $T = 10^5$, and $T = 10^6$ K are given in Table 1.

2.1.15. Atomic phosphorous, P

Cross section: TOPbase does not provide a photoionization cross section for phosphorus. We use the photoionization cross section from fits prepared by Verner and co-workers.

Threshold: The ionization threshold $\lambda_{th} = 1182.30$ Å is given by Martin et al. (1985).

Rate coefficient: The rate coefficient is $6.47 \times 10^{-7}\ s^{-1}$ for the quiet Sun and $1.37 \times 10^{-6}\ s^{-1}$ for the active Sun. Rate coefficients for the blackbody radiation fields at $T = 10^3$ K, $T = 10^4$ K, $T = 10^5$ K, and $T = 10^6$ K are given in Table 1.

Excess energy: The excess energy is 3.61 eV for the quiet Sun and 4.77 eV for the active Sun. The excess energies for four BBRFs at $T = 10^3$, $T = 10^4$, $T = 10^5$, and $T = 10^6$ K are given in Table 1.

2.1.16. Atomic sulfur, S

Cross section: Figs. 20–22 display the photoionization cross sections of the S(^{3}P) ground state and the S(^{1}D) and S(^{1}S) metastable states from various sources. In Fig. 20 we compare (1) the S(^{3}P) cross section generated from TOPbase data supplemented by an extension of the cross section based on fit coefficients prepared by Verner and co-workers for $\lambda < 480$ Å, with (2) the cross section from fits made by Verner and co-workers without TOPbase data and with (3) the calculated cross section of Chapman and Henry (1971) supplemented with data below $\lambda = 122$ Å from Barfield et al. (1972). The cross section of Chapman and Henry deviates significantly.

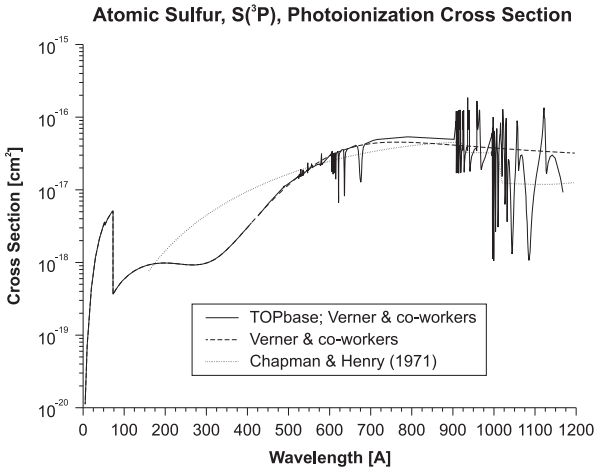

Fig. 20. Comparison of the photoionization cross section from TOPbase data with extension of the cross section from Verner and co-workers (solid curve) with the cross section from fit parameters prepared by Verner and co-workers without TOPbase data (dashed curve) and with the cross section calculated by Chapman and Henry (1971) (dotted curve).

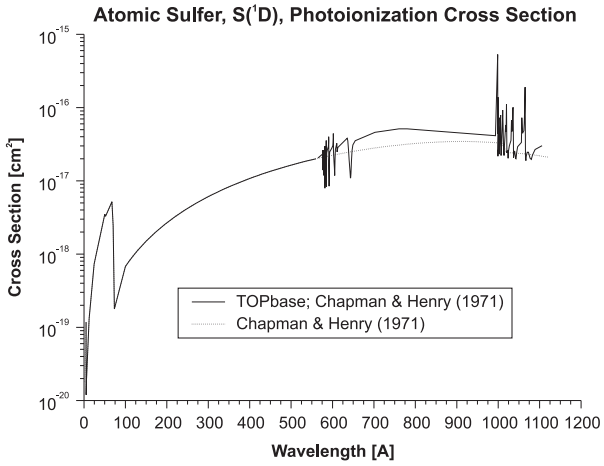

Fig. 21. Comparison of the photoionization cross section from Verner and co-workers (solid curve) with the cross section of Chapman and Henry (1971) (dotted curve) for the S(^{1}D) metastable state of sulfur.

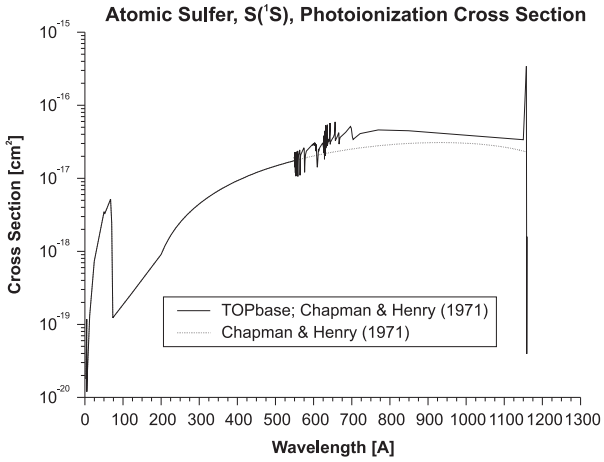

Fig. 22. Comparison of the photoionization cross section from Verner and co-workers (solid curve) with the cross section of Chapman and Henry (1971) (dotted curve) for the S(^{1}S) metastable state of sulfur.

In Fig. 21 we show the photoionization cross sections of the S(^{1}D) metastable state of sulfur and compare results from TOPbase, as extended by the cross section from Chapman and Henry (1971) between $\lambda \approx 100$ and 560 Å, and further extended by Barfield et al. (1972) for $\lambda < 100$ Å with the calculated cross section from Chapman and Henry (1971) without TOPbase but including the same extension from Barfield et al. (1972). There are significant deviations in the results from TOPbase and from Chapman and Henry.

In Fig. 22 we show the photoionization cross sections of the S(^{1}S) metastable state and compare results from TOPbase, as extended by the cross section from Chapman and Henry (1971) between $\lambda \approx 200$ and 547 Å, and further extended by Barfield et al. (1972) for $\lambda < 200$ Å with the calculated cross section from Chapman and Henry (1971) without TOPbase but including the same extension from Barfield et al. (1972). Again, significant deviations exist in the results from TOPbase and from Chapman and Henry. In all cases we used threshold wavelengths from the NIST database.

Please cite this article as: Huebner, W.F., Mukherjee, J., Photoionization and photodissociation rates in solar and blackbody radiation fields. Planetary and Space Science (2015), http://dx.doi.org/10.1016/j.pss.2014.11.022

Threshold: According to NIST, the ionization threshold for S(^{3}P) is at a wavenumber of 83,559.1 cm^{-1}, equivalent to $\lambda_{th}=$ 1196.76 Å as given by Moore (1993). The $3s^23p^4$ S(^{1}D) state is 9238.609 cm^{-1} above the ^{3}P ground state and the $3s^23p^4$ S(^{1}S) state is 22,179.954 cm^{-1} above the ^{3}P ground state (Martin et al., 1990). Just as for oxygen the ionization limits for S(^{1}D) and S(^{1}S) are different than that for the S(^{3}P). For S(^{1}D) the line absorption series limit is the $3s^23p^3\ ^2D^o_{3/2}$ state of singly ionized sulfur. This state is 14,852.94 cm^{-1} above the ground state of the ion. Thus, the ionization potential is 83,559.1 − 9238.609 + 14,852.94= 89,173.4 cm^{-1}, equivalent to $\lambda_{th}=1121.41$ Å (Moore, 1993). Similarly, the absorption line series limit of S(^{1}S) is the $3s^22p^3\ ^2P^o_{1/2}$ state of singly ionized sulfur. It is 24,524.83 cm^{-1} above the ground state of the ion (Moore, 1993). Thus the ionization potential for S(^{1}S) is 83,559.1 −22,179.95 + 24,524.83= 85,904.0 cm^{-1}. This is equivalent to $\lambda_{th}=1164.09$ Å. For comparison, TOPbase gives the ionization threshold for the S(^{3}P) state as 86,698.2 cm^{-1}, for the S(^{1}D) state as 92,117.2 cm^{-1}, and for the S(^{1}S) as 89,464.7 cm^{-1}. These TOPbase values differ from the NIST values by about 3–4%. However, the onset of the TOPbase cross section for the S(^{1}S) state is about 7% below their presumably consistently calculated threshold energy. This means that most of the autoionization resonances are below the ionization threshold. The onset of the TOPbase cross section for the S(^{1}S) state gives nearly the same discrepancy with respect to the NIST threshold value that we use. Discrepancies for the S(^{1}D) state are much smaller and are negligible for the S^{3}P ground state.

Rate coefficient: The rate coefficients for the quiet and the active Sun are

for S(^{3}P):

Solar activity	QS	AS
TOPbase, Verner and co-workers	1.37×10^{-6}	3.00×10^{-6}
Verner and co-workers	1.34×10^{-6}	2.91×10^{-6}
Chapman and Henry (1971); Barfield et al. (1972)	1.83×10^{-6}	3.96×10^{-6}

for S(^{1}D):

Solar activity	QS	AS
TOPbase, Chapman and Henry (1971), Barfield et al. (1972)	1.49×10^{-6}	3.33×10^{-6}
Chapman and Henry (1971), Barfield et al. (1972)	1.08×10^{-6}	2.45×10^{-6}

for S(^{1}S):

Solar activity	QS	AS
TOPbase, Chapman and Henry (1971), Barfield et al. (1972)	1.83×10^{-6}	4.01×10^{-6}
Chapman and Henry (1971), Barfield et al. (1972)	1.05×10^{-6}	2.31×10^{-6}

Here Chapman and Henry (1971) and Barfield et al. (1972) refers to the cross section of Chapman and Henry (1971) with the Barfield et al. (1972) extension of the cross section. The rate coefficients based on the cross section from Chapman and Henry are about 35% larger than those based on the cross section from TOPbase or fit parameter data for S(^{3}P) and about 30–40% smaller for the S(^{1}D) and S(^{1}S) states. Rate coefficients for blackbody radiation fields (BBRFs) without dilution factors for four temperatures from $T=10^3$ K to $T=10^6$ K are presented in Table 1.

Excess energy: The excess energies in eV for the quiet and the active Sun are

for S(^{3}P):

Solar activity	QS	AS
TOPbase, Verner and co-workers	4.39	4.93
Verner and co-workers	4.29	4.85
Chapman and Henry (1971), Barfield et al. (1972)	4.39	5.10

for S(^{1}D):

Solar activity	QS	AS
TOPbase, Chapman and Henry (1971), Barfield et al. (1972)	5.22	6.36
Chapman and Henry (1971), Barfield et al. (1972)	6.21	7.68

for S(^{1}S):

Solar activity	QS	AS
TOPbase; Chapman and Henry (1971), Barfield et al. (1972)	3.72	4.29
Chapman and Henry (1971), Barfield et al. (1972)	5.42	6.38

Here Chapman and Henry (1971) and Barfield et al. (1972) refers to excess energies based on the cross section of Chapman and Henry (1971) with the Barfield et al. (1972) extension of the cross section. Excess energies based on TOPbase cross sections for blackbody radiation fields (BBRFs) without dilution factors for four temperatures from $T=10^3$ K to $T=10^6$ K are presented in Table 1.

2.1.17. Atomic chlorine, Cl

Cross section: In Fig. 23 we compare the photoionization cross section from fits made by Verner and co-workers with the calculated cross section of Brown et al. (1980) supplemented with data for $\lambda<270.4$ Å from Barfield et al. (1972). The cross sections obtained from the calculated values of Brown et al. diverge significantly from the fit data.

Threshold: The ionization threshold $\lambda_{th}=956.11$ Å is given by Radziemski and Kaufman (1969). The previously used threshold wavelength, $\lambda_{th}=953$ Å (Huebner et al., 1992), was taken from Moore (1970).

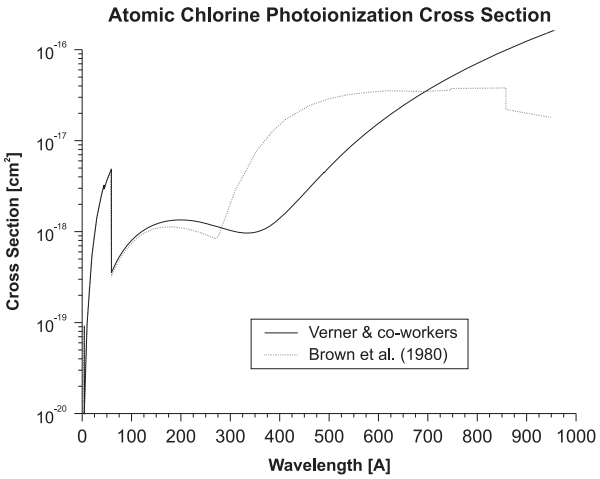

Fig. 23. Comparison of the photoionization cross section for chlorine from fits of Verner and co-workers (solid curve) and calculations of Brown et al. (1980) (dashed curve).

Please cite this article as: Huebner, W.F., Mukherjee, J., Photoionization and photodissociation rates in solar and blackbody radiation fields. Planetary and Space Science (2015), http://dx.doi.org/10.1016/j.pss.2014.11.022

Rate coefficient: The rate coefficients in units of s^{-1} for the quiet and the active Sun are

Solar activity	QS	AS
Verner and co-workers	1.41×10^{-6}	3.28×10^{-6}
Brown et al. (1980)	5.67×10^{-7}	1.30×10^{-6}

Here Brown et al. (1980) refers to rate coefficients based on the cross section of Brown et al. (1980) with the Barfield et al. (1972) extension of the cross section. The rate coefficients for the two different sources for the cross section and the threshold energy are, not surprisingly, very different for the solar radiation field, as well as for the blackbody radiation fields. Rate coefficients for blackbody radiation fields (BBRFs) without dilution factors based on cross sections from Verner and co-workers are presented in Table 1 for four temperatures from $T = 10^3$ K to $T = 10^6$ K.

Excess energy: The excess energies in eV for the quiet and the active Sun are

Solar activity	QS	AS
Verner and co-workers	2.23	2.74
Brown et al. (1980)	6.75	7.94

Here Brown et al. (1980) refers to cross section of Brown et al. (1980) with the Barfield et al. (1972) extension of the cross section. The excess energies for four BBRFs at $T = 10^3$, $T = 10^4$, $T = 10^5$, and $T = 10^6$ K are given in Table 1

2.1.18. Atomic argon, Ar

Cross section: As shown in Fig. 24, the cross section from fits made by Verner and co-workers traces the cross section using TOPbase data well and is in excellent agreement with the cross section of Marr and West (1976) up to $\lambda = 783$ Å. It has been extended above this value up to threshold using data measured by Huffman et al. (1963), as used in our earlier calculations (Huebner et al., 1992). Except for resonances, the cross section curves practically overlap over most of the wavelength range.

Threshold: The ionization threshold $\lambda_{th} = 786.72$ Å is given by Velchev et al. (1999). This is very close to our previous value of $\lambda_{th} = 786$ Å as given by Huffman et al. (1963).

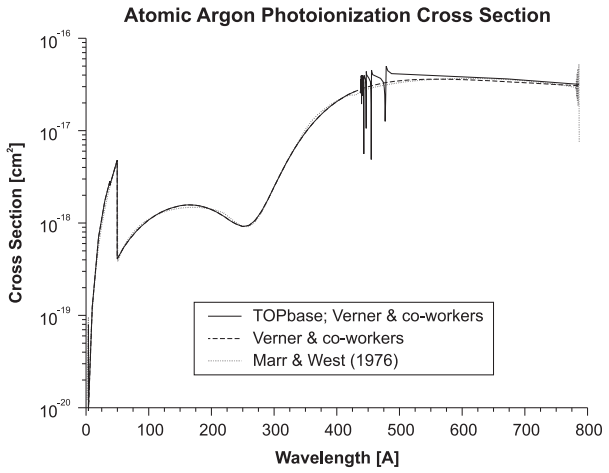

Fig. 24. Comparison of the photoionization cross section for argon from TOPbase (solid curve), from fit parameters of Verner and co-workers (dashed curve), and calculations of Brown et al. (1980) (dotted curve).

Rate coefficient: The rate coefficients in s^{-1} for the quiet and the active Sun are

Solar activity	QS	AS
TOPbase, Verner and co-workers	3.42×10^{-7}	7.74×10^{-7}
Verner and co-workers	3.03×10^{-7}	6.86×10^{-7}
Marr and West (1976)	3.06×10^{-7}	6.93×10^{-7}

Here Marr and West (1976) refers to rate coefficients based on the cross sections of Marr and West (1976) with the Huffman et al. (1963) extension of the cross section. Rate coefficients based on TOPbase cross sections for blackbody radiation fields (BBRFs) without dilution factors for four temperatures from $T = 10^3$ K to $T = 10^6$ K are presented in Table 1.

Excess energy: The excess energies for the quiet and the active Sun are

Solar activity	QS	AS
TOPbase, Verner and co-workers	9.40	11.8
Verner and co-workers	10.1	12.8
Marr and West (1976)	10.1	12.8

Here Marr and West (1976) again refers to excess energies based on the cross sections of Marr and West (1976) with the Huffman et al. (1963) extension of the cross section. Excess energies for the blackbody radiation fields are presented in Table 1.

2.1.19. Atomic potassium, K

Cross section: TOPbase does not provide the cross section for potassium. In Fig. 25 we compare the cross section from fits made by Verner and co-workers with the cross section of Hudson and Carter (1965) for wavelengths from $\lambda = 1200$ Å to threshold supplemented with data from Barfield et al. (1972) for $\lambda < 1128.19$ Å. The two sets of cross sections differ significantly.

Threshold: The ionization threshold $\lambda_{th} = 2856.34$ Å is given by Sugar and Corliss (1985). This threshold value is in very good agreement with the value of $\lambda_{th} = 2856$ Å used by us earlier and quoted by Hudson and Carter (1965).

Rate coefficient: The rate coefficients in s^{-1} for the quiet and the active Sun are

Solar activity	QS	AS
Verner and co-workers	2.70×10^{-5}	2.79×10^{-5}
Hudson and Carter (1965)	2.22×10^{-5}	2.36×10^{-5}

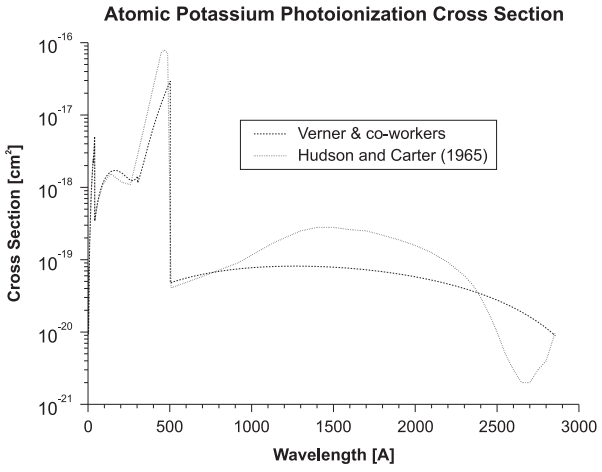

Fig. 25. Comparison of photoionization cross section for potassium from Verner and co-workers with the cross section from Hudson and Carter (1965).

Please cite this article as: Huebner, W.F., Mukherjee, J., Photoionization and photodissociation rates in solar and blackbody radiation fields. Planetary and Space Science (2015), http://dx.doi.org/10.1016/j.pss.2014.11.022

Here Hudson and Carter (1965) refers to rate coefficients based on the cross section of Hudson and Carter (1965) with the Barfield et al. (1972) extension of the cross section. The rate coefficients from the two different sources for the cross sections and threshold energies agree to be within 25% for the solar radiation field. Agreement is worse for the blackbody radiation fields. Table 1 is based on TOPbase cross sections.

Excess energy: The excess energies in eV for the quiet and the active Sun are

Solar activity	QS	AS
Verner and co-workers	0.735	0.921
Hudson and Carter (1965)	1.36	1.78

Here again Hudson and Carter (1965) refers to excess energies based on the cross sections of Hudson and Carter (1965) with the Barfield et al. (1972) extension of the cross section. Excess energies for the blackbody radiation fields are presented in Table 1. The excess energies from the two sets of sources vary by a factor of about 2; except for the BBRF at about $T = 100,000$ K where agreement is much better.

2.1.20. Atomic calcium, Ca

Cross section: In Fig. 26 we compare the photoionization cross section from TOPbase with the cross section made from fits prepared by Verner and co-workers for wavelengths from $\lambda = 1390$ Å to threshold.

Threshold: The ionization threshold $\lambda_{th} = 2028.15$ Å is given by Sugar and Corliss (1985).

Rate coefficient: The rate coefficients in s^{-1} for the quiet and the active Sun are

Solar activity	QS	AS
TOPbase, Verner and co-workers	3.05×10^{-4}	3.25×10^{-4}
Verner and co-workers	6.95×10^{-5}	7.80×10^{-5}

Rate coefficients based on TOPbase cross sections for blackbody radiation fields (BBRFs) without dilution factors for four temperatures from $T = 10^3$ K to $T = 10^6$ K are presented in Table 1.

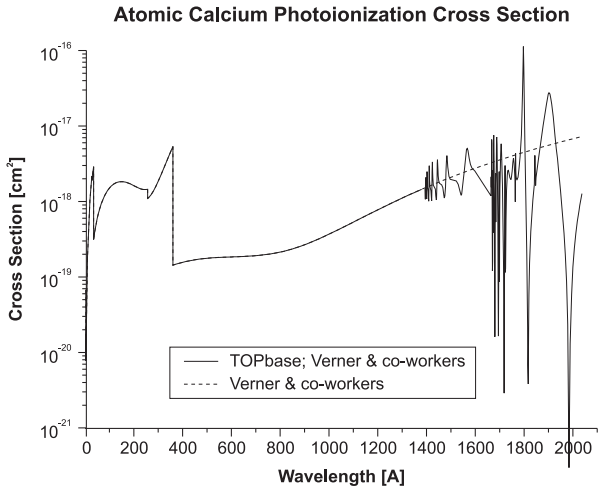

Fig. 26. Comparison of photoionization cross section for calcium from TOPbase with the cross section from Verner and co-workers.

Excess energy: The excess energies in eV for the quiet and the active Sun are

Solar activity	QS	AS
TOPbase, Verner and co-workers	0.112	0.140
Verner and co-workers	0.386	0.470.

Excess energies based on TOPbase data for blackbody radiation fields without dilution factors are presented in Table 1.

2.1.21. Atomic scandium, Sc

Cross section: TOPbase does not provide photoionization cross sections for scandium. We use the photoionization cross section from fits prepared by Verner and co-workers. An error in a fit coefficient (the ionization potential of the ground state of scandium) in the subroutine PHFIT2 in the FORTRAN program of Verner and Yakovlev (1995) has been corrected by replacing 7.342 eV by the NIST value of 6.561 eV.

Threshold: The ionization threshold $\lambda_{th} = 1889.57$ Å is given by Sugar and Corliss (1985).

Rate coefficient: The rate coefficient is $2.59 \times 10^{-6}\,s^{-1}$ for the quiet Sun and $4.97 \times 10^{-6}\,s^{-1}$ for the active Sun. Rate coefficients based on cross sections from fit parameters of Verner and co-workers are presented for blackbody radiation fields (BBRFs) without dilution factors for four temperatures from $T = 10^3$ K to $T = 10^6$ K in Table 1.

Excess energy: The excess energy is 3.75 eV for the quiet Sun and 5.04 eV for the active Sun. Excess energies for the blackbody radiation fields are presented in Table 1.

2.1.22. Atomic titanium, Ti

Cross section: TOPbase does not provide the photoionization cross section for titanium. We use the photoionization cross section from fits prepared by Verner and co-workers.

Threshold: The ionization threshold $\lambda_{th} = 1815.79$ Å is given by Sohl et al. (1990).

Rate coefficient: The rate coefficient is $2.47 \times 10^{-6}\,s^{-1}$ for the quiet Sun and $5.68 \times 10^{-6}\,s^{-1}$ for the active Sun. Rate coefficients based on cross sections from fit parameters of Verner and co-workers are presented for blackbody radiation fields (BBRFs) without dilution factors for four temperatures from $T = 10^3$ K to $T = 10^6$ K in Table 1.

Excess energy: The excess energy is 4.64 eV for the quiet Sun and 5.64 eV for the active Sun. Excess energies for the blackbody radiation fields are presented in Table 1.

2.1.23. Atomic vanadium, V

Cross section: TOPbase does not provide the photoionization cross section for vanadium. We use the photoionization cross section from fits prepared by Verner and co-workers.

Threshold: The ionization threshold $\lambda_{th} = 1837.84$ Å is given by James et al. (1994).

Rate coefficient: The rate coefficient is $1.48 \times 10^{-6}\,s^{-1}$ for the quiet Sun and $2.09 \times 10^{-6}\,s^{-1}$ for the active Sun. Rate coefficients based on cross sections from fit parameters of Verner and co-workers are presented for blackbody radiation fields (BBRFs) without dilution factors for four temperatures ranging from $T = 10^3$ K to $T = 10^6$ K in Table 1.

Excess energy: The excess energy is 4.31 eV for the quiet Sun and 9.51 eV for the active Sun. Excess energies for the blackbody radiation fields are presented in Table 1.

Please cite this article as: Huebner, W.F., Mukherjee, J., Photoionization and photodissociation rates in solar and blackbody radiation fields. Planetary and Space Science (2015), http://dx.doi.org/10.1016/j.pss.2014.11.022

2.1.24. Atomic chromium, Cr

Cross section: TOPbase does not provide the photoionization cross section for chromium. We use the photoionization cross section from fits prepared by Verner and co-workers.

Threshold: The ionization threshold $\lambda_{th} = 1832.32$ Å is given by Sugar and Corliss (1985).

Rate coefficient: The rate coefficient is $3.78 \times 10^{-6}\ s^{-1}$ for the quiet Sun and $8.88 \times 10^{-6}\ s^{-1}$ for the active Sun. Rate coefficients based on cross sections from fit parameters of Verner and co-workers are presented for blackbody radiation fields (BBRFs) without dilution factors for four temperatures ranging from $T = 10^3$ K to $T = 10^6$ K in Table 1.

Excess energy: The excess energy is 5.02 eV for the quiet Sun and 5.95 eV for the active Sun. Excess energies for the blackbody radiation fields are presented in Table 1.

2.1.25. Atomic manganese, Mn

Cross section: TOPbase does not provide the photoionization cross section for manganese. We use the photoionization cross section from fits prepared by Verner and co-workers.

Threshold: The ionization threshold $\lambda_{th} = 1667.80$ Å is given by Sugar and Corliss (1985).

Rate coefficient: The rate coefficient is $5.76 \times 10^{-7}\ s^{-1}$ for the quiet Sun and $1.17 \times 10^{-6}\ s^{-1}$ for the active Sun. Rate coefficients for blackbody radiation fields without dilution factors are presented in Table 1 for four temperatures in the range from 1000 K to 1,000,000 K.

Excess energy: The excess energy is 13.1 eV for the quiet Sun and 22.4 eV for the active Sun. Excess energies for blackbody radiation fields are presented in Table 1.

2.1.26. Atomic iron, Fe

Cross section: In Fig. 27 we compare the photoionization cross section from NORAD with the cross section obtained from fit parameters prepared by Verner and co-workers for wavelengths from $\lambda = 820$ Å to threshold.

Threshold: The ionization threshold $\lambda_{th} = 1568.9$ Å is given by Sugar and Corliss (1985).

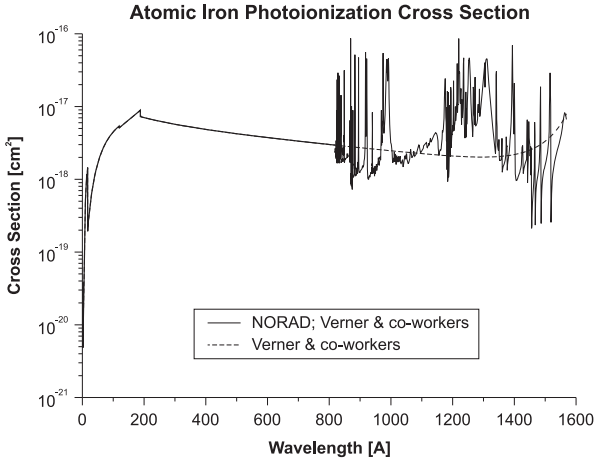

Fig. 27. Comparison of the photoionization cross section for iron from NORAD data with the cross section from fit parameters prepared by Verner and co-workers. There are very large differences between these cross sections at wavelengths $\lambda < 820$ Å. NORAD uses a hydrogenic approximation for the cross section at large photon energies (small wavelengths) as an extension to the values calculated with the R-matrix method. Thus, as already mentioned earlier in the subsection on Neutral Atoms, we have also replaced the hydrogenic approximation for the extension of the NORAD cross section with the cross section using the fit parameters of Verner and co-workers. In the case of iron this replacement is for the wavelength region $\lambda < 820$ Å.

Rate coefficient: The rate coefficients in units s^{-1} for the quiet and the active Sun are

Solar activity	QS	AS
NORAD, Verner and co-workers	8.20×10^{-6}	1.95×10^{-5}
Verner and co-workers	1.68×10^{-6}	3.56×10^{-6}.

Rate coefficients based on cross sections from NORAD data as modified with data from Verner and co-workers are presented for blackbody radiation fields (BBRFs) without dilution factors for four temperatures ranging from $T = 10^3$ K to $T = 10^6$ K in Table 1.

Excess energy: The excess energies in eV for the quiet and the active Sun are

Solar activity	QS	AS
NORAD, Verner and co-workers	2.70	3.21
Verner and co-workers	4.87	7.72

Excess energies for blackbody radiation fields at four temperatures from 10^3 to 10^6 K are presented in Table 1.

2.1.27. Atomic cobalt, Co

Cross section: TOPbase does not provide the photoionization cross section for cobalt. We use the photoionization cross section from fits prepared by Verner and co-workers.

Threshold: The ionization threshold $\lambda_{th} = 1573.2$ Å is given by Page and Gudeman (1990).

Rate coefficient: The rate coefficient is $5.32 \times 10^{-7}\ s^{-1}$ for the quiet Sun and $1.24 \times 10^{-6}\ s^{-1}$ for the active Sun. Rate coefficients based on the cross section from fit parameters of Verner and co-workers are presented for blackbody radiation fields (BBRFs) without dilution factors for four temperatures ranging from $T = 10^3$ K to $T = 10^6$ K in Table 1.

Excess energy: The excess energy is 15.4 eV for the quiet Sun and 23.2 eV for the active Sun. Excess energies for the blackbody radiation fields are presented in Table 1.

2.1.28. Atomic nickel, Ni

Cross section: TOPbase does not provide the photoionization cross section for nickel. We use the photoionization cross sections from fits prepared by Verner and co-workers.

Threshold: The ionization threshold $\lambda_{th} = 1622.8$ Å is given by Kessler et al. (2007).

Rate coefficient: The rate coefficient is $9.43 \times 10^{-7}\ s^{-1}$ for the quiet Sun and $1.87 \times 10^{-6}\ s^{-1}$ for the active Sun. Rate coefficients based on cross section data from fit parameters of Verner and co-workers are presented for blackbody radiation fields (BBRFs) without dilution factors for four temperatures ranging from $T = 10^3$ K to $T = 10^6$ K in Table 1.

Excess energy: The excess energy is 8.94 eV for the quiet Sun and 15.8 eV for the active Sun. Excess energies for the blackbody radiation fields are presented in Table 1.

2.1.29. Atomic copper, Cu

Cross section: TOPbase does not provide the photoionization cross section for copper. We use the photoionization cross section from fits prepared by Verner and co-workers.

Threshold: The ionization threshold $\lambda_{th} = 1604.7$ Å is given by Shenstone (1948), Longmire et al. (1980), and Loock et al. (1999).

Rate coefficient: The rate coefficient is $6.13 \times 10^{-7}\ s^{-1}$ for the quiet Sun and $1.48 \times 10^{-6}\ s^{-1}$ for the active Sun. Rate coefficients based on cross sections from fit parameters of Verner and co-

Please cite this article as: Huebner, W.F., Mukherjee, J., Photoionization and photodissociation rates in solar and blackbody radiation fields. Planetary and Space Science (2015), http://dx.doi.org/10.1016/j.pss.2014.11.022

workers are presented for blackbody radiation fields (BBRFs) without dilution factors for four temperatures ranging from $T = 10^3$ K to $T = 10^6$ K in Table 1.

Excess energy: The excess energy is 17.0 eV for the quiet Sun and 24.1 eV for the active Sun. Excess energies for the blackbody radiation fields are presented in Table 1.

2.1.30. Atomic zinc, Zn

Cross section: TOPbase does not provide the photoionization cross section for zinc. We use the photoionization cross sections from fit parameters prepared by Verner and co-workers.

Threshold: The ionization threshold $\lambda_{th} = 1319.8$ Å is given by Brown et al. (1975).

Rate coefficient: The rate coefficient is $5.06 \times 10^{-7}\ s^{-1}$ for the quiet Sun and $1.42 \times 10^{-6}\ s^{-1}$ for the active Sun. Rate coefficients based on cross sections from fit parameters of Verner and co-workers are presented for blackbody radiation fields (BBRFs) without dilution factors for four temperatures ranging from $T = 10^3$ K to $T = 10^6$ K in Table 1.

Excess energy: The excess energy is 15.4 eV for the quiet Sun and 20.2 eV for the active Sun. Excess energies for the blackbody radiation fields are presented in Table 1.

2.1.31. Atomic xenon, Xe

Cross section: TOPbase does not provide the photoionization cross section for xenon. We use the photoionization cross section from fit parameters prepared by Verner and co-workers.

Threshold: The ionization threshold $\lambda_{th} = 1022.15$ Å is given by Huffman et al. (1963), Knight and Wang (1985), and Brandi et al. (2001).

Rate coefficient: The rate coefficient is $1.44 \times 10^{-6}\ s^{-1}$ for the quiet Sun and $3.35 \times 10^{-6}\ s^{-1}$ for the active Sun. Rate coefficients based on cross sections from fit parameters of Verner and co-workers are presented for blackbody radiation fields (BBRFs) without dilution factors for four temperatures ranging from $T = 10^3$ K to $T = 10^6$ K in Table 1.

Excess energy: The excess energy is 4.30 eV for the quiet Sun and 5.41 eV for the active Sun. Excess energies for the blackbody radiation fields are presented in Table 1.

2.2. Monatomic ions

Just as we did for neutral atoms, we have supplemented the data for monatomic ions to complete the list of elements up to atomic number $Z = 30$. The new photoionization cross sections are taken from two related databases: (1) TOPbase and NORAD that contain results from close-coupling approximations using the R-matrix method and (2) analytic fits to partial photoionization cross sections including subshells made by Verner et al. (1993, 1996) and Verner and Yakovlev (1995). We will again refer to these references simply as Verner and co-workers. TOPbase and NORAD not only include autoionization resonances but also contain a hydrogenic approximation for extending the calculated cross sections. These extensions become unrealistic with increasing atomic number, Z, and are in direct contradiction with the high-quality close-coupling calculations. Also, both TOPbase and NORAD lack cross section data for inner shell ionizations. The analytic fits made by Verner and co-workers for the partial photoionization cross sections are based on TOPbase R-matrix methods supplemented with results from Hartree–Dirac–Slater calculations. Just as for the neutral atoms, we use TOPbase and NORAD data that include the autoionization structures, but replace the unrealistic hydrogenic cross section extensions with the appropriately fitted photoionization cross sections from Verner and co-workers. Although TOPbase claims to contain cross section data for all elements and their ions up to atomic number $Z = 30$, many of the atomic ions are missing in the database at http://cdsweb.u-strasbg.fr/topbase/xsections.html. Our discussion about autoionizing line transitions of atomic neutrals also applies to atomic ions.

We use the ionization threshold wavelengths from the Handbook of Basic Atomic Spectroscopic Data [here simply referred to as NIST, http://www.nist.gov/pml/data/handbook/index.cfm]. When rate coefficients and excess energies are insignificantly different from our earlier results, we do not discuss the details of the changes. In general, when two different sets of cross section data are compared for an ion the corresponding rate coefficients and excess energies are discussed in the appropriate subsection about that ion and are not listed separately in the tables. Rate coefficients for blackbody radiation fields (BBRFs) without dilution factors for four temperatures from $T = 10^3$ K to $T = 10^6$ K and associated average excess energies are summarized in Table 2. "QS" and "AS" mean quiet Sun and active Sun, respectively.

2.2.1. Negative hydrogen ion, H^-

We consider photodetachment of H^- leading to H + e and two-electron photo-ejection leading to H^+ + 2e.

Cross section: From $\lambda = 180$ Å to 16,640 Å the cross section for photodetachment was calculated by Broad and Reinhardt (1976). These values were supplemented with calculated data from Geltman (1962). They are the same cross sections as previously used by Huebner et al. (1992). In the wavelength region $\lambda = 180.26$–863.4 Å we have added the cross sections for two electron photo-ejection from H^- as calculated by Broad and Reinhardt (1976) and presented in their Fig. 4.

Threshold: The photodetachment threshold $\lambda_{th} = 16439$ Å is given by Lykke et al. (1991) and Rienstra-Kiracofe et al. (2002). This value is lower than the one previously used ($\lambda_{th} = 16,640$ Å, Broad and Reinhardt, 1976). The threshold for photo-ejection of two electrons is $\lambda_{th} = 847.36$ Å, as given by Broad and Reinhardt (1976).

Rate coefficient: The rate coefficient for photodetachment is $1.40 \times 10^1\ s^{-1}$ for the quiet as well as for the active Sun. This remains unchanged from the previous value. The rate coefficient for two electron photo-ejection is $1.17 \times 10^{-9}\ s^{-1}$ for the quiet Sun and $2.69 \times 10^{-9}\ s^{-1}$ for the active Sun. Rate coefficients for blackbody radiation fields (BBRFs) without dilution factors are presented in Table 2 for four temperatures ranging from $T = 10^3$ K to $T = 10^6$ K.

Excess energy: The rounded value of the excess energy for photodetachment is 0.93 eV for both the quiet Sun and the active

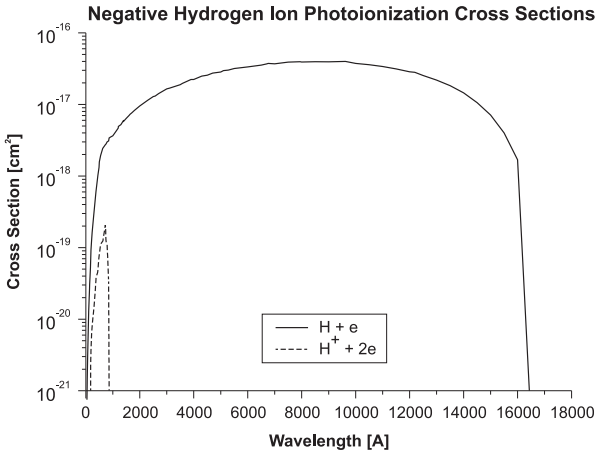

Fig. 28. Photo cross sections of H^- leading to H plus ejection of one electron (solid curve) and to H^+ plus two electrons (dashed curve).

Please cite this article as: Huebner, W.F., Mukherjee, J., Photoionization and photodissociation rates in solar and blackbody radiation fields. Planetary and Space Science (2015), http://dx.doi.org/10.1016/j.pss.2014.11.022

Sun. It is less than 0.01 eV smaller than the previous value (Huebner et al., 1992), which, when rounded, also was 0.93 eV. The rounded values of the excess energies for the two electron photo-ejection process are 9.6 eV for the quiet Sun and 11 eV for the active Sun. This excess energy is almost entirely shared by both of the photo ejected electrons. Excess energies for the blackbody radiation fields are presented in Table 2.

2.2.2. Singly ionized helium, He^+

Cross section: The photoionization cross section is hydrogenic. We use the cross section based on fit parameters produced by Verner and co-workers.

Threshold: The ionization threshold $\lambda_{th} = 227.84$ Å is given by Mohr and Kotochigova (2000).

Rate coefficient: The rate coefficient is $6.12 \times 10^{-9}\ s^{-1}$ for the quiet Sun and $3.20 \times 10^{-8}\ s^{-1}$ for the active Sun. Rate coefficients for blackbody radiation fields (BBRFs) without dilution factors are presented in Table 2 for four temperatures ranging from $T = 10^3$ K to $T = 10^6$ K.

Excess energy: The excess energy is 11.1 eV for the quiet Sun and 10.4 eV for the active Sun. Excess energies for the blackbody radiation fields are presented in Table 2.

2.2.3. Singly ionized lithium, Li^+

Cross section: The photoionization cross section from TOPbase shows no autoionizing structures. We use the cross section of Verner and co-workers, which is very closely the same as the TOPbase cross section.

Threshold: The ionization threshold $\lambda_{th} = 163.91$ Å is given by Drake and Martin (2001).

Rate coefficient: The rate coefficient is $1.82 \times 10^{-9}\ s^{-1}$ for the quiet Sun and $7.07 \times 10^{-9}\ s^{-1}$ for the active Sun. Rate coefficients for blackbody radiation fields (BBRFs) without dilution factors are presented in Table 2 for four temperatures ranging from $T = 10^3$ K to $T = 10^6$ K.

Excess energy: The excess energy is 17.8 eV for the quiet Sun and 14.7 eV for the active Sun. Excess energies for the blackbody radiation fields are presented in Table 2.

2.2.4. Singly ionized beryllium, Be^+

Cross section: The TOPbase photoionization cross section shows no autoionizing structures. We use the cross section of Verner and co-workers, which is very closely the same as the TOPbase cross section.

Threshold: The ionization threshold $\lambda_{th} = 680.81$ Å is given by Kramida and Martin (2000).

Rate coefficient: The rate coefficient is $1.51 \times 10^{-8}\ s^{-1}$ for the quiet Sun and $3.93 \times 10^{-8}\ s^{-1}$ for the active Sun. Rate coefficients for blackbody radiation fields (BBRFs) without dilution factors are presented in Table 2 for four temperatures ranging from $T = 10^3$ K to $T = 10^6$ K. Fig. 28

Excess energy: The excess energy is 20.8 eV for the quiet Sun and 25.6 eV for the active Sun. Excess energies for the blackbody radiation fields are presented in Table 2.

2.2.5. Singly ionized boron, B^+

Cross section: In Fig. 29 we show the photoionization cross section from TOPbase, as extended with data from Verner and co-workers for $\lambda < 250$ Å, and the cross section from Verner and co-workers for the entire wavelength range. From about 250 Å to threshold, the cross section from fit data of Verner and co-workers tracks the average cross section through the regions where strong autoionization resonances dominate very well.

Threshold: The ionization threshold $\lambda_{th} = 492.89$ Å is given by Ryabtsev (1998).

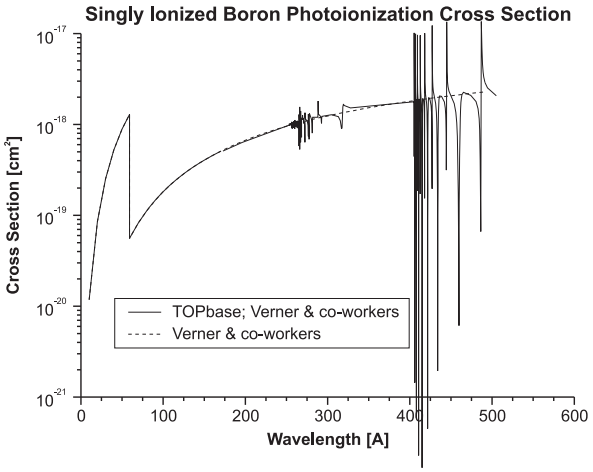

Fig. 29. The photoionization cross section of the boron ion, B^+, from TOPbase is compared with the corresponding cross section from Verner and co-workers.

Rate coefficient: The rate coefficients in s^{-1} for the quiet and the active Sun are

Solar activity	QS	AS
TOPbase, Verner and co-workers	2.17×10^{-8}	6.80×10^{-8}
Verner and co-workers	2.33×10^{-8}	7.19×10^{-8}.

Rate coefficients based on the TOPbase cross section for blackbody radiation fields without dilution factors at four temperatures ranging from $T = 10^3$ to $T = 10^6$ K are given in Table 2.

Excess energy: The excess energies in eV for the quiet and the active Sun are

Solar activity	QS	AS
TOPbase, Verner and co-workers	21.0	24.7
Verner and co-workers	19.8	23.5

The excess energies for four BBRFs at $T = 10^3$, $T = 10^4$, $T = 10^5$, and $T = 10^6$ K are given in Table 2.

2.2.6. Singly ionized carbon, C^+

Cross section: In Fig. 30 we show the photoionization cross section from TOPbase, as extended with data from Verner and

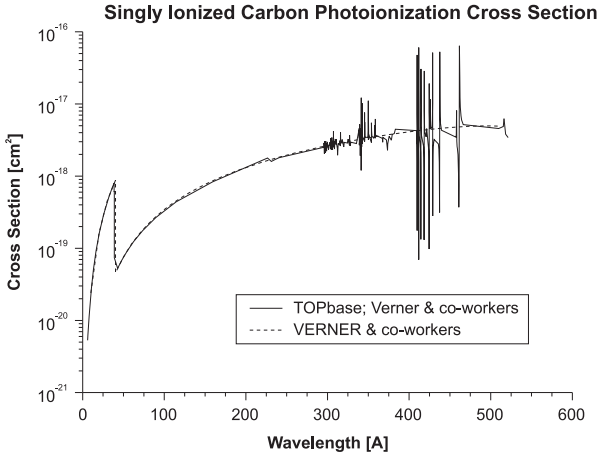

Fig. 30. The photoionization cross section of the carbon ion, C^+, from TOPbase is compared with the corresponding cross section from Verner and co-workers.

Please cite this article as: Huebner, W.F., Mukherjee, J., Photoionization and photodissociation rates in solar and blackbody radiation fields. Planetary and Space Science (2015), http://dx.doi.org/10.1016/j.pss.2014.11.022

co-workers for $\lambda < 6$ Å, and the cross section from Verner and co-workers for the entire wavelength range. From about 6 Å to threshold, the cross section from fit data of Verner and co-workers tracks the average cross section through the regions where autoionization resonances dominate very well.

Threshold: The ionization threshold $\lambda_{th} = 508.48$ Å is given by Moore (1993).

Rate coefficient: The rate coefficients in units of s^{-1} for the quiet and the active Sun are

Solar activity	QS	AS
TOPbase, Verner and co-workers	5.29×10^{-8}	1.59×10^{-7}
Verner and co-workers	5.13×10^{-8}	1.54×10^{-7}.

Rate coefficients for blackbody radiation fields without factors for radiation dilution at four temperatures ranging from $T = 10^3$ K to $T = 10^6$ K are given in Table 2.

Excess energy: The excess energies in eV for the quiet and the active Sun are

Solar activity	QS	AS
TOPbase, Verner and co-workers	17.8	20.8
Verner and co-workers	18.3	21.1

The excess energies for four BBRFs at $T = 10^3$, $T = 10^4$, $T = 10^5$, and $T = 10^6$ K are given in Table 2.

2.2.7. Singly ionized nitrogen, N^+

Cross section: In Fig. 31 we show the photoionization cross section from TOPbase, as extended with data from Verner and co-workers for $\lambda < 190$ Å, and the cross section from Verner and co-workers for the entire wavelength range. From about 190 Å to threshold, the cross section from fit data of Verner and co-workers tracks the average cross section through the regions where autoionization resonances dominate very well.

Threshold: The ionization threshold $\lambda_{th} = 418.85$ Å is given by Eriksson (1983).

Rate coefficient: The rate coefficients for the quiet and the active Sun are

Solar activity	QS	AS
TOPbase, Verner and co-workers	9.20×10^{-8}	2.83×10^{-7}
Verner and co-workers	9.18×10^{-8}	2.82×10^{-7}.

Rate coefficients for the blackbody radiation fields without factors for radiation dilution at four temperatures ranging from $T = 10^3$ K to $T = 10^6$ K are given in Table 2.

Excess energy: The excess energies in eV for the quiet and the active Sun are

Solar activity	QS	AS
TOPbase, Verner and co-workers	14.9	17.3
Verner and co-workers	14.9	17.3

The excess energies for four BBRFs at $T = 10^3$, $T = 10^4$, $T = 10^5$, and $T = 10^6$ K are given in Table 2.

2.2.8. Singly ionized oxygen, O^+

Cross section: In Fig. 32 we show the photoionization cross section from TOPbase, as extended with data from Verner and co-workers for $\lambda < 240$ Å, and the cross section from Verner and co-workers for the entire wavelength range. From 240 Å to threshold, the cross section from fit data of Verner and co-workers tracks the average cross section through the regions where strong autoionization resonances dominate very well.

Threshold: The ionization threshold $\lambda_{th} = 353.02$ Å is given by Martin et al. (1993).

Rate coefficient: The rate coefficients in s^{-1} for the quiet and the active Sun are

Solar activity	QS	AS
TOPbase, Verner and co-workers	1.27×10^{-7}	4.09×10^{-7}
Verner and co-workers	1.29×10^{-7}	4.15×10^{-7}.

Rate coefficients for the blackbody radiation fields without dilution factors at four temperatures ranging from $T = 10^3$ K to $T = 10^6$ K are given in Table 2.

Excess energy: The excess energies in units of eV for the quiet and the active Sun are

Solar activity	QS	AS
TOPbase; Verner and co-workers	12.0	14.5
Verner and co-workers	11.9	14.4

The excess energies for four BBRFs at $T = 10^3$, $T = 10^4$, $T = 10^5$, and $T = 10^6$ K are given in Table 2.

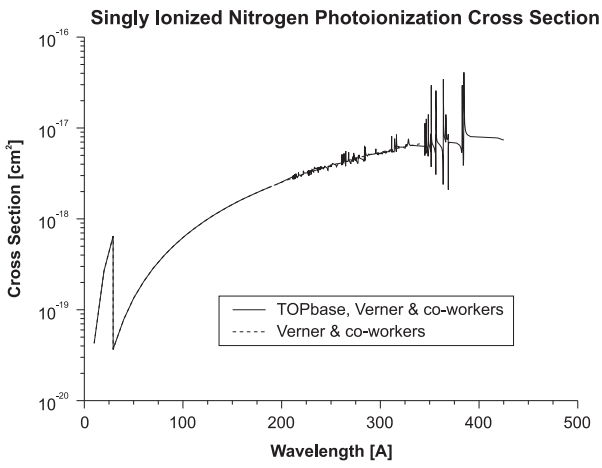

Fig. 31. The photoionization cross section of the nitrogen ion, N^+, from TOPbase is compared with the corresponding cross section from Verner and co-workers.

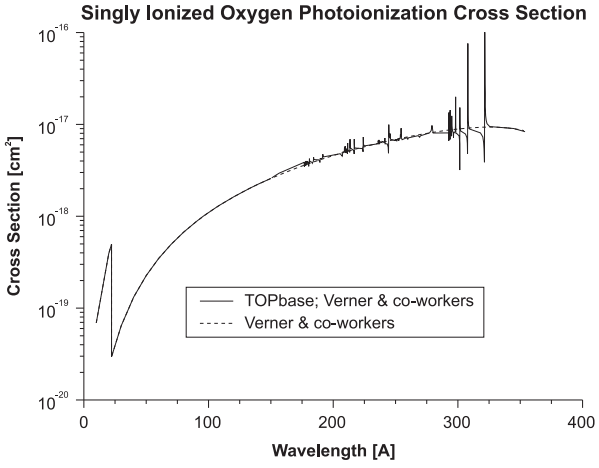

Fig. 32. The photoionization cross section of the oxygen ion, O^+, from TOPbase is compared with the corresponding cross section from Verner and co-workers.

Please cite this article as: Huebner, W.F., Mukherjee, J., Photoionization and photodissociation rates in solar and blackbody radiation fields. Planetary and Space Science (2015), http://dx.doi.org/10.1016/j.pss.2014.11.022

2.2.9. Singly ionized fluorine, F^+

Cross section: In Fig. 33 we show the photoionization cross section from TOPbase, as extended with data from Verner and co-workers for $\lambda < 180$ Å, and the cross section from Verner and co-workers for the entire wavelength range without the TOPbase cross section. From about 180 Å to threshold, the cross section from fit data of Verner and co-workers tracks the average cross section through the regions where strong autoionization resonances dominate very well.

Threshold: The ionization threshold $\lambda_{th} = 354.54$ Å is given by Palenius (1969).

Rate coefficient: The rate coefficients in s^{-1} for the quiet and the active Sun are

Solar activity	QS	AS
TOPbase, Verner and co-workers	1.48×10^{-7}	4.91×10^{-7}
Verner and co-workers	1.42×10^{-7}	4.72×10^{-7}

Rate coefficients for the blackbody radiation fields without dilution factors at four temperatures ranging from $T = 10^3$ K to $T = 10^6$ K are given in Table 2.

Excess energy: The excess energies in eV for the quiet and the active Sun are

Solar activity	QS	AS
TOPbase, Verner and co-workers	13.4	16.1
Verner and co-workers	13.4	16.6

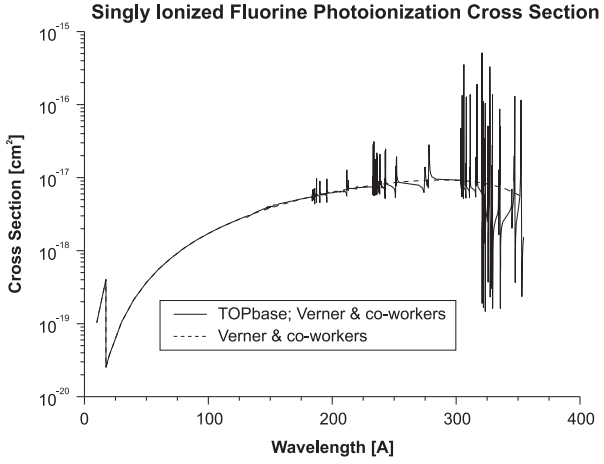

Fig. 33. The photoionization cross section of the fluorine ion, F^+, from TOPbase is compared with the corresponding cross section from Verner and co-workers.

The excess energies for four BBRFs at $T = 10^3$, $T = 10^4$, $T = 10^5$, and $T = 10^6$ K are given in Table 2.

2.2.10. Singly ionized neon, Ne^+

Cross section: In Fig. 34 we show the photoionization cross section from TOPbase, as extended with data from Verner and co-workers for $\lambda < 150$ Å, and the cross section from Verner and co-workers for the entire wavelength range. From about 150 Å to threshold, the cross section from fit data of Verner and co-workers tracks the average cross section through the regions where strong autoionization resonances dominate very well.

Threshold: The ionization threshold $\lambda_{th} = 302.67$ Å is given by Persson (1971).

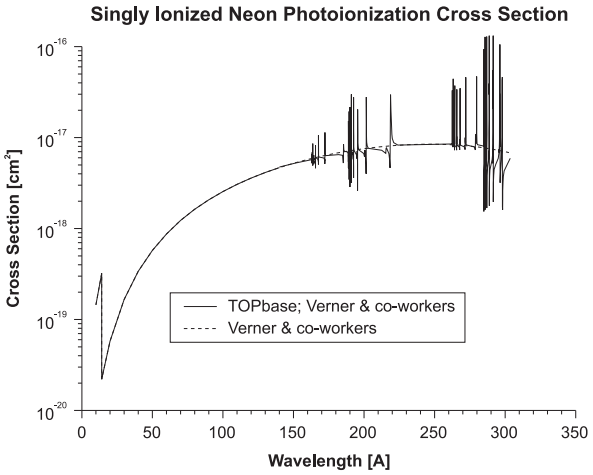

Fig. 34. The photoionization cross section of the neon ion, Ne^+, from TOPbase is compared with the corresponding cross section from Verner and co-workers.

Rate coefficient: The rate coefficients for the quiet and the active Sun are

Solar activity	QS	AS
TOPbase, Verner and co-workers	9.74×10^{-8}	3.60×10^{-7}
Verner and co-workers	8.85×10^{-8}	3.35×10^{-7}

Rate coefficients for the blackbody radiation fields without dilution factors at four temperatures ranging from $T = 10^3$ K to $T = 10^6$ K are given in Table 2.

Excess energy: The excess energies in eV for the quiet and the active Sun are

Solar activity	QS	AS
TOPbase, Verner and co-workers	14.6	17.6
Verner and co-workers	16.2	19.1

The excess energies for four BBRFs at $T = 10^3$, $T = 10^4$, $T = 10^5$, and $T = 10^6$ K are given in Table 2.

2.2.11. Singly ionized sodium, Na^+

Cross section: In Fig. 35 we show the photoionization cross section from TOPbase, as extended with data from Verner and co-workers for $\lambda < 150$ Å, and the cross section from Verner and co-workers for the entire wavelength range. From about 150 Å to

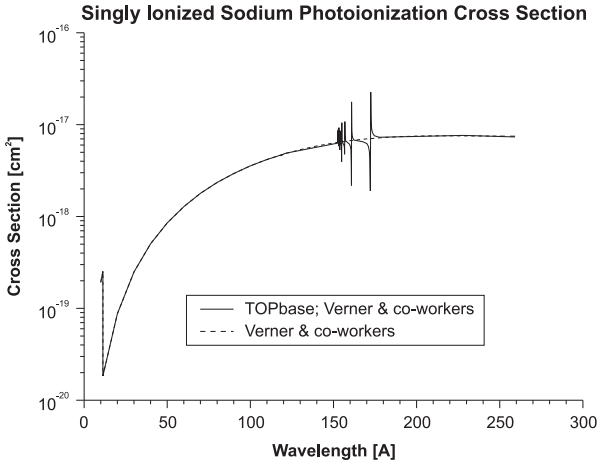

Fig. 35. The photoionization cross section of the sodium ion, Na^+, from TOPbase is compared with the corresponding cross section from Verner and co-workers.

Please cite this article as: Huebner, W.F., Mukherjee, J., Photoionization and photodissociation rates in solar and blackbody radiation fields. Planetary and Space Science (2015), http://dx.doi.org/10.1016/j.pss.2014.11.022

threshold, the cross section from fit data of Verner and co-workers tracks the average cross section through the region where autoionization resonances dominate very well.

Threshold: The ionization threshold $\lambda_{th} = 262.20$ Å is given by Martin and Zalubas (1981).

Rate coefficient: The rate coefficients in s^{-1} for the quiet and the active Sun are

Solar activity	QS	AS
TOPbase; Verner and co-workers	6.33×10^{-8}	2.76×10^{-7}
Verner and co-workers	6.33×10^{-8}	2.75×10^{-7}.

Rate coefficients for the blackbody radiation fields without the radiation dilution factors at four temperatures ranging from $T = 10^3$ K to $T = 10^6$ K are given in Table 2.

Excess energy: The excess energies in eV for the quiet and the active Sun are

Solar activity	QS	AS
TOPbase; Verner and co-workers	16.7	17.6
Verner and co-workers	16.7	17.6

The excess energies for four BBRFs at $T = 10^3$, $T = 10^4$, $T = 10^5$, and $T = 10^6$ K are given in Table 2.

2.2.12. Singly ionized magnesium, Mg^+

Cross section: In Fig. 36 we show the photoionization cross section from TOPbase, as extended with data from Verner and co-workers, and the cross section from Verner and co-workers for the entire wavelength range. From about 500 Å to threshold, the cross section from fit data of Verner and co-workers is increasingly larger than the cross sections from TOPbase, which shows no autoionization resonances. TOPbase photoionization cross section data incorrectly extend to energies below (wavelengths above) the ionization threshold.

Threshold: The ionization threshold $\lambda_{th} = 824.62$ Å is given by Kaufman and Martin (1991a).

Rate coefficient: The rate coefficients in s^{-1} for the quiet and the active Sun are

Solar activity	QS	AS
TOPbase, Verner and co-workers	2.34×10^{-8}	9.92×10^{-8}
Verner and co-workers	2.31×10^{-8}	9.86×10^{-8}

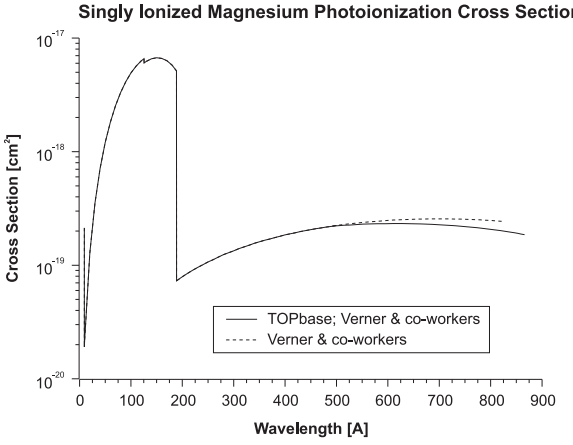

Fig. 36. The photoionization cross section of the magnesium ion, Mg^+, from TOPbase is compared with the corresponding cross section from Verner and co-workers. The TOPbase cross section extends to longer wavelengths than the threshold at $\lambda_{th} = 824.62$ Å.

Rate coefficients for the blackbody radiation fields without dilution factors at four temperatures ranging from $T = 10^3$ K to $T = 10^6$ K are given in Table 2.

Excess energy: The excess energies in eV for the quiet and the active Sun are

Solar activity	QS	AS
TOPbase, Verner and co-workers	56.1	56.7
Verner and co-workers	56.8	57.1

The excess energies for four BBRFs at $T = 10^3$, $T = 10^4$, $T = 10^5$, and $T = 10^6$ K are given in Table 2.

2.2.13. Singly ionized aluminum, Al^+

Cross section: In Fig. 37 we show the photoionization cross section from TOPbase, as extended with data from Verner and co-workers for $\lambda < 310$ Å, and the cross section from Verner and co-workers for the entire wavelength range. From about 310 Å to threshold, the cross section from fit data of Verner and co-workers tracks the average cross section through the regions where strong autoionization resonances dominate very well.

Threshold: The ionization threshold $\lambda_{th} = 658.49$ Å is given by Kaufman and Martin (1991b).

Rate coefficient: The rate coefficients in s^{-1} for the quiet and the active Sun are

Solar activity	QS	AS
TOPbase, Verner and co-workers	9.92×10^{-9}	2.97×10^{-8}
Verner and co-workers	9.89×10^{-9}	2.97×10^{-8}

Rate coefficients for the blackbody radiation fields without dilution factors at four temperatures ranging from $T = 10^3$ K to $T = 10^6$ K are given in Table 2.

Excess energy: The excess energies in eV for the quiet and the active Sun are

Solar activity	QS	AS
TOPbase; Verner and co-workers	54.8	58.6
Verner and co-workers	55.0	58.6

The excess energies for four BBRFs at $T = 10^3$, $T = 10^4$, $T = 10^5$, and $T = 10^6$ K are given in Table 2.

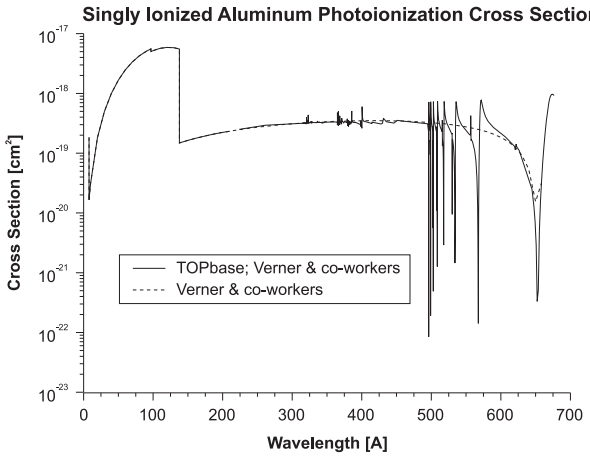

Fig. 37. The photoionization cross section of the aluminum ion, Al^+, from TOPbase is compared with the corresponding cross section from Verner and co-workers. The TOPbase data very clearly defines the Cooper minimum at about 652.3 Å.

Please cite this article as: Huebner, W.F., Mukherjee, J., Photoionization and photodissociation rates in solar and blackbody radiation fields. Planetary and Space Science (2015), http://dx.doi.org/10.1016/j.pss.2014.11.022

2.2.14. Singly ionized silicon, Si^+

Cross section: In Fig. 38 we show the photoionization cross section from TOPbase, as extended with data from Verner and co-workers for $\lambda < 320$ Å, and the cross section from Verner and co-workers for the entire wavelength range. From about 320 Å to threshold, the cross section from fit data of Verner and co-workers tracks the average cross section through a large region where autoionization resonances dominate very well.

Threshold: The ionization threshold $\lambda_{th} = 758.51$ Å is given by Martin and Zalubas (1983).

Rate coefficient: The rate coefficients in s^{-1} for the quiet and the active Sun are

Solar activity	QS	AS
TOPbase; Verner and co-workers	1.70×10^{-8}	5.03×10^{-8}
Verner and co-workers	1.69×10^{-8}	5.00×10^{-8}

Rate coefficients for blackbody radiation fields without dilution factors at four temperatures ranging from $T = 10^3$ K to $T = 10^6$ K are given in Table 2.

Excess energy: The excess energies in eV for the quiet and the active Sun are

Solar activity	QS	AS
TOPbase; Verner and co-workers	41.2	47.0
Verner and co-workers	41.5	47.2

The excess energies for four BBRFs at $T = 10^3$, $T = 10^4$, $T = 10^5$, and $T = 10^6$ K are given in Table 2.

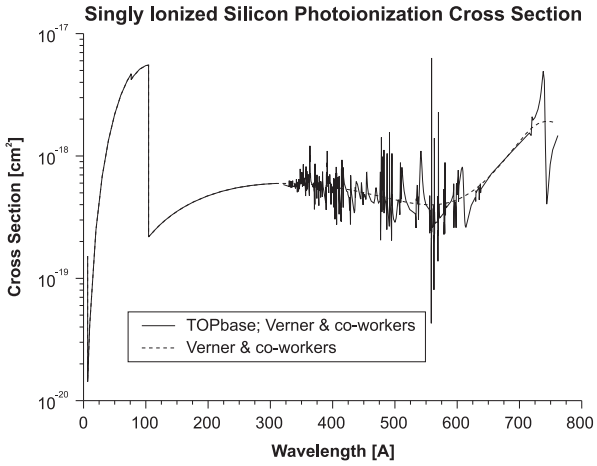

Fig. 38. The photoionization cross section of the silicon ion, Si^+, from TOPbase is compared with the corresponding cross section from Verner and co-workers.

2.2.15. Singly ionized phosphorus, P^+

Cross section: TOPbase does not provide the photoionization cross section for singly ionized phosphorus. We use the photoionization cross sections from fits prepared by Verner and co-workers.

Threshold: The ionization threshold $\lambda_{th} = 627.15$ Å is given by Martin et al. (1985).

Rate coefficient: The rate coefficient is $2.30 \times 10^{-8}\ s^{-1}$ for the quiet Sun and $7.16 \times 10^{-8}\ s^{-1}$ for the active Sun. Rate coefficients for blackbody radiation fields without dilution factors at four temperatures ranging from $T = 10^3$ K to $T = 10^6$ K are given in Table 2.

Excess energy: The excess energy is 33.2 eV for the quiet Sun and 39.9 eV for the active Sun. Excess energies for blackbody radiation fields are presented in Table 2.

2.2.16. Singly ionized sulfur, S^+

Cross section: In Fig. 39 we show the photoionization cross section from TOPbase, as extended with data from Verner and co-workers for $\lambda < 300$ Å, and the cross section from Verner and co-workers for the entire wavelength range. From about 300 Å to threshold, the cross section from fit data of Verner and co-workers tracks the average TOPbase cross section through the regions where strong autoionization resonances dominate very well.

Threshold: The ionization threshold $\lambda_{th} = 531.26$ Å is given by Martin et al. (1990).

Rate coefficient: The rate coefficients in s^{-1} for the quiet and the active Sun are

Solar activity	QS	AS
TOPbase, Verner and co-workers	2.60×10^{-8}	7.98×10^{-8}
Verner and co-workers	2.54×10^{-8}	7.86×10^{-8}

Rate coefficients based on the TOPbase cross section with the extension from Verner and co-workers for blackbody radiation fields without dilution factors are given in Table 2 at four temperatures ranging from $T = 10^3$ K to $T = 10^6$ K.

Excess energy: The excess energies in eV for the quiet and the active Sun are

Solar activity	QS	AS
TOPbase, Verner and co-workers	22.8	30.9
Verner and co-workers	23.2	30.9

The excess energies for four BBRFs at $T = 10^3$, $T = 10^4$, $T = 10^5$, and $T = 10^6$ K are given in Table 2.

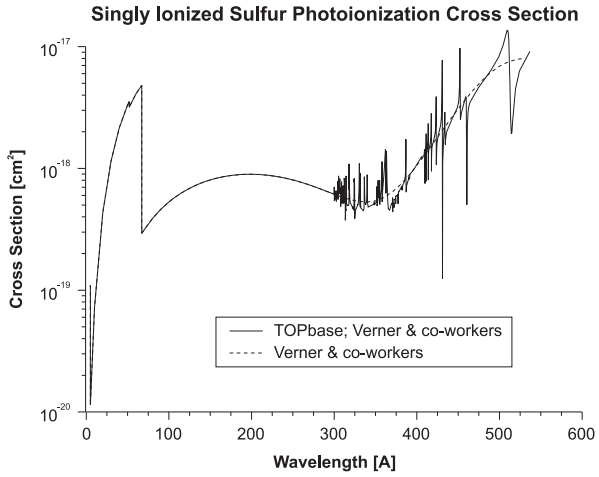

Fig. 39. The photoionization cross section of the sulfur ion, S^+, from TOPbase is compared with the corresponding cross section from Verner and co-workers.

2.2.17. Singly ionized chlorine, Cl^+

Cross section: TOPbase does not provide the photoionization cross section for singly ionized chlorine. We use the photoionization cross section from fits prepared by Verner and co-workers.

Threshold: The ionization threshold $\lambda_{th} = 520.64$ Å is given by Radziemski and Kaufman (1974).

Rate coefficient: The rate coefficient is $2.90 \times 10^{-8}\ s^{-1}$ for the quiet Sun and $9.63 \times 10^{-8}\ s^{-1}$ for the active Sun. Rate coefficients for blackbody radiation fields without dilution factors at four temperatures ranging from $T = 10^3$ K to $T = 10^6$ K are given in Table 2.

Excess energy: The excess energy is 25.3 eV for the quiet Sun and 31.7 eV for the active Sun. Excess energies for the blackbody radiation fields without dilution factors are presented in Table 2.

Please cite this article as: Huebner, W.F., Mukherjee, J., Photoionization and photodissociation rates in solar and blackbody radiation fields. Planetary and Space Science (2015), http://dx.doi.org/10.1016/j.pss.2014.11.022

2.2.18. Singly ionized argon ion, Ar^+

Cross section: In Fig. 40 we show the photoionization cross section from TOPbase, as extended with data from Verner and co-workers for $\lambda < 335$ Å, and the cross section from Verner and co-workers for the entire wavelength range. From about 335 Å to threshold, the cross section from fit data of Verner and co-workers tracks the average cross section through the regions where autoionization resonances dominate very well.

Threshold: The ionization threshold $\lambda_{th} = 448.74$ Å is given by Minnhagen (1960).

Rate coefficient: The rate coefficients in s^{-1} for the quiet and the active Sun are

Solar activity	QS	AS
TOPbase; Verner and co-workers	1.24×10^{-7}	3.55×10^{-7}
Verner and co-workers	1.25×10^{-7}	3.58×10^{-7}

Rate coefficients based on TOPbase cross sections for blackbody radiation fields without dilution factors at four temperatures ranging from $T = 10^3$ K to $T = 10^6$ K are given in Table 2.

Excess energy: The excess energies in eV for the quiet and the active Sun are

Solar activity	QS	AS
TOPbase, Verner and co-workers	12.5	14.5
Verner and co-workers	12.4	14.4

The excess energies for four BBRFs at $T = 10^3$, $T = 10^4$, $T = 10^5$, and $T = 10^6$ K are given in Table 2.

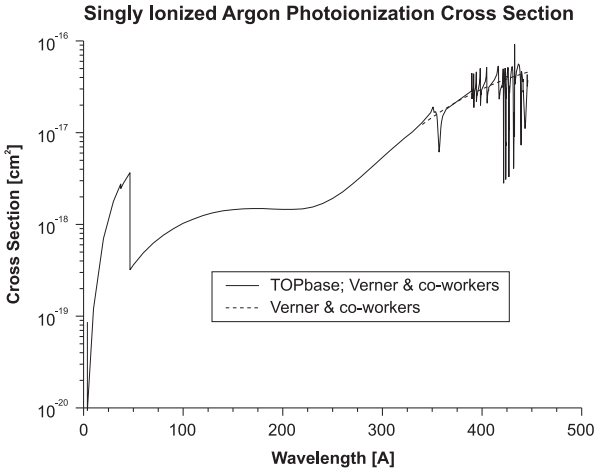

Fig. 40. The photoionization cross section of the argon ion, Ar^+, from TOPbase is compared with the corresponding cross section from Verner and co-workers.

2.2.19. Singly ionized potassium, K^+

Cross section: TOPbase does not provide the photoionization cross section for singly ionized potassium. We use the photoionization cross section from fits prepared by Verner and co-workers.

Threshold: The ionization threshold $\lambda_{th} = 392.00$ Å is given by Kelly (1987).

Rate coefficient: The rate coefficient is $3.02 \times 10^{-8}\ s^{-1}$ for the quiet Sun and $1.04 \times 10^{-7}\ s^{-1}$ for the active Sun. Rate coefficients for blackbody radiation fields without dilution factors at four temperatures ranging from $T = 10^3$ K to $T = 10^6$ K are given in Table 2.

Excess energy: The excess energy is 19.2 eV for the quiet Sun and 23.1 eV for the active Sun. Excess energies for blackbody radiation fields are presented in Table 2.

2.2.20. Singly ionized calcium, Ca^+

Cross section: TOPbase does not provide the photoionization cross section for singly ionized calcium. We use the photoionization cross section from fits prepared by Verner and co-workers.

Threshold: The ionization threshold $\lambda_{th} = 1044.37$ Å is given by Sugar and Corliss (1985).

Rate coefficient: The rate coefficient is $4.23 \times 10^{-8}\ s^{-1}$ for the quiet Sun and $1.29 \times 10^{-7}\ s^{-1}$ for the active Sun. Rate coefficients for blackbody radiation fields without dilution factors at four temperatures ranging from $T = 10^3$ K to $T = 10^6$ K are given in Table 2.

Excess energy: The excess energy is 27.8 eV for the quiet Sun and 34.5 eV for the active Sun. Excess energies for the blackbody radiation fields are presented in Table 2.

2.2.21. Singly ionized scandium, Sc^+

Cross section: TOPbase does not provide the photoionization cross section for singly ionized scandium. We use the photoionization cross section from fits prepared by Verner and co-workers.

Threshold: The ionization threshold $\lambda_{th} = 968.65$ Å is given by Sugar and Corliss (1985).

Rate coefficient: The rate coefficient is $9.50 \times 10^{-8}\ s^{-1}$ for the quiet Sun and $2.65 \times 10^{-7}\ s^{-1}$ for the active Sun. Rate coefficients for blackbody radiation fields without dilution factors at four temperatures ranging from $T = 10^3$ K to $T = 10^6$ K are given in Table 2.

Excess energy: The excess energy is 20.8 eV for the quiet Sun and 26.0 eV for the active Sun. Excess energies for blackbody radiation fields are presented in Table 2.

2.2.22. Singly ionized titanium, Ti^+

Cross section: TOPbase does not provide the photoionization cross section for singly ionized titanium. We use the photoionization cross section from fits prepared by Verner and co-workers.

Threshold: The ionization threshold $\lambda_{th} = 913.29$ Å is given by Sugar and Corliss (1985).

Rate coefficient: The rate coefficient is $1.18 \times 10^{-7}\ s^{-1}$ for the quiet Sun and $3.41 \times 10^{-7}\ s^{-1}$ for the active Sun. Rate coefficients for blackbody radiation fields without dilution factors at four temperatures ranging from $T = 10^3$ K to $T = 10^6$ K are given in Table 2.

Excess energy: The excess energy is 26.0 eV for the quiet Sun and 31.2 eV for the active Sun. Excess energies for blackbody radiation fields are presented in Table 2.

2.2.23. Singly ionized vanadium, V^+

Cross section: TOPbase does not provide the photoionization cross section for singly ionized vanadium. We use the photoionization cross section from fits prepared by Verner and co-workers.

Threshold: The ionization threshold $\lambda_{th} = 848.18$ Å is given by Iglesias et al. (1988).

Rate coefficient: The rate coefficient is $2.33 \times 10^{-7}\ s^{-1}$ for the quiet Sun and $6.48 \times 10^{-7}\ s^{-1}$ for the active Sun. Rate coefficients for blackbody radiation fields without dilution factors at four temperatures ranging from $T = 10^3$ K to $T = 10^6$ K are given in Table 2.

Excess energy: The excess energy is 19.8 eV for the quiet Sun and 24.5 eV for the active Sun. Excess energies for blackbody radiation fields are presented in Table 2.

2.2.24. Singly ionized chromium, Cr^+

Cross section: TOPbase does not provide the photoionization cross section for singly ionized chromium. We use the photoionization cross section from fits prepared by Verner and co-workers.

Threshold: The ionization threshold $\lambda_{th} = 752.07$ Å is given by Sugar and Corliss (1985).

Rate coefficient: The rate coefficient is $2.15 \times 10^{-7}\ s^{-1}$ for the quiet Sun and $6.30 \times 10^{-7}\ s^{-1}$ for the active Sun. Rate coefficients for

Please cite this article as: Huebner, W.F., Mukherjee, J., Photoionization and photodissociation rates in solar and blackbody radiation fields. Planetary and Space Science (2015), http://dx.doi.org/10.1016/j.pss.2014.11.022

blackbody radiation fields without dilution factors at four temperatures ranging from $T = 10^3$ K to $T = 10^6$ K are given in Table 2.

Excess energy: The excess energy is 24.1 eV for the quiet Sun and 29.0 eV for the active Sun. Excess energies for blackbody radiation fields are presented in Table 2.

2.2.25. Singly ionized manganese, Mn^+

Cross section: TOPbase does not provide the photoionization cross section for singly ionized manganese. We use the photoionization cross section from fits prepared by Verner and co-workers.

Threshold: The ionization threshold $\lambda_{th} = 792.74$ Å is given by Sugar and Corliss (1985).

Rate coefficient: The rate coefficient is 1.79×10^{-7} s^{-1} for the quiet Sun and 5.68×10^{-7} s^{-1} for the active Sun. Rate coefficients for blackbody radiation fields without dilution factors at four temperatures ranging from $T = 10^3$ K to $T = 10^6$ K are given in Table 2.

Excess energy: The excess energy is 30.2 eV for the quiet Sun and 34.2 eV for the active Sun. Excess energies for blackbody radiation fields are presented in Table 2.

2.2.26. Singly ionized iron, Fe^+

Cross section: In Fig. 41 we show the photoionization cross section from NORAD after removing the hydrogenic extension and replacing it with data from Verner and co-workers for $\lambda < 370$ Å. For comparison we also show the cross section from Verner and co-workers for the entire wavelength range. From about 370 Å to threshold, the cross section from fit data of Verner and co-workers tracks the average cross section through an extensive wavelength regions where autoionization resonances dominate very well.

Threshold: The ionization threshold $\lambda_{th} = 765.91$ Å is given by Sugar and Corliss (1985).

Rate coefficient: The rate coefficients in s^{-1} for the quiet and the active Sun are

Solar activity	QS	AS
NORAD, Verner and co-workers	2.55×10^{-7}	7.79×10^{-7}
Verner and co-workers	2.26×10^{-7}	7.23×10^{-7}

Rate coefficients based on NORAD data with the extension from Verner and co-workers are given in Table 2 for blackbody radiation fields without dilution factors at four temperatures ranging from $T = 10^3$ K to $T = 10^6$ K.

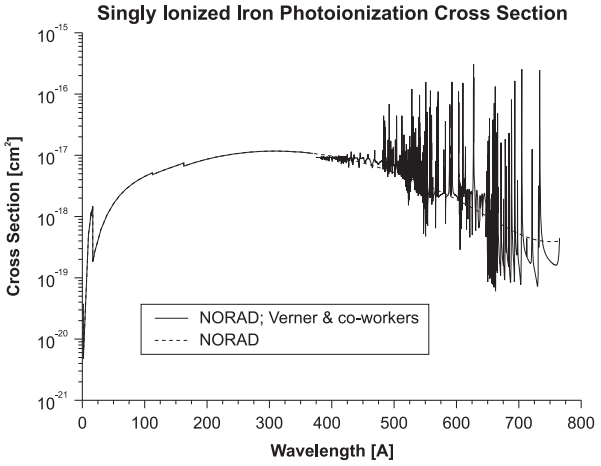

Fig. 41. The photoionization cross section of the iron ion, Fe^+, from NORAD for $\lambda > 374.5$ Å is compared with the cross section from Verner and co-workers (shown for the entire wavelength range).

Excess energy: The excess energies in eV for the quiet and the active Sun are

Solar activity	QS	AS
NORAD, Verner and co-workers	27.2	31.6
Verner and co-workers	30.3	33.8

The excess energies for four BBRFs at $T = 10^3$, $T = 10^4$, $T = 10^5$, and $T = 10^6$ K are given in Table 2.

2.2.27. Singly ionized cobalt, Co^+

Cross section: TOPbase does not provide the photoionization cross section for singly ionized cobalt. We use the photoionization cross section from fits prepared by Verner and co-workers.

Threshold: The ionization threshold $\lambda_{th} = 725.72$ Å is given by Sugar and Corliss (1985).

Rate coefficient: The rate coefficient is 2.52×10^{-7} s^{-1} for the quiet Sun and 7.72×10^{-7} s^{-1} for the active Sun. Rate coefficients for blackbody radiation fields without dilution factors at four temperatures ranging from $T = 10^3$ K to $T = 10^6$ K are given in Table 2.

Excess energy: The excess energy is 26.6 eV for the quiet Sun and 31.2 eV for the active Sun. Excess energies for blackbody radiation fields are presented in Table 2.

2.2.28. Singly ionized nickel, Ni^+

Cross section: TOPbase does not provide the photoionization cross section for singly ionized nickel. We use the photoionization cross section from fits prepared by Verner and co-workers.

Threshold: The ionization threshold $\lambda_{th} = 682.40$ Å is given by Shenstone (1970).

Rate coefficient: The rate coefficient is 2.52×10^{-7} s^{-1} for the quiet Sun and 7.88×10^{-7} s^{-1} for the active Sun. Rate coefficients for blackbody radiation fields without dilution factors at four temperatures ranging from $T = 10^3$ K to $T = 10^6$ K are given in Table 2.

Excess energy: The excess energy is 26.7 eV for the quiet Sun and 31.3 eV for the active Sun. Excess energies for the blackbody radiation fields are presented in Table 2.

2.2.29. Singly ionized copper, Cu^+

Cross section: TOPbase does not provide the photoionization cross section for singly ionized copper. We use the photoionization cross section from fits prepared by Verner and co-workers.

Threshold: The ionization threshold $\lambda_{th} = 610.99$ Å is given by Sugar and Musgrove (1990).

Rate coefficient: The rate coefficient is 2.38×10^{-7} s^{-1} for the quiet Sun and 7.67×10^{-7} s^{-1} for the active Sun. Rate coefficients for blackbody radiation fields without dilution factors at four temperatures ranging from $T = 10^3$ K to $T = 10^6$ K are given in Table 2.

Excess energy: The excess energy is 26.5 eV for the quiet Sun and 30.8 eV for the active Sun. Excess energies for blackbody radiation fields are presented in Table 2.

2.2.30. Singly ionized zinc, Zn^+

Cross section: TOPbase does not provide the photoionization cross section for singly ionized zinc. We use the photoionization cross section from fits prepared by Verner and co-workers.

Threshold: The ionization threshold $\lambda_{th} = 690.17$ Å is given by Sugar and Musgrove (1995).

Rate coefficient: The rate coefficient is 1.67×10^{-7} s^{-1} for the quiet Sun and 5.92×10^{-7} s^{-1} for the active Sun. Rate coefficients for blackbody radiation fields without dilution factors at four temperatures ranging from $T = 10^3$ K to $T = 10^6$ K are given in Table 2.

Please cite this article as: Huebner, W.F., Mukherjee, J., Photoionization and photodissociation rates in solar and blackbody radiation fields. Planetary and Space Science (2015), http://dx.doi.org/10.1016/j.pss.2014.11.022

Excess energy: The excess energy is 34.8 eV for the quiet Sun and 38.2 eV for the active Sun. Excess energies for blackbody radiation fields are presented in Table 2.

2.3. Diatomic molecules

No new diatomic species or revised cross sections have been added. Table 3 summarizes the results from previous

Table 1
Photoionization rate coefficients (s^{-1}) (first entry) and average excess energies (eV) (second entry) of all photo products for monatomic neutrals. BB refers to blackbody radiation at the specified temperature without the factor for radiation dilution with distance from the source. Numbers in parentheses after numerical entries are powers of 10.

Mother species	*Photo products*	*Quiet Sun*	*Active Sun*	*BB*			
				10^3 K	10^4 K	10^5 K	10^6 K
H	$H^+ + e$	7.26(−8)	1.72(−7)	5.69(−62)	1.35(+1)	1.74(+8)	8.60(+9)
		3.54(0)	3.97(0)	1.56(−1)	8.56(−1)	6.35(0)	2.23(+1)
He	$He^+ + e$	5.64(−8)	1.68(−7)		1.83(−4)	2.37(+8)	5.09(+10)
		1.73(+1)	2.00(+1)		9.16(−1)	8.90(0)	4.39(+1)
Li	$Li^+ + e$	1.97(−4)	2.07(−4)	2.72(−22)	1.04(+4)	9.65(+7)	7.86(+10)
		3.51(−1)	3.89(−1)	9.31(−2)	1.11(0)	1.45(+1)	1.16(+2)
Be	$Be^+ + e$	8.91(−7)	2.23(−6)	3.64(−41)	3.40(+2)	1.64(+8)	8.80(+10)
		1.67(0)	1.80(0)	2.53(−2)	9.95(−1)	1.26(+1)	1.58(+2)
B	$B^+ + e$	6.76(−6)	1.51(−5)	6.53(−35)	7.84(+3)	6.26(+8)	8.87(+10)
		1.66(0)	1.86(0)	3.01(−2)	8.01(−1)	9.10(0)	1.66(+2)
C(^{3}P)	$C^+ + e$	5.63(−7)	1.26(−6)	4.22(−50)	4.58(+2)	9.78(+8)	1.05(+11)
		5.55(0)	6.99(0)	8.95(−2)	9.51(−1)	9.77(0)	1.19(+2)
C(^{1}D)	$C^+ + e$	4.80(−6)	1.18(−5)	4.80(−44)	1.91(+3)	1.26(+9)	1.17(+11)
		1.14(0)	1.21(0)	8.89(−2)	1.37(0)	8.54(0)	1.16(+2)
C(^{1}S)	$C^+ + e$	5.36(−6)	1.22(−5)	6.86(−37)	4.90(+3)	1.24(+9)	1.10(+11)
		2.38(0)	2.52(0)	9.29(−2)	1.23(0)	9.84(0)	1.19(+2)
N	$N^+ + e$	2.31(−7)	5.90(−7)	1.13(−65)	1.34(+1)	1.04(+9)	1.44(+11)
		1.55(+1)	1.90(+1)	2.04(−1)	1.03(0)	1.11(+1)	8.22(+1)
O(^{3}P)	$O^+ + e$	2.44(−7)	6.59(−7)	2.93(−62)	1.06(1)	9.78(+8)	1.91(+11)
		2.01(+1)	2.41(+1)	1.71(−1)	1.26(0)	1.45(+1)	7.73(+1)
O(^{1}D)	$O^+ + e$	2.38(−7)	6.25(−7)	7.87(−69)	5.50(0)	1.15(+9)	1.96(+11)
		1.90(+1)	2.33(+1)	2.64(−1)	1.58(0)	1.16(+1)	7.32(+1)
O(^{1}S)	$O^+ + e$	2.47(−7)	6.45(−7)	1.09(−65)	1.08(1)	1.05(+9)	1.84(+11)
		1.79(+1)	2.17(+1)	2.47(−1)	1.03(0)	1.24(+1)	7.56(+1)
F	$F^+ + e$	2.10(−7)	6.10(−7)	9.24(−79)	2.95(−1)	8.14(+8)	2.39(+11)
		2.29(+1)	2.72(+1)	2.25(−2)	1.23(0)	1.39(+1)	7.93(+1)
Ne	$Ne^+ + e$	1.84(−7)	5.87(−7)		4.12(−3)	5.88(+8)	2.96(+11)
		2.43(+1)	2.78(+1)		1.03(0)	1.41(+1)	8.61(+1)
Na	$Na^+ + e$	7.26(−6)	7.91(−6)	1.89(−22)	2.17(+2)	1.53(+8)	3.38(+11)
		9.72(−1)	2.98(0)	7.22(−2)	1.51(0)	4.51(+1)	1.20(+2)
Mg	$Mg^+ + e$	6.49(−7)	1.17(−6)	5.35(−33)	9.96(+2)	6.13(+7)	3.50(+11)
		4.09(0)	9.51(0)	7.42(−2)	5.10(−1)	3.48(+1)	1.39(+2)
Al	$Al^+ + e$	1.20(−3)	1.30(−3)	3.73(−23)	1.67(+5)	5.44(+8)	3.47(+11)
		2.53(−1)	2.81(−1)	3.13(−2)	6.08(−1)	4.26(0)	1.62(+2)
Si	$Si^+ + e$	2.29(−5)	4.81(−5)	1.06(−33)	3.35(+4)	1.05(+9)	3.44(+11)
		1.36(0)	1.57(0)	4.51(−2)	6.97(−1)	3.93(0)	1.75(+2)
P	$P^+ + e$	6.47(−7)	1.37(−6)	6.75(−46)	2.03(+3)	6.76(+8)	3.07(+11)
		3.61(0)	4.77(0)	8.73(−2)	7.32(−1)	4.71(0)	1.98(+2)
S(^{3}P)	$S^+ + e$	1.37(−6)	3.00(−6)	8.84(−47)	1.56(+3)	2.42(+9)	3.44(+11)
		4.39(0)	4.93(0)	3.21(−1)	1.47(0)	7.24(0)	1.81(+2)
S(^{1}D)	$S^+ + e$	1.49(−6)	3.33(−6)	7.38(−49)	1.35(+3)	2.77(+9)	4.02(+11)
		5.22(0)	6.36(0)	8.51(−2)	1.16(0)	8.55(0)	1.63(+2)
S(^{1}S)	$S^+ + e$	1.83(−6)	4.01(−6)	5.19(−43)	4.20(+3)	2.73(+9)	3.54(+11)
		3.72(0)	4.29(0)	2.98(−5)	4.66(−1)	7.88(0)	1.76(+2)
Cl	$Cl^+ + e$	1.41(−6)	3.28(−6)	1.53(−57)	5.89(+2)	2.42(+9)	3.09(+11)
		2.23(0)	2.74(0)	8.47(−2)	7.54(−1)	3.65(0)	1.90(+2)
Ar	$Ar^+ + e$	3.42(−7)	7.74(−7)	1.70(−70)	1.20(+1)	2.34(+9)	3.38(+11)
		9.40(0)	1.18(+1)	1.72(−1)	8.58(−1)	7.99(0)	1.65(+2)
K	$K^+ + e$	2.70(−5)	2.79(−5)	2.66(−19)	5.85(+2)	4.12(+8)	2.24(+11)
		7.35(−1)	9.21(−1)	1.13(−1)	1.76(0)	2.53(+1)	2.31(+2)
Ca	$Ca^+ + e$	3.05(−4)	3.25(−4)	2.76(−23)	2.40(+4)	1.45(+8)	1.84(+11)
		1.12(−1)	1.40(−1)	4.43(−4)	5.00(−1)	2.01(+1)	2.25(+2)
Sc	$Sc^+ + e$	2.59(−6)	4.97(−6)	5.34(−29)	3.24(+3)	4.92(+8)	2.19(+11)
		3.75(0)	5.04(0)	7.74(−2)	2.134(0)	2.02(+1)	1.81(+2)
Ti	$Ti^+ + e$	2.47(−6)	5.68(−6)	4.60(−30)	6.87(+2)	6.14(+8)	2.54(+11)
		4.640)	5.64(0)	8.12(−2)	2.85(0)	2.06(+1)	1.58(+2)
V	$V^+ + e$	1.48(−6)	2.09(−6)	2.55(−29)	6.13(+2)	6.67(+8)	2.99(+11)
		4.31(0)	9.51(0)	8.08(−2)	9.32(−1)	2.24(+1)	1.43(+2)

Please cite this article as: Huebner, W.F., Mukherjee, J., Photoionization and photodissociation rates in solar and blackbody radiation fields. Planetary and Space Science (2015), http://dx.doi.org/10.1016/j.pss.2014.11.022

Table 1 (*continued*)

Mother species	*Photo products*	*Quiet Sun*	*Active Sun*	*BB*			
				10^3 K	10^4 K	10^5 K	10^6 K
Cr	$Cr^+ + e$	3.78(−6)	8.88(−6)	4.61(−30)	2.92(+3)	1.15(+9)	3.82(+11)
		5.02(0)	5.95(0)	8.18(−2)	2.79(0)	1.92(+1)	1.29(+2)
Mn	$Mn^+ + e$	5.76(−7)	1.17(−6)	1.94(−32)	5.64(+2)	6.90(+8)	4.08(+11)
		1.31(+1)	2.24(+1)	9.21(−2)	5.84(−1)	2.46(+1)	1.32(+2)
Fe	$Fe^+ + e$	8.20(−6)	1.95(−5)	2.18(−33)	4.82(+3)	6.58(+8)	4.41(+11)
		2.70(0)	3.21(0)	3.09(−2)	1.16(0)	1/91(+1)	1.38(+2)
Co	$Co^+ + e$	5.32(−7)	1.24(−6)	2.24(−34)	6.09(+2)	6.38(+8)	5.21(+11)
		1.54(+1)	2.32(+1)	7.75(−2)	5.87(−1)	2.63(+1)	1.36(+2)
Ni	$Ni^+ + e$	9.43(−7)	1.87(−6)	5.69(−33)	1.301(+3)	5.89(+8)	5.74(+11)
		8.94(0)	1.58(+1)	7.78(−2)	6.03(−1)	2.73(+1)	1.41(+2)
Cu	$Cu^+ + e$	6.13(−7)	1.48(−6)	5.93(−34)	6.25(+2)	9.74(+8)	6.60(+11)
		1.70(+1)	2.41(+1)	8.44(−2)	2.07(0)	2.22(+1)	1.38(+2)
Zn	$Zn^+ + e$	5.06(−7)	1.42(−6)	5.42(−42)	1.53(+2)	5.27(+8)	6.73(+11)
		1.54(+1)	2.02(+1)	8.27(−2)	6.30(−1)	2.65(+1)	1.46(+2)
Xe	$Xe^+ + e$	1.44(−6)	3.35(−6)	6.69(−54)	7.76(+2)	2.84(+9)	7.60(+11)
		4.30(0)	5.41(0)	9.34(−2)	9.64(−1)	6.80(0)	1.16(+2)

Table 2
Photoionization (including photo detachment and two electron ejection from H^-) rate coefficients (s^{-1}) (first entry) and average excess energy (eV) (second entry) of all photo products for monatomic ions. All other table entries have the same meaning as in Table 1.

Mother species	*Photo products*	*Quiet Sun*	*Active Sun*	*BB*			
				10^3 K	10^4 K	10^5 K	10^6 K
H^-	$H + e$	1.40(+1)	1.40(+1)	1.02(+1)	3.58(+6)	5.53(+8)	1.40(+10)
		9.28(−1)	9.28(−1)	1.98(−1)	1.47(0)	9.32(0)	2.41(+1)
	$H^+ + 2e$	1.17(−9)	2.69(−9)	1.56(−67)	8.68(−2)	6.87(+6)	3.89(+8)
		9.62(0)	1.12(+1)	1.05(−1)	1.52(0)	8.06(0)	1.88(+1)
He^+	$He^{2+} + e$	6.12(−9)	3.20(−8)		9.33(−19)	6.59(+6)	1.92(+10)
		1.11(+1)	1.04(+1)		3.04(0)	8.53(0)	4.64(+1)
Li^+	$Li^{2+} + e$	1.82(−9)	7.07(−9)		7.52(−27)	1.98(+6)	5.42(+10)
		1.78(+1)	1.47(+1)		2.70(0)	8.52(0)	6.27(+1)
Be^+	$Be^{2+} + e$	1.51(−8)	3.93(−8)	4.77(−83)	3.46(−2)	7.26(+7)	7.17(+10)
		2.08(+1)	2.56(+1)	1.75(−2)	1.02(0)	9.44(0)	1.65(+2)
B^+	$B^{2+} + e$	2.17(−8)	6.80(−8)		4.65(−7)	5.81(+7)	6.45(+10)
		2.10(+1)	2.47(+1)		5.03(−0)	1.37(+1)	1.87(+2)
C^+	$C^{2+} + e$	5.29(−8)	1.59(−7)		2.62(−4)	2.13(+8)	7.13(+10)
		1.78(+1)	2.08(+1)		7.07(−1)	9.13(0)	1.28(+2)
N^+	$N^{2+} + e$	9.28(−8)	2.83(−7)		1.57(−6)	2.41(+8)	1.05(+11)
		1.49(+1)	1.73(+1)		1.01(0)	9.22(0)	8.86(+1)
O^+	$O^{2+} + e$	1.27(−7)	4.09(−7)		3.90(−9)	2.16(+8)	1.55(+11)
		1.20(+1)	1.45(+1)		1.04(0)	9.62(0)	7.03(+1)
F^+	$F^{2+} + e$	1.48(−7)	4.91(−7)		3.78(−9)	2.32(+8)	2.13(+11)
		1.34(+1)	1.61(+1)		1.01(0)	1.12(+1)	7.21(+1)
Ne^+	$Ne^{2+} + e$	9.74(−8)	3.60(−7)		1.59(−11)	1.51(+8)	2.63(+11)
		1.46(+1)	1.76(+1)		3.64(−1)	1.09(+1)	7.68(+1)
Na^+	$Na^{2+} + e$	6.33(−8)	2.76(−7)		2.98(−14)	8.37(+7)	3.10(+11)
		1.67(+1)	1.76(+1)		3.19(0)	1.14(+1)	8.33(+1)
Mg^+	$Mg^{2+} + e$	2.34(−8)	9.92(−8)	2.21(−67)	2.25(−1)	3.43(+7)	3.33(+11)
		5.61(+1)	5.67(+1)	6.63(+4)	5.88(−1)	3.36(+1)	1.36(+2)
Al^+	$Al^{2+} + e$	9.92(−9)	2.97(−8)	5.03(−94)	8.79(−4)	2.47(+7)	3.22(+11)
		5.48(+1)	5.86(+1)	1.05(0)	2.11(0)	1.89(+1)	1.57(+2)
Si^+	$Si^{2+} + e$	1.70(−8)	5.03(−8)	7.19(−75)	2.91(−1)	6.08(+7)	2.99(+11)
		4.12(+1)	4.70(+1)	2.05(−1)	7.18(−1)	1.27(+1)	1.84(+2)
P^+	$P^{2+} + e$	2.30(−8)	7.16(−8)	4.36(−93)	4.64(−3)	6.10(+7)	2.81(+11)
		3.32(+1)	3.99(+1)	1.41(−1)	7.75(−1)	1.53(+1)	2.03(+2)
S^+	$S^{2+} + e$	2.60(−8)	7.98(−8)		6.94(−4)	1.34(+8)	2.42(+11)
		2.28(+1)	3.09(+1)		8.67(−1)	6.45(0)	2.19(+2)
Cl^+	$Cl^{2+} + e$	2.90(−8)	9.63(−8)		2.43(−4)	1.01(+8)	2.18(+11)
		2.53(+1)	3.17(+1)		8.46(−1)	1.03(+1)	2.30(+2)
Ar^+	$Ar^{2+} + e$	1.24(−7)	3.55(−7)		5.44(−5)	7.29(+8)	2.57(+11)
		1.25(+1)	1.45(+1)		9.52(−1)	5.19(0)	1.74(+2)
K^+	$K^{2+} + e$	3.02(−8)	1.04(−7)		9.58(−8)	7.12(+7)	1.90(+11)
		1.92(+1)	2.31(+1)		1.03(0)	9.57(0)	2.23(+2)

Please cite this article as: Huebner, W.F., Mukherjee, J., Photoionization and photodissociation rates in solar and blackbody radiation fields. Planetary and Space Science (2015), http://dx.doi.org/10.1016/j.pss.2014.11.022

Table 2 (*continued*)

Mother species	*Photo products*	*Quiet Sun*	*Active Sun*	*BB*			
				10^3 K	10^4 K	10^5 K	10^6 K
Ca^+	Ca^{2+} + e	4.23(−8)	1.29(−7)	1.12(−54)	7.31(0)	8.27(+7)	1.74(+11)
		2.78(+1)	3.45(+1)	9.60(−2)	9.42(−1)	2.27(+1)	2.20(+2)
Sc^+	Sc^{2+} + e	9.50(−8)	2.65(−7)	1.12(−59)	7.85(0)	3.26(+8)	1.99(+11)
		2.08(+1)	2.60(+1)	9.73(−2)	2.23(0)	1.44(+1)	1.83(+2)
Ti^+	Ti^{2+} + e	1.18(−7)	3.41(−7)	2.04(−63)	2.13(0)	4.95(+8)	2.41(+11)
		2.60(+1)	3.12(+1)	1.40(−1)	2.91(0)	1.53(+1)	1.54(+2)
V^+	V^{2+} + e	2.33(−7)	6.48(−7)	1.10(−65)	1.29(+1)	8.89(8)	3.13(+11)
		1.98(+1)	2.45(+1)	1.62(−1)	8.66(−1)	1.29(+1)	1.31(+2)
Cr^+	Cr^{2+} + e	2.15(−7)	6.30(−7)	3.08(−74)	1.71(0)	8.75(+8)	3.65(+11)
		2.41(+1)	2.90(+1)	1.35(−1)	9.10(−1)	1.33(+1)	1.21(+2)
Mn^+	Mn^{2+} + e	1.79(−7)	5.68(−7)	3.84(−73)	4.28(−2)	5.57(+8)	4.00(+11)
		3.02(+1)	3.42(+1)	2.32(−1)	2.29(0)	1.96(+1)	1.24(+2)
Fe^+	Fe^{2+} + e	2.55(−7)	7.79(−7)	2.11(−71)	1.04(0)	7.50(+8)	4.83(+11)
		2.72(+1)	3.16(+1)	6.37(−5)	5.46(−1)	1.82(+1)	1.20(+2)
Co^+	Co^{2+} + e	2.52(−7)	7.72(−7)	1.38(−77)	6.02(−1)	8.82(+8)	5.39(+11)
		2.66(+1)	3.12(+1)	1.89(−1)	1.03(0)	1.54(+1)	1.22(+2)
Ni^+	Ni^{2+} + e	2.52(−7)	7.88(−7)	6.34(−82)	1.85(−1)	8.21(+8)	5.97(+11)
		2.67(+1)	3.13(+1)	3.46(−2)	1.07(0)	1.56(+1)	1.24(+2)
Cu^+	Cu^{2+} + e	2.38(−7)	7.67(−7)	1.10(−93)	2.32(−2)	7.30(+8)	6.51(+11)
		2.65(+1)	3.08(+1)	1.86(−1)	9.26(−1)	1.50(+1)	1.26(+2)
Zn^+	Zn^{2+} + e	1.67(−7)	5.92(−7)	9.01(−84)	9.58(−4)	3.62(+8)	6.67(+11)
		3.48(+1)	3.82(+1)	1.35(−1)	1.28(0)	2.46(+1)	1.38(+2)

Table 3
Photodissociation, photoionization, and dissociative photoionization rate coefficients (s^{-1}) (first entry) and average excess energies (eV) (second entry) of all photo products for diatomic molecules. All other table entries have the same meaning as in Table 1; (theo) and (exp) refer to theoretical and experimental cross section data, respectively.

Mother species	*Photo products*	*Quiet Sun*	*Active Sun*	*BB*			
				10^3 K	10^4 K	10^5 K	10^6 K
H_2	H + H	4.80(−8)	1.09(−7)	1.37(−54)	4.55(+1)	3.31(+7)	7.03(+8)
		8.23(0)	8.22(0)	7.50(0)	8.15(0)	8.25(0)	8.26(0)
	H + H(2s, 2p)	3.44(−8)	8.21(−8)	9.83(−66)	8.53(0)	8.53(+7)	2.20(+9)
		5.02(−1)	4.88(−1)	1.32(−1)	4.69(−1)	9.35(−1)	9.93(−1)
	H_2^+ + e	5.41(−8)	1.15(−7)	6.68(−70)	2.75(0)	3.65(+8)	1.64(+10)
		6.57(0)	7.17(0)	5.12(−2)	1.20(0)	6.41(0)	9.30(0)
	H^+ + H + e	9.52(−9)	2.79(−8)	2.18(−83)	3.31(−3)	2.21(+7)	6.94(9)
		2.48(+1)	2.70(+1)	7.84(−2)	1.05(0)	1.99(+1)	5.08(+1)
CH	$C(^3P)$ + H	9.20(−3)	9.20(−3)	1.12(−13)	1.70(+4)	5.04(+6)	6.68(+7)
		4.46(−1)	4.46(−1)	1.50(−1)	7.62(−1)	1.61(0)	1.68(0)
	$C(^1D)$ + H	5.12(−6)	7.61(−6)	1.82(−31)	9.74(+3)	4.91(+8)	9.79(+9)
		3.60(0)	3.82(0)	2.69(0)	3.76(0)	6.89(0)	7.05(0)
CH	$C(^1S)$ + H	5.03(−5)	5.55(−5)	2.17(−25)	7.93(+3)	1.21(+7)	1.74(+8)
		1.79(−1)	1.81(−1)	7.37(−2)	2.09(−1)	2.39(−1)	2.41(−1)
	CH^+ + e	7.58(−7)	1.69(−6)	4.20(−47)	6.97(+2)	1.42(+9)	1.39(+11)
		6.35(0)	7.80(0)	8.63(−2)	1.31(0)	1.05(+1)	1.11(+2)
OH (theo)	$O(^3P)$ + H	6.54(−6)	7.17(−6)	1.69(−20)	2.36(+3)	1.43(+7)	2.25(+8)
		1.27(0)	1.43(0)	3.52(−1)	3.30(0)	3.58(0)	3.60(0)
	$O(^1S)$ + H	6.71(−8)	1.64(−7)	2.60(−16)	3.77(+1)	5.28(+6)	1.01(+8)
		9.80(0)	9.94(0)	2.40(0)	1.07(+1)	1.10(+1)	1.10(+1)
	$O(^1D)$ + H	6.35(−7)	1.51(−6)	2.55(−19)	5.64(+2)	6.85(+7)	1.33(+9)
		7.90(0)	7.88(0)	1.81(−1)	7.97(0)	8.95(0)	9.02(0)
	OH^+ + e	2.47(−7)	6.52(−7)	2.14(−61)	1.20(+1)	1.04(+9)	1.87(+11)
		1.91(+1)	2.32(+1)	6.91(−2)	1.69(0)	1.36(+1)	7.41(+1)
OH (exp)	$O(^3P)$ + H	1.20(−5)	1.37(−5)	1.69(−20)	6.31(+3)	3.82(+7)	6.03(+8)
		2.00(0)	2.14(0)	3.52(−1)	3.24(0)	3.66(0)	3.69(0)
	$O(^1S)$ + H	8.33(−7)	2.11(−6)	2.60(−16)	1.79(+2)	2.35(+7)	4.52(+8)
		1.00(+1)	1.00(+1)	2.40(0)	1.06(+1)	1.10(+1)	1.10(+1)
	$O(^1D)$ + H	7.01(−6)	1.76(−5)	2.55(−19)	2.32(+3)	1.35(+8)	2.50(+9)
		7.73(0)	7.74(0)	1.81(−1)	7.42(0)	8.13(0)	8.20(0)
	OH^+ + e	2.43(−7)	6.43(−7)	5.12(−62)	1.06(+1)	1.03(+9)	1.87(+11)
		1.94(+1)	2.36(+1)	1.83(−1)	1.82(0)	1.37(+1)	7.42(+1)
HF	F + H	1.58(−7)	3.83(−7)	7.51(−30)	9.77(+1)	2.13(+7)	4.67(+8)
		4.61(0)	4.61(0)	1.72(−1)	4.33(0)	7.20(0)	7.41(0)

Please cite this article as: Huebner, W.F., Mukherjee, J., Photoionization and photodissociation rates in solar and blackbody radiation fields. Planetary and Space Science (2015), http://dx.doi.org/10.1016/j.pss.2014.11.022

Table 3 (*continued*)

Mother species	*Photo products*	*Quiet Sun*	*Active Sun*	*BB*			
				10^3 K	10^4 K	10^5 K	10^6 K
	$HF^+ + e$	2.04(−7)	5.64(−7)	5.41(−73)	1.54(0)	8.96(+8)	1.94(+11)
		2.14(+1)	2.60(+1)	6.97(−2)	1.42(0)	1.26(+1)	7.46(+1)
	$H^+ + F + e$	6.10(−8)	1.77(−7)	1.78(−84)	1.33(−2)	2.57(+8)	6.54(+10)
		2.12(+1)	2.52(+1)	8.54(−3)	1.80(0)	1.22(+1)	7.27(+1)
	$F^+ + H + e$	1.39(−8)	4.72(−8)	8.15(−72)	4.01(−1)	2.75(+7)	2.41(+10)
		2.70(+1)	3.20(+1)	1.37(−16)	1.11(−3)	1.88(+1)	9.46(+1)
C_2	$C(^1D) + C(^1D)$	1.03(−7)	2.09(−7)	3.35(−41)	1.80(+2)	6.94(+7)	1.61(+9)
		3.62(0)	3.65(0)	1.59(−1)	2.87(0)	4.36(0)	9.49(0)
	$C_2^+ + e$	9.08(−7)	2.16(−6)	1.72(−56)	2.55(+2)	2.44(+9)	2.26(+11)
		6.76(0)	8.15(0)	8.46(−2)	1.52(0)	8.40(0)	1.15(+2)
CN	C + N	3.17(−6)	7.43(−6)	5.45(−36)	1.72(+3)	4.57(+9)	2.89(+11)
		7.41(0)	7.97(0)	1.16(−1)	5.11(0)	9.89(0)	8.41(+1)
$CO(X\ ^1\Sigma^+)$	C + O	2.81(−7)	6.60(−7)	1.24(−55)	1.24(+2)	2.24(+8)	5.11(+9)
		2.56(0)	2.58(0)	1.15(0)	2.32(0)	2.67(0)	2.70(0)
	$C(^1D) + O(^1D)$	3.46(−8)	7.87(−8)	1.45(−66)	5.97(0)	1.97(+8)	8.18(+9)
		2.29(0)	2.39(0)	9.47(−2)	1.61(0)	2.92(0)	4.44(+1)
	$CO^+ + e$	3.80(−7)	9.59(−7)	5.10(−63)	3.04(+1)	1.55(+9)	1.71(+11)
		1.40(+1)	1.68(+1)	2.04(−1)	8.70(−1)	1.18(+1)	4.56(+1)
	$C^+ + O + e$	2.94(−8)	9.88(−8)		1.27(−4)	7.23(+7)	5.56(+10)
		2.64(+1)	2.99(+1)		1.38(0)	1.74(+1)	1.27(+2)
	$O^+ + C + e$	2.42(−8)	8.31(−8)		7.18(−7)	4.23(+7)	4.94(+10)
		2.60(+1)	2.91(+1)		1.65(0)	2.17(+1)	1.32(+2)
$CO(Xa\ ^3\Pi)$	C + O	7.20(−5)	9.18(−5)	4.05(−26)	4.17(+4)	4.39(+8)	1.53(+10)
		2.16(0)	2.41(0)	1.15(0)	2.48(0)	7.16(0)	3.30(+1)
	$CO^+ + e$	8.58(−6)	1.82(−5)	8.03(−34)	1.15(+4)	1.89(+9)	1.40(+11)
		2.24(0)	2.66(0)	8.43(−2)	9.29(−1)	1.32(+1)	4.20(+1)
	$C^+ + O + e$	2.45(−8)	8.17(−8)	2.36(−76)	2.88(−2)	6.14(+7)	5.35(+10)
		3.17(+1)	3.60(+1)	2.04(−1)	1.54(0)	2.13(+1)	1.44(+2)
	$O^+ + C + e$	2.06(−8)	7.24(−8)	6.95(−87)	6.15(−4)	3.78(+7)	5.14(+10)
		3.27(+1)	3.60(+1)	4.86(−1)	9.15(−1)	2.64(+1)	1.46(+2)
N_2	N + N	6.61(−7)	1.56(−6)	9.10(−56)	1.94(+2)	4.02(+8)	1.01(+10)
		3.38(0)	3.38(0)	2.80(0)	3.33(0)	5.21(0)	5.57(0)
	$N_2^+ + e$	3.52(−7)	9.11(−7)	7.30(−71)	6.13(0)	1.77(+9)	2.24(+11)
		1.78(+1)	2.14(+1)	2.64(−1)	1.13(0)	1.15(+1)	6.28(+1)
	$N^+ + N + e$	1.50(−8)	5.47(−8)		3.22(−6)	3.25(+7)	4.37(+10)
		2.89(+1)	3.24(+1)		2.05(0)	1.96(+1)	1.60(+2)
NO	N + O	2.20(−6)	3.21(−6)	2.67(−28)	1.48(+3)	3.68(+8)	1.47(+10)
		1.84(0)	2.72(0)	7.29(−2)	2.19(0)	1.00(+1)	2.87(+1)
	$NO^+ + e$	1.28(−6)	3.19(−6)	8.83(−42)	4.74(+2)	1.79(+9)	2.82(+11)
		8.23(0)	9.89(0)	1.04(−1)	2.13(0)	1.67(+1)	8.24(+1)
	$N^+ + O + e$	3.18(−8)	1.02(−7)	4.13(−99)	4.13(−4)	8.72(+7)	4.85(+10)
		2.52(+1)	2.85(+1)	1.70(−1)	1.52(0)	1.66(+1)	1.05(+2)
	$O^+ + N + e$	1.81(−9)	5.08(−9)	1.17(−95)	4.17(−4)	7.71(+6)	1.71(+9)
		1.86(+1)	2.25(+1)	2.73(−1)	1.18(0)	1.03(+1)	7.72(+1)
O_2	$O(^3P) + O(^3P)$	1.45(−7)	2.15(−7)	7.13(−27)	4.11(+1)	1.50(+8)	4.12(+9)
		4.39(0)	5.85(0)	1.24(−1)	3.51(0)	1.13(+1)	1.15(+1)
	$O(^3P) + O(^1D)$	4.05(−6)	6.47(−6)	4.91(−31)	7.45(+3)	1.40(+8)	2.78(+9)
		1.33(0)	1.55(0)	1.92(−1)	1.31(0)	4.15(0)	5.02(0)
	$O(^1S) + O(^1S)$	3.90(−8)	9.35(−8)	7.83(−62)	9.74(0)	3.41(+7)	8.07(+8)
		7.38(−1)	7.38(−1)	2.07(−1)	7.14(−1)	9.10(−1)	9.25(−1)
	$O_2^+ + e$	4.67(−7)	1.18(−6)	4.82(−34)	7.77(+1)	1.61(+9)	2.35(+11)
		1.58(+1)	1.92(+1)	5.60(−23)	1.31(0)	1.43(+1)	6.96(+1)
	$O^+ + O + e$	1.10(−7)	3.47(−7)	9.86(−98)	4.02(−3)	3.50(+8)	1.49(+11)
		2.38(+1)	2.73(+1)	9.19(−2)	1.02(0)	1.40(+1)	8.71(+1)
HCl	H + Cl	7.21(−6)	1.16(−5)	3.80(−22)	8.54(+3)	2.06(+9)	2.93(+11)
		4.41(0)	5.30(0)	1.73(−1)	4.56(0)	1.31(+1)	2.08(+2)
F_2	F + F	5.65(−4)	5,81(−4)	1.14(−7)	2.06(+4)	2.54(+9)	4.98(+11)
		1.78(0)	1.98(0)	1.80(−1)	6.16(0)	2.29(+1)	9.59(+1)
SO	S + O	6.16(−4)	6.62(−4)	2.50(−22)	5.65(+4)	2.32(+8)	3.73(+9)
		6.18(−1)	6.81(−1)	2.18(−1)	1.39(0)	2.90(0)	3.00(0)
	$SO^+ + e$	8.62(−7)	1.99(−6)	2.22(−45)	1.16(+3)	2.30(+9)	4.89(+11)
		9.86(0)	1.29(+1)	8.62(−2)	1.07(0)	1.19(+1)	1.54(+2)
Cl_2	Cl + Cl	5.14(−3)	5.31(−3)	2.00(−11)	2.04(+5)	6.01(+9)	6.28(+11)
		2.10(0)	2.19(0)	2.41(−1)	4.57(0)	1.30(+1)	1.97(+2)
BrO	$Br + O(^3P)$	6.93(−3)	7.01(−3)	4.12(−11)	6.81(+4)	1.77(+9)	4.09(+11)
		1.73(0)	1.75(0)	1.80(−1)	3.77(0)	1.61(+1)	1.69(+2)
	$Br + O(^1D)$	2.14(−3)	2.22(−3)	6.77(−18)	6.28(+4)	1.77(+9)	4.09(+11)
		7.96(−1)	8.28(−1)	1.72(−1)	2.00(0)	1.41(+1)	1.67(+2)

calculations for the solar radiation field and adds the results for the blackbody radiation fields without dilution factors for selected temperatures from 1000 K to 1,000,000 K.

2.4. Triatomic molecules

No new triatomic species or revised cross sections have been added. Table 4 summarizes the results from previous calculations

Table 4
Photodissociation, photoionization, and dissociative photoionization rate coefficients (s^{-1}) (first entry) and average excess energies (eV) (second entry) of all photo products for triatomic molecules. All other table entries have the same meaning as in Table 1. SO_2^* is an excited state.

Mother species	*Photo products*	*Quiet Sun*	*Active Sun*	*BB*			
				10^3 K	10^4 K	10^5 K	10^6 K
NH_2	NH + H	2.15(−6)	3.40(−6)	4.03(−24)	3.25(+3)	1.26(+9)	1.40(+11)
		6.38(0)	8.49(0)	1.73(−1)	4.07(0)	1.87(+1)	9.63(+1)
H_2O	H + OH	1.03(−5)	1.76(−5)	3.94(−29)	5.58(+3)	4.09(+8)	3.18(+10)
		3.41(0)	4.04(0)	1.77(0)	2.89(0)	1.37(+1)	6.68(+1)
	H_2 + O(^{1}D)	5.97(−7)	1.48(−6)	5.54(−39)	2.40(+2)	1.16(+8)	1.02(+10)
		3.84(0)	3.94(0)	1.71(0)	3.00(0)	1.34(+1)	6.71(+1)
	O + H + H	7.54(−7)	1.91(−6)	1.08(−42)	1.49(+2)	1.46(+7)	2.78(+8)
		6.99(−1)	6.97(−1)	8.69(−2)	8.36(−1)	1.56(0)	1.62(0)
	H_2O^+ + e	3.31(−7)	8.28(−7)	2.69(−57)	5.71(+1)	1.09(+9)	1.37(+11)
		1.24(+1)	1.52(+1)	1.03(−1)	1.32(0)	1.22(+1)	6.32(+1)
	H^+ + OH + e	1.31(−8)	4.07(−8)	4.84(−86)	6.13(−3)	4.38(+7)	2.39(+10)
		2.50(+1)	3.05(+1)	4.80(−1)	1.25(0)	1.40(+1)	1.07(+2)
	O^+ + H_2 + e	5.85(−9)	2.21(−8)	7.61(−88)	1.07(−4)	1.03(+7)	1.92(+10)
		3,65(+1)	3.98(+1)	5.15(−1)	1.52(0)	2.83(+1)	1.22(+2)
	OH^+ + H + e	5.54(−8)	1.51(−7)	1.92(−83)	7.08(−2)	2.50(+8)	5,45(+10)
		1.86(+1)	2.32(+1)	9.09(−2)	1.33(0)	1.09(+1)	7.92(+1)
HCN	H + CN(A $^2\Pi_i$)	1.26(−5)	3.13(−5)	1.40(−30)	3.95(+3)	4.14(+8)	8.06(+9)
		3.82(0)	3.84(0)	2.48(−1)	3.73(0)	5.01(0)	5.09(0)
	HCN^+ + e	4.51(−7)	1.12(−6)	1.43(−61)	5.10(+1)	1.59(+9)	2.26(+11)
		1.12(+1)	1.38(+1)	1.58(−1)	1.14(0)	1.04(+1)	1.16(+2)
HO_2	OH + O	6.61(−3)	6.67(−3)	1.58(−11)	3.88(+4)	3.10(+9)	4.73(+11)
		1.02(0)	1.04(0)	1.77(−1)	3.10(0)	2.20(+1)	8.84(+1)
H_2S	HS + H	3.20(−4)	3.66(−4)	2.08(−19)	3.97(+4)	6.74(+8)	1.22(+10)
		2.14(0)	2.45(0)	1.96(−1)	3.79(0)	6.17(0)	6.34(0)
	H_2S^+ + e	5.64(−7)	1.19(−6)	2.72(−46)	1.17(+3)	4.29(+8)	9.09(+9)
		2.18(0)	2.27(0)	9.41(−2)	1.04(0)	2.19(0)	2.30(0)
	S^+ + H_2 + e	1.47(−7)	3.53(−7)	1.36(−61)	2.46(+1)	4.41(+8)	1.45(+11)
		6.86(0)	8.73(0)	2.09(−1)	1.27(0)	7.67(0)	2.06(+2)
	HS^+ + H + e	7.26(−8)	1.74(−7)	2.62(−65)	5.78(0)	3.62(+8)	1.43(+11)
		1.20(+1)	1.58(+1)	9.02(−2)	1.50(0)	8.16(0)	2.08(+2)
CO_2	CO(X $^1\Sigma^+$) + O(^{3}P)	1.71(−8)	1.99(−8)	1.15(−28)	9.16(0)	3.10(+4)	4.65(+5)
		1.69(0)	1.70(0)	1.68(−1)	1.77(0)	1.80(0)	1.80(0)
	CO(X $^1\Sigma^+$) + O(^{1}D)	9.24(−7)	1.86(−6)	2.07(−33)	1.76(+3)	5.86(+8)	1.29(+10)
		4.34(0)	4.55(0)	1.17(−1)	3.57(0)	5.60(0)	6.01(0)
	CO(a $^3\Pi$) + O(^{3}P)	2.82(−7)	6.35(−7)	1.26(−52)	1.77(2)	2.79(+8)	6.79(+9)
		1.99(0)	2.02(0)	1.74(−1)	1.55(0)	3.02(0)	3.49(0)
	CO_2^+ + e	6.55(−7)	1.76(−6)	1.42(−61)	5.13(+1)	2.21(+9)	3.16(+11)
		1.69(+1)	2.08(+1)	8.96(−2)	8.39(−1)	1.39(+1)	4.78(+1)
	C^+ + O_2 + e	2.89(−8)	1.07(−7)		7.56(−7)	4.84(+7)	4.79(+10)
		3.02(+1)	3.36(+1)		2.40(0)	2.50(+1)	9.22(+1)
	O^+ + CO + e	6.38(−8)	2.11(−7)	7.66(−87)	2.16(−3)	1.81(+8)	7.34(+10)
		2.79(+1)	3.16(+1)	3.07(−1)	1.83(0)	1.85(+1)	7.54(+1)
	CO^+ + O + e	5.02(−8)	1.66(−7)	1.05(−86)	4.07(−3)	1.57(+8)	6.23(+10)
		2.71(+1)	3.14(+1)	1.07(−1)	1.32(0)	1.64(+1)	8.04(+1)
N_2O	N_2($^1\Sigma$) + O(^{1}S)	4.90(−6)	1.03(−5)	8.74(−28)	9.28(+3)	3.52(+9)	4.55(+11)
		6.80(0)	8.25(0)	2.68(−1)	4.04(0)	1.64(+1)	9.15(+1)
	N_2($^1\Sigma$) + O(^{1}D)	1.02(−6)	1.13(−6)	4.64(−20)	2.62(+2)	1.34(+6)	2.11(+7)
		2.75(0)	2.80(0)	1.75(−1)	3.63(0)	4.37(0)	4.41(0)
NO_2	NO(X $^2\Pi$) + O(^{3}P)	8.47(−3)	8.48(−3)	9.97(−12)	2.18(+4)	1.53(+8)	2.64(+9)
		3.45(−1)	3.49(−1)	8.86(−2)	2.94(0)	6.33(0)	6.49(0)
	NO(X $^2\Pi$) + O(^{1}D)	4.34(−5)	5.01(−5)	2.36(−22)	1.29(+4)	1.36(+8)	2.31(+9)
		1.21(0)	1.47(0)	1.52(−1)	2.67(0)	4.16(0)	4.28(0)
	NO_2^+ + e	1.30(−6)	3.20(−6)	8.67(−46)	4.37(+2)	3.34(+9)	5.09(+11)
		1.30(+1)	1.60(+1)	1.31(−1)	3.14(0)	1.46(+1)	8,74(+1)
O_3	O(^{3}P) + O_2($^3\Sigma_g^-$)	4.68(−4)	4.68(−4)	2.13(−6)	2.46(+2)	2.72(+4)	3.32(+5)
		1.40(0)	1.40(0)	2.22(−1)	2.11(0)	2.61(0)	2.63(0)

Please cite this article as: Huebner, W.F., Mukherjee, J., Photoionization and photodissociation rates in solar and blackbody radiation fields. Planetary and Space Science (2015), http://dx.doi.org/10.1016/j.pss.2014.11.022

Table 4 (*continued*)

Mother species	*Photo products*	*Quiet Sun*	*Active Sun*	*BB*			
				10^3 K	10^4 K	10^5 K	10^6 K
	$O(^1D) + O_2(a'\Delta g)$	9.72(−3)	9.94(−3)	4.57(−16)	8.48(+4)	3.06(+9)	5.30(+11)
		7.93(−1)	8.06(−1)	3.30(−1)	1.29(0)	2.07(+1)	9.31(+1)
HOCl	OH + Cl	5.58(−4)	5.67(−4)	5.69(−12)	1.06(+4)	3.04(+9)	3.29(+11)
		1.71(0)	1.79(0)	1.29(−1)	5.75(0)	1.92(+1)	1.16(+2)
OCS	$CO + S(^3P)$	1.53(−5)	1.68(−5)	1.33(−20)	4.57(+3)	6.77(+7)	1.18(+9)
		2.72(0)	2.85(0)	6.46(−1)	5.08(0)	6.42(0)	6.54(0)
	$CO + S(^1S)$	3.01(−5)	4.36(−5)	1.66(−27)	5.37(+4)	4.66(+8)	7.53(+9)
		2.13(0)	2.21(0)	1.38(−1)	2.25(0)	2.56(0)	2.60(0)
	$CO + S(^1D)$	4.99(−5)	5.48(−5)	1.54(−21)	1.32(+4)	4.54(+7)	6.84(+8)
		1.96(0)	2.01(0)	5.40(−1)	2.93(0)	3.04(0)	3.04(0)
	$CS + O(^3P)$	6.92(−8)	7.91(−8)	1.18(−30)	2.46(+1)	6.39(+4)	9.45(+5)
		1.31(−1)	1.32(−1)	6.74(−2)	1.48(−1)	1.61(−1)	1.61(−1)
	$CS + O(^1D)$	6.35(−6)	1.37(−5)	3.85(−37)	1.41(+4)	3.69(+8)	6.36(+9)
		8.46(−1)	9.27(−1)	8.26(−2)	4.60(−1)	6.53(−1)	6.68(−1)
OCS	$COS^+ + e$	2.37(−7)	4.62(−7)	8.05(−49)	5.88(+2)	1.66(+8)	5.25(+10)
		1.50(0)	2.15(0)	5.21(−2)	5.12(−1)	1.56(0)	2.03(+2)
	$C^+ + SO + e$	5.58(−10)	2.52(−9)		8.22(−8)	5.92(+5)	1.72(+10)
		6.10(+1)	6.02(+1)		1.59(0)	3.80(+1)	2.05(+2)
	$O^+ + CS + e$	1.85(−10)	8.27(−10)	1.61(−89)	3.53(−6)	2.01(+5)	5.40(+9)
		6.16(+1)	6.13(+1)	1.51(−8)	8.34(−1)	3.88(+1)	2.06(+2)
	$S^+ + CO + e$	8.66(−9)	3.52(−8)	3.71(−65)	1.00(−1)	1.77(+7)	2.12(+11)
		5.75(+1)	6.22(+1)	1.85(−1)	2.08(0)	2.46(+1)	2.12(+2)
	$CO^+ + S + e$	2.04(−9)	8.96(−9)	1.41(−81)	2.81(−4)	2.86(+6)	5.90(+10)
		6.21(+1)	6.29(+1)	5.79(−4)	1.49(0)	3.24(+1)	2.09(+2)
	$CS^+ + O + e$	2.73(−10)	1.15(−9)	8.37(−89)	2.32(−5)	4.76(+5)	7.13(+9)
		5.66(+1)	5.91(+1)	3.61(−1)	1.54(0)	2.56(+1)	2.06(+2)
SO_2	SO_2^*	4.00(−5)	4.16(−5)	1.23(−22)	8.09(+2)	5.75(+5)	7.83(+6)
		–	–	–	–	–	–
	$S + O_2$	5.09(−5)	6.35(−5)	5.91(−25)	1.10(+4)	2.51(+8)	4.68(+9)
		7.48(−1)	1.17(0)	1.13(−1)	1.62(0)	4.67(0)	4.84(0)
	SO + O	1.59(−4)	1.76(−4)	1.66(−23)	1.51(+4)	2.54(+8)	4.74(+9)
		4.40(−1)	6.30(−1)	1.13(−1)	1.45(0)	4.90(0)	5.08(0)
	$SO_2^+ + e$	1.06(−6)	2.61(−6)	4.95(−53)	2.37(+2)	3.32(+9)	7.08(+11)
		1.20(+1)	1.54(+1)	3.44(−4)	1.14(0)	1.17(+1)	1.35(+2)
ClNO	Cl + NO	6.32(−3)	6.49(−3)	4.45(−8)	1.83(+5)	5.02(+9)	6.05(+11)
		2.73(0)	2.79(0)	2.12(−1)	4.85(0)	1.82(+1)	1.31(+2)
OClO	$ClO + O(^3P)$	1.14(−1)	1.14(−1)	5.85(−10)	1.08(+5)	1.25(+7)	1.52(+8)
		9.20(−1)	9.20(−1)	3.64(−1)	9.85(−1)	1.04(0)	1.05(0)
	$ClO + O(^1D)$	8.07(−5)	1.04(−4)	3.57(−19)	1.76(+4)	4.76(+9)	6.01(+11)
		1.66(0)	2.75(0)	8.49(−2)	4.56(0)	1.61(+1)	1.29(+2)
ClOO	ClO + O	9.00(−3)	9.21(−3)	2.84(−12)	9.60(+4)	4.79(+9)	6.02(+11)
		2.16(0)	2.18(0)	2.26(−1)	3.20(0)	1.79(+1)	1.31(+2)
CS_2	$CS(X\,^1\Sigma) + S(^3P)$	2.03(−3)	2.17(−3)	2.40(−19)	1.94(+5)	2.62(+8)	3.72(+9)
		1.52(0)	1.53(0)	2.51(−1)	1.77(0)	1.84(0)	1.84(0)
	$CS(X\,^1\Sigma^+) + S(^1D)$	8.92(−4)	9.60(−4)	1.40(−22)	9.53(+4)	1.30(+8)	1.85(+9)
		5.06(−1)	5.13(−1)	7.28(−2)	6.47(−1)	7.01(−1)	7.05(−1)
	$CS(a^3\Pi) + S(^3P)$	4.72(−6)	7.70(−6)	1.12(−33)	1.31(+4)	2.01(+8)	3.35(+9)
		6.86(−1)	7.40(−1)	1.58(−1)	7.76(−1)	1.05(0)	1.07(0)
	$CS(A^1\Pi) + S(^3P)$	5.15(−6)	1.26(−5)	2.38(−40)	3.59(+3)	3.11(+8)	5.89(+9)
		9.16(−1)	9.19(−1)	1.26(−1)	9.42(−1)	1.64(0)	1.69(0)
	$CS_2^+ + e$	5.50(−7)	1.24(−6)	1.06(−45)	1.01(+3)	2.54(+8)	1.88(+11)
		2.41(0)	3.14(0)	2.05(−1)	1.23(0)	5.29(0)	2.19(+2)
	$C^+ + S_2 + e$	1.17(−9)	4.65(−9)	3.75(−86)	1.22(−5)	1.78(+6)	2.14(+10)
		5.02(+1)	5.39(+1)	1.71(−3)	5.52(−1)	3.40(+1)	2.23(+2)
	$S^+ + CS + e$	1.19(−8)	4.69(−8)	1.93(−71)	1.29(−2)	1.89(+7)	2.14(+11)
		5.34(+1)	5.75(+1)	3.55(−1)	1.65(0)	3.60(+1)	2.27(+2)
CS_2	$CS^+ + S + e$	7.75(−9)	3.02(−8)	2.01(−75)	6.29(−3)	1.31(+7)	1.35(+11)
		5.13(+1)	5.57(+1)	7.02(−2)	1.52(0)	3.26(+1)	2.25(+2)
	$S_2^+ + C + e$	3.45(−10)	1.32(−9)	8.00(−82)	1.37(−4)	6.29(+5)	5.52(+9)
		4.84(+1)	5.33(+1)	2.52(−1)	1.83(0)	2.93(+1)	2.23(+2)
HOBr	OH + Br	1.83(−3)	1.84(−3)	4.84(−11)	1.95(+4)	3.38(+9)	8.21(+11)
		1.25(0)	1.29(0)	2.23(−1)	5.52(0)	1.71(+1)	1.69(+2)
HOI	OH + I	8.65(−4)	8.75(−4)	9.77(−12)	1.29(+4)	2.81(+9)	8.88(+11)
		1.57(0)	1.67(0)	1.53(−1)	5.60(0)	2.05(+1)	1.12(+2)
INO	I + NO	9.82(−2)	9.89(−2)	1.75(−3)	4.29(+5)	2.42(+9)	9.58(+11)
		2.79(0)	2.81(0)	1.89(−1)	4.38(0)	2.36(+1)	1.15(+2)

for the solar radiation field and adds the results for the blackbody radiation fields without dilution factors for selected temperatures from 1000 K to 1,000,000 K. SO_2^* indicates an excited state ($SO_2 + \nu \rightarrow SO_2^*$), which is needed to get the correct cross sections from branching ratios and the total photo cross section.

2.5. Tetratomic and pentatomic molecules

No new tetratomic species or revised cross sections have been added. Table 5 for tetratomic and Table 6 for pentatomic molecules summarize the results from previous calculations for the solar

Table 5
Photodissociation, photoionization, and dissociative photoionization rate coefficients (s^{-1}) (first entry) and average excess energies (eV) (second entry) of all photo products for tetratomic molecules. All other table entries have the same meaning as in Table 1. $C_2H_2^*$ is an excited state.

Mother species	*Photo products*	*Quiet Sun*	*Active Sun*	*BB*			
				10^3 K	10^4 K	10^5 K	10^6 K
NH_3	$NH(X\,^3\Sigma^-) + H + H$	1.99(−6)	4.80(−6)	6.17(−38)	1.52(+3)	3.25(+8)	7.25(+9)
		2.10(0)	2.09(0)	1.52(−1)	1.78(0)	4.85(0)	5.14(0)
	$NH(a^1\Delta) + H_2$	3.95(−6)	5.47(−6)	3.11(−26)	1.33(+3)	9.16(+7)	1.98(+9)
		1.72(0)	2.32(0)	4.43(−1)	2.80(0)	7.20(0)	7.60(0)
	$NH_2(X^2B_1) + H$	1.70(−4)	1.87(−4)	2.63(−23)	2.51(+4)	1.05(+8)	1.72(+9)
		1.84(0)	1.89(0)	4.88(−1)	2.26(0)	4.11(0)	4.27(0)
	$NH_3^+ + e$	6.10(−7)	1.42(−6)	5.10(−46)	4.46(+2)	1.25(+9)	8.23(+10)
		5.77(0)	6.42(0)	1.44(−1)	1.55(0)	1.13(+1)	4.95(+1)
	$H^+ + NH_2 + e$	3.33(−9)	1.19(−8)		1.14(−9)	5.42(+6)	1.01(+10)
		2.03(+1)	2.36(+1)		9.98(−1)	1.57(+1)	1.57(+2)
	$N^+ + H_2 + H + e$	3.25(−9)	1.15(−8)		8.98(−6)	7.45(+6)	1.01(+10)
		2.95(+1)	3.31(+1)		1.19(0)	1.96(+1)	1.66(+2)
	$NH^+ + H_2 + e$	6.92(−9)	2.10(−8)	4.19(−75)	9.42(−3)	3.28(+7)	1.25(+10)
		2.62(+1)	3.05(+1)	6.89(−2)	1.56(0)	1.55(+1)	1.45(+2)
	$NH_2^+ + H + e$	1.77(−7)	4.00(−7)	9.28(−72)	3.84(0)	1.18(+9)	8.67(+10)
		1.13(+1)	1.39(+1)	1.69(−1)	1.55(0)	7.99(0)	4.33(+1)
C_2H_2	$C_2H_2^*$	1.68(−5)	3.31(−5)	3.32(−29)	1.95(+4)	3.98(+8)	6.91(+9)
		–	–	–	–	–	–
	$C_2 + H_2$	2.74(−6)	5.51(−6)	4.05(−30)	3.17(+3)	1.35(+8)	2.81(+9)
		3.07(0)	3.36(0)	6.40(−1)	2.58(0)	5.95(0)	6.47(0)
	$C_2H + H$	1.02(−5)	1.86(−5)	1.02(−24)	9.08(+3)	4.02(+8)	8.42(+9)
		3.16(0)	3.72(0)	1.74(−1)	3.38(0)	6.80(0)	7.31(0)
	$C_2H_2^+ + e$	7.80(−7)	1.74(−6)	7.12(−51)	4.89(+2)	1.63(+9)	1.28(+11)
		5.06(0)	6.10(0)	9.87(−2)	1.10(0)	8.69(0)	1.03(+2)
	$C_2H^+ + H + e$	7.43(−8)	1.90(−7)	1.79(−81)	2.01(−1)	3.77(+8)	7.80(+10)
		1.59(+1)	2.02(+1)	2.23(−1)	1.25(0)	9.40(0)	1.46(+2)
H_2CO	$CO + H + H$	3.20(−5)	4.44(−5)	6.41(−21)	1.70(+4)	1.16(+9)	6.88(+10)
		3.03(0)	3.57(0)	7.88(−2)	3.44(0)	1.47(+1)	4.42(+1)
	$CO + H_2$	1.16(−4)	1.16(−4)	4.42(−15)	1.78(+2)	3.06(+4)	3.80(+5)
		2.07(0)	2.08(0)	1.72(0)	2.18(0)	2.24(0)	2.25(0)
	$HCO + H$	6.64(−5)	6.68(−5)	1.42(−16)	1.69(+2)	4.46(+4)	5.76(+5)
		3.89(−1)	3.91(−1)	1.43(−1)	6.32(−1)	9.30(−1)	9.58(−1)
	$H_2CO^+ + e$	4.03(−7)	8.77(−7)	2.84(−49)	3.65(+2)	4.90(+8)	2.05(+10)
		3.19(0)	3.58(0)	1.69(−1)	1.39(0)	6.16(0)	2.76(+1)
	$CO^+ + H_2 + e$	1.21(−7)	3.69(−7)	3.92(−59)	9.76(−1)	4.10(+8)	1.79(+11)
		2.85(+1)	3.27(+1)	4.99(−8)	2.00(0)	1.89(+1)	1.27(+2)
	$HCO^+ + H + e$	1.97(−7)	4.55(−7)	7.35(−55)	6.64(+1)	6.08(+8)	3.98(+10)
		7.34(0)	8.68(0)	1.66(−1)	1.62(0)	9.21(0)	3.77(+1)
PH_3	$PH_2 + H$	6.05(−5)	7.61(−5)	4.75(−17)	2.23(+4)	1.25(+9)	3.53(+11)
		3.52(0)	3.96(0)	1.76(−1)	4.36(0)	1.45(+1)	1.96(+2)
H_2O_2	$OH + OH$	1.37(−4)	1.48(−4)	1.90(−11)	1.01(+4)	3.08(+9)	4.72(+11)
		3.01(0)	3.48(0)	1.79(−1)	5.68(0)	2.28(+1)	8.91(+1)
HNCO	$H + NCO(A^2\Sigma)$	1.38(−5)	2.49(−5)	1.42(−23)	9.00(+3)	1.86(+9)	2.15(+11)
		4.05(0)	4.99(0)	1.41(−1)	4.15(0)	1.61(+1)	9.51(+1)
	$NH(c\,^1\Pi) + CO$	1.49(−5)	2.59(−5)	7.03(−18)	9.00(+3)	1.86(+9)	2.15(+11)
		5.10(0)	6.14(0)	1.72(−1)	5.55(0)	1.75(+1)	9.65(+1)
HONO	$OH + NO$	2.33(−3)	2.36(−3)	5.56(−10)	3.85(+4)	3.81(+9)	5.18(+11)
		1.72(0)	1.80(0)	1.80(−1)	5.15(0)	2.05(+1)	9.37(+1)
NO_3	$NO + O_2$	1.67(−1)	1.67(−1)	5.18(−1)	4.22(+4)	1.46(+6)	1.62(+7)
		1.81(0)	1.81(0)	2.16(−1)	1.83(0)	1.84(0)	1.84(0)
	$NO_2 + O$	1.19(−1)	1.19(−1)	2.22(−6)	7.31(+4)	4.60(+9)	7.12(+11)
		2.99(−1)	3.00(−1)	9.14(−2)	2.53(0)	2.19(+1)	9.57(+1)
COF_2	$COF + F$	2.12(−5)	3.86(−5)	1.74(−26)	1.77(+4)	4.23(+9)	7.54(+11)
		4.10(0)	5.30(0)	1.95(−1)	3.01(0)	1.85(+1)	9.19(+1)

Please cite this article as: Huebner, W.F., Mukherjee, J., Photoionization and photodissociation rates in solar and blackbody radiation fields. Planetary and Space Science (2015), http://dx.doi.org/10.1016/j.pss.2014.11.022

Table 5 (*continued*)

Mother species	*Photo products*	*Quiet Sun*	*Active Sun*	*BB*			
				10^3 K	10^4 K	10^5 K	10^6 K
COFCl	COF + Cl	7.35(−5)	1.00(−4)	5.93(−18)	2.82(+4)	5.63(+9)	7.18(+11)
		2.86(0)	4.01(0)	1.73(−1)	4.57(0)	1.82(+1)	1.02(+2)
$ClNO_2$	Cl + NO_2	2.89(−3)	3.00(−3)	7.09(−7)	1.50(5)	6.78(+9)	7.61(+11)
		2.81(0)	2.94(0)	1.81(−1)	5.85(0)	1.92(+1)	1.01(+2)
ClONO	Cl + NO_2	1.09(−2)	1.10(−2)	3.05(−7)	1.40(+5)	6.31(+9)	7.52(+11)
		3.40(0)	3.43(0)	3.67(−1)	5.94(0)	2.07(+1)	1.03(+2)
ClO_3	ClO_2 + O	2.59(−2)	2.61(−2)	1.90(−13)	1.44(+5)	6.11(+9)	7.49(+11)
		5.91(−1)	6.04(−1)	1.26(−1)	2.40(0)	1.82(+1)	1.01(+2)
$COCl_2$	COCl + Cl	1.58(−4)	2.10(−4)	5.99(−16)	6.15(+4)	6.81(+9)	6.77(+11)
		3.29(0)	4.13(0)	1.76(−1)	4.70(0)	1.78(+1)	1.12(+2)

Table 6
Photodissociation, photoionization, and dissociative photoionization rate coefficients (s^{-1}) (first entry) and average excess energies (eV) (second entry) of all photo products for pentatomic molecules. All other table entries have the same meaning as in Table 1.

Mother species	*Photo products*	*Quiet Sun*	*Active Sun*	*BB*			
				10^3 K	10^4 K	10^5 K	10^6 K
CH_4	CH + H_2 + H	6.39(−7)	1.55(−6)	1.98(−41)	3.74(+2)	1.13(+8)	2.04(+9)
		1.72(0)	1.67(0)	2.27(−1)	1.96(0)	3.59(0)	3.69(0)
	CH_2 + H + H	2.14(−6)	5.45(−6)	1.11(−42)	4.11(+2)	3.89(+7)	7.49(+8)
		8.29(−1)	8.27(−1)	1.74(−1)	1.02(0)	1.77(0)	1.92(0)
	$CH_2(a^1A_1)$ + H_2	3.96(−6)	9.58(−6)	4.82(−30)	2.85(+3)	5.21(+8)	1.09(+10)
		5.29(0)	5.27(0)	1.92(−1)	5.12(0)	7.19(0)	7.33(0)
	CH_3 + H	2.64(−7)	6.09(−7)	2.18(−26)	2.99(+2)	7.40(+7)	1.58(+9)
		6.52(0)	6.52(0)	1.71(−1)	5.95(0)	8.29(0)	8.41(0)
	CH_4^+ + e	3.58(−7)	8.41(−7)	7.56(−60)	7.14(+1)	1.11(+9)	6.94(+10)
		5.45(0)	6.23(0)	1.52(−1)	1.22(0)	8.08(0)	5.36(+1)
	H^+ + CH_3 + e	9.12(−9)	2.85(−8)	7.94(−85)	1.02(−3)	2.61(+7)	1.51(+10)
		2.70(+1)	3.02(+1)	9.09(−2)	1.40(0)	1.94(+1)	1.57(+2)
	CH^+ + H_2 + H + e	4.21(−9)	1.38(−8)	1.59(−95)	8.48(−5)	1.32(+7)	1.14(+10)
		2.78(+1)	3.17(+1)	2.46(−1)	1.87(0)	1.79(+1)	1.88(+2)
CH_4	CH_2^+ + H_2 + e	2.08(−8)	5.58(−8)	8.41(−70)	4.80(−1)	9.92(+7)	2.03(+10)
		1.96(+1)	2.38(+1)	2.10(−1)	1.32(0)	1.25(+1)	1.27(+2)
	CH_3^+ + H + e	1.98(−7)	4.57(−7)	4.28(−64)	1.97(+1)	1.00(+9)	6.69(+10)
		8.02(0)	9.54(0)	6.04(−2)	1.18(0)	7.87(0)	5.40(+1)
HCOOH	CO_2 + H_2	3.16(−4)	4.07(−4)	2.26(−20)	1.21(+5)	2.32(+9)	6.59(+10)
		4.75(0)	5.35(0)	3.17(0)	6.45(0)	1.03(+1)	2.73(+1)
	HCO + OH	5.64(−4)	7.25(−4)	4.02(−20)	2.21(+5)	5.38(+9)	1.42(+11)
		1.76(0)	2.36(0)	1.73(−1)	3.54(0)	7.20(0)	2.13(+1)
	$HCOOH^+$ + e	9.11(−7)	2.01(−6)	1.03(−50)	7.15(+2)	8.51(+8)	1.18(+11)
		3.89(0)	5.29(0)	1.23(−1)	1.03(0)	8.48(0)	1.01(+2)
	HCO^+ + OH + e	2.82(−7)	8.01(−7)	2.56(−62)	1.57(+1)	9.40(+8)	2.85(+11)
		2.14(+1)	2.61(+1)	1.17(−1)	1.11(0)	1.55(+1)	1.04(+2)
HC_3N	CN + C_2H	3.92(−5)	6.79(−5)	7.67(−27)	5.69(+4)	4.33(+9)	4.31(+11)
		2.65(0)	3.26(0)	1.51(−1)	2.54(0)	1.29(+1)	1.25(+2)
CH_3Cl	CH_3 + Cl	1.38(−5)	2.72(−5)	5.63(−20)	1.12(+4)	3.53(+9)	3.14(+11)
		6.20(0)	6.96(0)	1.73(−1)	5.30(0)	1.76(+1)	1.14(+2)
HNO_3	OH + NO_2	2.09(−4)	2.39(−4)	2.63(−12)	4.16(+4)	4.60(+9)	7.12(+11)
		4.32(0)	4.70(0)	1.79(−1)	5.16(0)	2.19(+1)	9.57(+1)
CHF_2Cl	CHF_2 + Cl	1.29(−5)	3.03(−5)	2.20(−28)	9.86(+3)	5.45(+9)	7.81(+11)
		6.03(0)	6.57(0)	2.17(−1)	3.95(0)	1.74(+1)	1.02(+2)
$ClONO_2$	Cl + NO_3	9.11(−4)	9.73(−4)	4.54(−10)	6.17(+4)	6.53(+9)	8.41(+11)
		3.59(0)	3.79(0)	1.68(−1)	5.79(0)	2.05(+1)	9.91(+1)
	ClONO + O	1.00(−4)	1, 07(−4)	1.36(−15)	6.86(+3)	7.26(+8)	9.35(+10)
		2.17(0)	2.37(0)	1.13(−1)	4.34(0)	1.91(+1)	9.76(+1)
CF_2Cl_2	CF_2 + Cl + Cl	1.57(−5)	3.41(−5)	4.21(−27)	1.08(+4)	5.62(+9)	7.97(+11)
		5.09(0)	5.88(0)	3.43(−1)	3.71(0)	1.69(+1)	1.13(+2)
	CF_2Cl + Cl	1.01(−5)	1.77(−5)	3.39(−20)	5.44(+3)	2.07(+9)	7.97(+11)
		5.45(0)	6.43(0)	1.48(−1)	5.32(0)	1.81(+1)	1.13(+2)
$CFCl_3$	CFCl + Cl + Cl	2.32(−5)	4.51(−5)	2.19(−26)	1.82(+4)	5.30(+9)	5.55(+11)
		3.85(0)	4.59(0)	2.51(−1)	3.13(0)	1.55(+1)	1.17(+2)
	$CFCl_2$ + Cl	3.26(−5)	5.09(−5)	1.33(−17)	1.68(+4)	4.02(+9)	3.96(+11)
		4.90(0)	5.85(0)	1.36(−1)	5.37(0)	1.79(+1)	1.14(+2)

Please cite this article as: Huebner, W.F., Mukherjee, J., Photoionization and photodissociation rates in solar and blackbody radiation fields. Planetary and Space Science (2015), http://dx.doi.org/10.1016/j.pss.2014.11.022

Table 6 (*continued*)

Mother species	*Photo products*	*Quiet Sun*	*Active Sun*	*BB*			
				10^3 K	10^4 K	10^5 K	10^6 K
$BrONO_2$	$BrO + NO_2$	3.24(−3)	3.32(−3)	1.98(−7)	9.25(+4)	7.15(+9)	1.28(+12)
		2.68(0)	2.78(0)	1.83(−1)	5.93(0)	1.92(+1)	1.42(+2)
CCl_4	$CCl_2 + Cl + Cl$	4.06(−5)	7.33(−5)	3.60(−26)	2.45(+4)	8.56(+9)	7.74(+11)
		3.21(0)	4.03(0)	1.72(−1)	2.96(0)	1.50(+1)	1.25(+1)
	$CCl_3 + Cl$	4.08(−5)	4.98(−5)	1.14(−16)	8.43(+3)	1.80(+9)	1.28(+11)
		3.57(0)	4.14(0)	1.48(−1)	4.99(0)	1.77(+1)	9.77(+1)
$IONO_2$	$IO + NO_2$	5.88(−3)	5.96(−3)	8.19(−7)	7.82(+4)	4.14(+9)	1.27(+12)
		1.87(0)	1.93(0)	1.81(−1)	5.24(0)	2.38(+1)	1.10(+2)

radiation field and add the results for selected blackbody radiation fields without dilution factors for temperatures from 1000 K to 1,000,000 K.

2.6. Hexatomic molecules

2.6.1. Methanethiol, CH_3SH

Cross sections: In the wavelength range $\lambda = 0.61$–1100 Å the cross sections are synthesized from cross sections of the atomic constituents of CH_3SH, namely the cross sections of C, plus four times that of H, plus that of S, using the data of Barfield et al. (1972). From $\lambda = 1925$ Å to 3095 Å the cross sections are given by Vaghjiani (1993).

Branching ratios: For the dissociation branch $CH_3SH \rightarrow CH_3S + H$, Vaghjiani (1993) gives branching ratios of 0.49 at $\lambda = 1930$ Å and 0.95 at $\lambda = 2220$ Å. Steer and Knight (1968) give a branching ratio of 1.00 at $\lambda = 2540$ Å. We assumed the branching ratio to vary linearly between these values and constant at 1.00 between $\lambda = 2540$ Å and threshold. We also assumed a branching ratio of 0.25 at $\lambda = 0.61$ Å, increasing linearly to Vaghjiani's value at $\lambda = 1930$ Å.

Threshold: The dissociation threshold $\lambda_{th} = 3095$ Å.

Rate coefficient: The rate coefficients are not sensitive to the assumed branching ratio at $\lambda = 0.61$ Å when changing it from 0.00 to 0.50. The rate coefficient is 1.01×10^{-3} s^{-1} for the quiet Sun and 1.03×10^{-3} s^{-1} for the active Sun. The rate coefficients, without dilution factors for four temperatures between $T = 10^3$ K and $T = 10^6$ K of the BBRF are summarized in Table 7.

Excess energy: Contrary to the rate coefficient, the excess energy is sensitive to the assumed branching ratio at $\lambda = 0.61$ Å, changing by about a factor of 2. The excess energy is 0.573 eV for the quiet Sun and 0.619 eV for the active Sun. The excess energies for four temperatures between $T = 10^3$ K and $T = 10^6$ K of the BBRF are summarized in Table 7.

Table 7
Photodissociation, photoionization, and dissociative photoionization rate coefficients (s^{-1}) (first entry) and average excess energies (eV) (second entry) of all photo products for hexatomic molecules. All other table entries have the same meaning as in Table 1.

Mother species	*Photo products*	*Quiet Sun*	*Active Sun*	*BB*			
				10^3 K	10^4 K	10^5 K	10^6 K
C_2H_4	$C_2H_2 + H + H$	2.29(−5)	3.36(−5)	1.87(−28)	1.91(+4)	6.89(+8)	2.40(+10)
		1.67(0)	2.10(0)	2.23(−1)	1.65(0)	8.93(0)	2.29(+1)
	$C_2H_2 + H_2$	2.36(−5)	3.45(−5)	2.13(−28)	1.95(+4)	4.56(+8)	1.44(+10)
		6.21(0)	6.62(0)	4.80(0)	6.19(0)	1.24(+1)	2.55(+1)
	$C_2H_4^+ + e$	5.80(−7)	1.35(−6)	4.17(−48)	2.97(+2)	1.26(+9)	9.46(+10)
		7.26(0)	8.50(0)	1.81(−1)	2.16(0)	1.06(+1)	4.79(+1)
	$C_2H_2^+ + H_2 + e$	1.97(−7)	4.89(−7)	3.47(−61)	2.04(+1)	7.82(+8)	8.16(+10)
		1.24(+1)	1.51(+1)	2.02(−1)	1.65(0)	1.14(+1)	5.23(+1)
	$C_2H_3^+ + H + e$	2.26(−7)	5.47(−7)	8.75(−64)	1.45(+1)	1.16(+9)	1.03(+11)
		1.31(+1)	1.59(+1)	2.53(−1)	1.83(0)	1.01(+1)	4.50(+1)
CH_3OH	$CH_3 + OH$	5.58(−7)	1.02(−6)	1.71(−21)	4.14(+2)	7.96(+7)	2.39(+9)
		4.96(0)	5.54(0)	1.19(−1)	4.92(0)	1.29(+1)	1.46(+1)
	$H_2CO + H_2$	1.01(−5)	1.82(−5)	4.32(−8)	7.23(+3)	2.06(+8)	3.92(+9)
		7.45(0)	8.07(0)	1.46(−1)	7.64(0)	9.87(0)	1.03(+1)
	$CH_3OH^+ + e$	4.88(−7)	1.02(−6)	9.29(−49)	5.79(+2)	6.55(+8)	1.95(+10)
		2.63(0)	6.54(0)	1.67(−1)	1.10(0)	5.91(0)	7.53(0)
	$H_2CO^+ + H_2 + e$	1.15(−7)	2.55(−7)	1.01(−58)	2.23(+1)	4.55(+8)	1.64(+10)
		4.43(0)	4.21(0)	1.44(−1)	1.69(0)	6.91(0)	8.20(0)
	$CH_3O^+ + H + e$	1.20(−7)	2.69(−7)	1.20(−56)	3.48(+1)	3.45(+8)	1.19(+10)
		3.52(0)	3.34(0)	1.66(−1)	1.40(0)	6.68(0)	8.05(0)
HO_2NO_2	$HO + NO_3$	2.98(−4)	3.19(−4)	6.02(−11)	2.59(+4)	3.34(+9)	6.26(+11)
		3.75(0)	3.98(0)	1.80(−1)	5.66(0)	2.17(+1)	1.16(+2)
	$HO_2 + NO_2$	2.98(−4)	3.19(−4)	6.02(−11)	2.59(+4)	3.34(+9)	6.26(+11)
		4.52(0)	4.75(0)	9.53(−1)	6.44(0)	2.24(+1)	1.17(+2)
CH_3SH	$CH_3 + SH$	1.49(−3)	1.50(−3)	3.89(−14)	1.94(+4)	1.90(+9)	3.09(+11)
		1.50(−1)	1.97(−1)	2.17(−4)	3.36(0)	1.70(+1)	1.75(+2)
	$CH_3S + H$	1.01(−3)	1.03(−3)	4.80(−15)	2.10(+4)	9.64(+8)	1.19(+11)
		5.73(−1)	6.19(−1)	2.38(−3)	2.70(0)	1.58(+1)	1.59(+2)

Please cite this article as: Huebner, W.F., Mukherjee, J., Photoionization and photodissociation rates in solar and blackbody radiation fields. Planetary and Space Science (2015), http://dx.doi.org/10.1016/j.pss.2014.11.022

2.7. Septatomic and supraseptatomic molecules

No new septatomic or supraseptatomic species or revised cross sections have been added. Table 8 for septatomic, Table 9 for octatomic, and Table 10 for supraoctatomic molecules summarize the results from previous calculations for the solar radiation field and add the results for blackbody radiation fields without dilution factors at four selected temperatures from 1000 K to 1,000,000 K.

Table 8
Photodissociation, photoionization, and dissociative photoionization rate coefficients (s^{-1}) (first entry) and average excess energies (eV) (second entry) of all photo products for septatomic molecules. All other table entries have the same meaning as in Table 1.

Mother species	*Photo products*	*Quiet Sun*	*Active Sun*	*BB*			
				10^3 K	10^4 K	10^5 K	10^6 K
CH_3CHO	CH_3 + HCO	4.09(−5)	4.18(−5)	1.62(−17)	1.71(+2)	9.31(+8)	1.46(+11)
		8.76(−1)	1.14(0)	4.96(−1)	2.39(0)	2.23(+1)	9.65(+1)
	$^3CH_3$ + CHO	1.22(−4)	1.23(−4)	8.36(−12)	2.89(+2)	1.80(+8)	1.45(+10)
		2.39(0)	2.40(0)	1.80(−1)	2.78(0)	2.24(+1)	4.75(+1)
	CH_4 + CO	1.64(−5)	1.71(−5)	3.78(−14)	1.09(+2)	1.27(+9)	2.08(+11)
		3.16(0)	4.04(0)	1.80(−1)	5.93(0)	2.43(+1)	1.01(+2)
CH_3OOH	CH_3O + OH	4.12(−4)	6.46(−4)	7.64(−13)	3.33(+5)	9.49(+9)	6.11(+11)
		5.81(0)	6.51(0)	1.80(−1)	6.46(0)	1.25(+1)	8.39(+1)
N_2O_5	NO_2 + NO_2 + O	8.49(−4)	9.01(−4)	5.32(−5)	7.28(+4)	8.26(+9)	1.23(+12)
		5.22(0)	5.42(0)	2.16(−1)	7.27(0)	2.35(+1)	9.70(+1)

Table 9
Photodissociation, photoionization, and dissociative photoionization rate coefficients (s^{-1}) (first entry) and average excess energies (eV) (second entry) of all photo products for octatomic molecules. All other table entries have the same meaning as in Table 1.

Mother species	*Photo products*	*Quiet Sun*	*Active Sun*	*BB*			
				10^3 K	10^4 K	10^5 K	10^6 K
C_2H_6	$^1CH_2$ + CH_4	2.22(−6)	5.44(−6)	2.13(−24)	1.24(+3)	5.12(+8)	1.90(+10)
		6.14(0)	6.13(0)	1.73(−1)	5.84(0)	1.25(+1)	2.88(+1)
	CH_3 + CH_3	8.80(−7)	2.12(−6)	1.10(−24)	5.42(+2)	3.77(+8)	1.44(+10)
		7.38(0)	7.36(0)	8.69(−1)	6.93(0)	1.37(+1)	3.02(+1)
	C_2H_4 + H_2	3.67(−6)	8.54(−6)	1.02(−22)	3.06(+3)	8.54(+8)	3.13(+10)
		8.96(0)	9.11(0)	3.30(0)	8.46(0)	1.55(+1)	3.21(+1)
	C_2H_5 + H	3.28(−6)	7.89(−6)	1.41(−23)	2.09(+3)	1.25(+9)	4.75(+10)
		6.78(0)	6.79(0)	4.44(−1)	6.31(0)	1.32(+1)	2.97(+1)
	$C_2H_6^+$ + e	4.86(−7)	1.15(−6)	2.82(−53)	1.20(+2)	1.61(+9)	2.04(+11)
		9.98(0)	1.22(+1)	1.52(−1)	1.75(0)	1.13(+1)	1.31(+2)
CH_3CCl_3	CH_3CCl_2 + Cl	3.41(−5)	4.08(−5)	2.28(−23)	1.01(+4)	4.76(+9)	6.98(+11)
		2.38(0)	3.34(0)	2.76(−1)	2.54(0)	2.16(+1)	1.35(+2)

Table 10
Photodissociation, photoionization, and dissociative photoionization rate coefficients (s^{-1}) (first entry) and average excess energies (eV) (second entry) of all photo products for supraoctatomic molecules. All other table entries have the same meaning as in Table 1.

Mother species	*Photo products*	*Quiet Sun*	*Active Sun*	*BB*			
				10^3 K	10^4 K	10^5 K	10^6 K
$CH_3O_2NO_2$	CH_3O + NO_3	8.24(−4)	8.48(−4)	3.65(−5)	3.47(+4)	3.96(+9)	7.64(+11)
		2.58(0)	2.73(0)	4.21(−3)	6.21(0)	2.18(+1)	1.13(+2)
	CH_3O_2 + NO_2	8.24(−4)	8.48(−4)	3.65(−5)	3.47(+4)	3.96(+9)	7.64(+11)
		3.04(0)	3.19(0)	1.88(−1)	6.68(0)	2.23(+1)	1.14(+2)
CH_3SSCH_3	CH_3S + CH_3S	1.12(−3)	1.17(−3)	5.70(−14)	4.94(+4)	2.82(+9)	6.10(+11)
		1.53(0)	1.63(0)	1.26(−1)	3.95(0)	1.71(+1)	1.84(+2)
	CH_3SS + CH_3	1.33(−3)	1.37(−3)	2.07(−11)	4.95(+4)	2.82(+9)	6.10(+11)
		1.94(0)	2.04(0)	1.77(−1)	4.63(0)	1.78(+1)	1.85(+2)
CH_3CNO_5	CH_3CO_2 + NO_3	7.96(−4)	8.44(−4)	2.73(−11)	6.37(+4)	5.02(+9)	7.41(+11)
		3.23(0)	3.48(0)	1.30(0)	6.11(0)	2.13(+1)	9.36(+1)
	CH_3CO_3 + NO_2	7.96(−4)	8.44(−4)	2.73(−11)	6.37(+4)	5.02(+9)	7.41(+11)
		3.44(0)	3.70(0)	1.52(0)	6.32(0)	2.16(+1)	9.38(+1)

Please cite this article as: Huebner, W.F., Mukherjee, J., Photoionization and photodissociation rates in solar and blackbody radiation fields. Planetary and Space Science (2015), http://dx.doi.org/10.1016/j.pss.2014.11.022

3. Summary

In Tables 1–10 we list (1) photo rate coefficients in units of transitions s^{-1} and (2) excess energies of photo products in eV. All known branching ratios for photodissociation, photoionization, and dissociative photoionization are taken into account. For the quiet Sun and the active Sun the radiation fields are diluted to values corresponding to a heliocentric distance of 1 AU and the data are for vacuum conditions. For blackbody conditions the radiation field has *not* been diluted. Tables are arranged in the order of number of atoms in each species: monatomic neutrals, monatomic ions, diatomics, triatomics, etc. In each table the mother species are listed in the order of increasing values for the sum of the atomic numbers of the constituent atoms. Species without state designation refer to the ground state.

Acknowledgments

This work was supported by a Grant from the NASA Planetary Astronomy Program (No. NNX08AF03G). We thank our colleagues from the Los Alamos National Laboratory, Drs. D.P. Kilcrease and J. Colgan for very valuable discussions. We also thank an unidentified reviewer for thoughtful suggestions.

References

Barfield, W.D., Koontz, G.D., Huebner, W.F., 1972. Fits to new calculations of photoionization cross sections for low-Z elements. J. Quant. Spectrosc. Radiat. Transf. 12, 1409–1433.

Baugh, J.F., Burkhardt, C.E., Leventhal, J.J., Bergeman, T., 1998. Precision Stark spectroscopy of sodium ^{2}P and ^{2}D states. Phys. Rev. A 58, 1585–1591.

Bethe, H.A., Salpeter, E.E., 1957. Quantum Mechanics of One- and Two-Electron Atoms. Springer Verlag, Berlin, Gottingen, Heidelberg.

Brandi, F., Velchev, I., Horgervorst, W., Ubachs, W., 2001. Vacuum-ultraviolet spectroscopy of Xe: hyperfine splittings, isotope shifts, and isotope-dependent ionization energies. Phys. Rev. A 64 032505-1–032505-6.

Broad, J.T., Reinhardt, W.P., 1976. One- and two-electron photoejection from H^-: a multichannel J-matrix calculation. Phys. Rev. A 14, 2159–2173.

Brown, C.M., Tilford, S.G., Ginter, M.L., 1975. Absorption spectra of Zn I and Cd I in the 1300–1750 Å region. J. Opt. Soc. Am. 65, 1404–1409.

Brown, E.R., Carter, S.L., Kelly, H.P., 1980. Photoionization cross section and resonance structure of Cl I. Phys. Rev. A 21, 1237–1248.

Chang, J.-J., Kelly, H.P., 1975. Photoabsorption of the neutral sodium atom: a many-body calculation. Phys. Rev. A 12, 92–98.

Chapman, R.D., Henry, R.J.W., 1971. Photoionization cross-sections for atoms and ions of sulfur. Astrophys. J. 168, 169–171.

Drake, G.W.F., Martin, W.C., Unpublished 2001; see ⟨http://physics.nist.gov/PhysRefData/Handbook/Tables/lithiumtable7.htm#DM01⟩.

Eriksson, K.B.S., 1983. Additions to the spectrum of the singly-ionized nitrogen atom. Phys. Scr. 28, 593–610.

Geltman, S., 1962. The bound–free absorption coefficient of the hydrogen negative ion. Astrophys. J. 136, 935–945.

Henry, R.J.W., 1970. Photoionization cross-sections for atoms and ions of carbon, nitrogen, oxygen, and neon. Astrophys. J. 161, 1153–1155.

Hudson, R.D., Carter, V.L., 1965. Absorption of light by potassium vapor between 2856 and 1150 Å. Phys. Rev. A 139, 1426–1428.

Hudson, R.D., Carter, V.L., 1967. Atomic absorption cross sections of lithium and sodium between 600 and 1000 Angstroms. J. Opt. Soc. Am. 57, 651–654.

Hudson, R.D., Carter, V.L., 1968. Atomic absorption cross sections of Na, 500–600 Å. J. Opt. Soc. Am. 58, 430–431.

Huebner, W.F., Carpenter, C.W., 1979. Solar Photo Rate Coefficients. Los Alamos Scientific Laboratory Report LA-8085-MS.

Huebner, W.F., Keady, J.J., Lyon, S.P., 1992. Solar photo rates for planetary atmospheres and atmospheric pollutants. Astrophys. Space Sci. 195, 1–294.

Huffman, R.E., Tanaka, Y., Larrabee, J.C., 1963. Absorption coefficients of xenon and argon in the 600–1025 Å wavelength regions. J. Chem. Phys. 39, 902–909.

Iglesias, L., Cabeza, M.I., de Luis, B., 1988. Pub. Inst. Opt. Madrid, No. 47; see ⟨http://physics.nist.gov/PhysRefData/Handbook/Tables/vanadiumtable7.htm⟩.

James, A.M., Kowalczyk, P., Langlois, E., Campell, M.D., Ogawa, A., Simard, B., 1994. Resonant two photon ionization spectroscopy of the molecules V_2, VNb, and Nb_2. J. Chem. Phys. 101, 4485–4495.

Johansson, L., 1966. Spectrum and term system of neutral carbon atom. Ark. Fys. Stockh. 31, 201.

Kaufman, V., Martin, W.C., 1991a. Wavelengths and energy level classifications of magnesium spectra for all stages of ionization (Mg I through Mg XII). J. Phys. Chem. Ref. Data 20, 83–152.

Kaufman, V., Martin, W.C., 1991b. Wavelengths and energy level classifications for the spectra of aluminum Al I through Al XIII. J. Phys. Chem. Ref. Data 20, 775–858.

Kaufman, V., Minnhagen, L., 1972. Accurate ground-term combinations in Ne I. J. Opt. Soc. Am. 62, 92–95.

Kaufman, V., Ward, J.F., 1966. Measurement and calculation of Cu II, Ge II, Si II, and C I vacuum-ultraviolet lines. J. Opt. Soc. Am. 56, 1591–1597.

Kelly, R.L., 1987. Atomic and ionic spectrum lines below 2000 Angstroms: hydrogen through krypton. J. Phys. Chem. Ref. Data 16 (Suppl. 1).

Kessler, T., Brück, K., Baktash, C., Beene, J.R., Geppert, Ch., Havener, C.C., Krause, H.F., Liu, Y., Schultz, D.R., Stracener, D.W., Vane, C.R., Wendt, K., 2007. Three-step resonant photoionization spectroscopy of Ni and Ge: ionization potential and odd-parity Rydberg levels. J. Phys. B 40, 4413–4432.

Knight, R.D., Wang, L.-G., 1985. One-photon laser spectroscopy of the np and nf Rydberg series in xenon. J. Opt. Soc. Am. B 2, 1084–1087.

Kramida, A.E., Martin, W.C., 1997. A compilation of energy levels and wavelengths for the spectrum of neutral beryllium (Be I). J. Phys. Chem. Ref. Data 26, 1185–1194.

Kramida, A.E., Martin, W.C., 2000. Unpublished Compilation; see ⟨http://www.nist.gov/pml/data/asd.cfm⟩.

Liden, K., 1949. The arc spectrum of fluorine. Ark. Fys. (Stockh.) 1, 229–267, Erratum: Ark. Fys. (Stockh.) 1 (1949), 268..

Longmire, M.S., Brown, C.M., Ginter, M.L., 1980. Absorption spectrum of Cu I between 1570 Å and 2500 Å. J. Opt. Soc. Am. 70, 423–429.

Loock, H.-P., Beaty, L.M., Simard, B., 1999. Reassessment of the first ionization potentials of copper, silver, and gold. Phys. Rev. A 59, 873–875.

Lykke, K.R., Murray, K.K., Lineberger, W.C., 1991. Threshold photodetachment of H^-. Phys. Rev. A 43, 6104–6107.

Manson, S.T., Msezane, A., Starace, A.F., Shahabi, S., 1979. Photoionization of chalcogen and halogen atoms: cross sections and angular distributions. Phys. Rev. A 20, 1005–1018.

Marr, G.V., West, J.B., 1976. Absolute photoionization cross-section tables for helium, neon, argon, and krypton in the VUV spectral regions. At. Data Nucl. Data Tables 18, 497–506.

Martin, W.C., 2002. Ongoing Compilation of Data for He I: ⟨http://physics.nist.gov/PhysRefData/Handbook/Tables/heliumtable1.htm⟩.

Martin, W.C., Zalubas, R.J., 1981. Energy levels of sodium Na I through Na XI. J. Phys. Chem. Ref. Data 10, 153–196.

Martin, W.C., Zalubas, R., 1983. Energy levels of silicon, Si I through Si XIV. J. Phys. Chem. Ref. Data 12, 323–379.

Martin, W.C., Zalubas, R., Musgrove, A., 1985. Energy levels of phosphorus, P I through P XV. J. Phys. Chem. Ref. Data 14, 751–802.

Martin, W.C., Zalubas, R., Musgrove, A., 1990. Energy levels of sulfur, S I through S XVI. J. Phys. Chem. Ref. Data 19, 821–880.

Martin, W.C., Kaufman, V., Musgrove, A., 1993. A compilation of energy levels and wavelengths for the spectrum of singly-ionized oxygen (O II). J. Phys. Chem. Ref. Data 22, 1179–1212.

Martin, W.C., Kaufman, V., Musgrove, A., Dalton, G.R., 1994. Unpublished; see ⟨http://physics.nist.gov/PhysRefData/Handbook/Tables/silicontable7.htm#MK%MD94⟩.

Minnhagen, L., 1960. The nf and ng levels of Ar II. Ark. Fys. (Stockh.) 18, 97–134.

Mohr, P., Kotochigova, S., 2000. Unpublished calculations; see ⟨http://physics.nist.gov/PhysRefData/Handbook/Tables/hydrogentable7.htm#M%K00a⟩.

Moore, C.E., 1970. Ionization Potentials and Ionization Limits Derived from the Analysis of Optical Spectra. Nat. Stand. Ref. Data Ser., Nat. Bur. Stand. Report NSRDS-NBS 34.

Moore, C.E., 1975. Selected Tables of Atomic Spectra—A: Atomic Energy Levels (2nd ed.)—B: Multiplet Table; N I, N II, N III. Data Derived From the Analyses of Optical Spectra, Nat. Stand. Ref. Data Ser., Nat. Bur. Stand. Report NSRDS-NBS 3.

Moore, C.E., 1993. In: J.W. Gallagher (Ed.) Tables of Spectra of Hydrogen Carbon Nitrogen and Oxygen. CRC Press, Inc., Boca Raton, FL.

Nahar, S.N., 2013. Private Communication; see NORAD.

NIST database: ⟨http://www.nist.gov/pml/data/handbook/index.cfm⟩.

NORAD, Nahar Ohio [State University] Radiative Atomic Data, ⟨http://www.astronomy.ohio-state.edu/~nahar/nahar_radiativeatomicdata/index.html⟩.

Page, R.H., Gudeman, C.S., 1990. Completing the iron period: double-resonance, fluorescence dip Rydberg spectroscopy and ionization potentials of titanium, vanadium, iron, cobalt, and nickel. J. Opt. Soc. Am. B 7, 1761–1771.

Palenius, H.P., 1969. Spectrum and term system of singly ionized fluorine, F II. Ark. Fys. (Stockh.) 39, 15–64.

Persson, W., 1971. The spectrum of singly ionized neon, Ne II. Phys. Scr. 3, 133–155.

Radziemski, L.J., Kaufman, V., 1969. Wavelengths, energy levels, and analysis of neutral atomic chlorine (Cl I). J. Opt. Soc. Am. 59, 424–443.

Radziemski Jr., L.J., Kaufman, V., 1974. Wavelengths, energy levels, and analysis of the second spectrum of chlorine (Cl II). J. Opt. Soc. Am. 64, 366–389.

Rienstra-Kiracofe, J.C., Tschumper, G.S., Schaefer Jr., F.H.F., Sreela, N., Ellison, G.B., 2002. Atomic and molecular electron affinities: photoelectron experiments and theoretical computations. Chem. Rev. 102, 231–282.

Ryabtsev, A.N., 1998. Private Communication; see Ryabtsev, A. N., Kink, I., Awaya, Y., Ekberg, J. O., Mannervik, S., Ölme, A., Martinson, I., 2005. Phys. Scripta 71, 489–501.

Ryabtsev, A.N., 2002. Private Communication; see ⟨http://physics.nist.gov/PhysRefData/Handbook/Tables/boron~table1.htm⟩.

Samson, J.A.R., 1982. Corpuscles and radiation in matter I. In: Mehlhorn, W. (Ed.), Handbuch der Physik, vol. 6. Springer, Berlin, Heidelberg, pp. 123–213.

Sauter, F., 1931a. Über den atomaren Photoeffekt bei großer Härte der anregenden Strahlung. Ann. Phys. 401, 217–248.

Please cite this article as: Huebner, W.F., Mukherjee, J., Photoionization and photodissociation rates in solar and blackbody radiation fields. Planetary and Space Science (2015), http://dx.doi.org/10.1016/j.pss.2014.11.022

Sauter, F., 1931b. Über den atomaren Photoeffekt in der K-Schale nach der relativistischen Wellenmechanik Diracs. Ann. Phys. 403, 454–488.
Seaton, M., 1995. The Opacity Project, vol. 1. Institute of Physics Publishing, Bristol, Philadelphia.
Shenstone, A.G., 1948. The first spectrum of copper (Cu I). Philos. Trans. R. Soc. Lond. A 241, 297–322.
Shenstone, A.G., 1970. The second spectrum of nickel (Ni II). J. Res. Natl. Bur. Stand. (U.S.) 74A, 801.
Sohl, J.E., Zhu, Y., Knight, R.D., 1990. Two-color laser photoionization spectroscopy of Ti I: multichannel quantum defect theory analysis and a new ionization potential. J. Opt. Soc. Am. B 7, 9–14.
Steer, R.P., Knight, A.R., 1968. Reactions of thioyl radicals. IV. Photolysis of methanethiol. J. Phys. Chem. 72, 2145–2153.
Stobbe, M., 1930. Zur Quantenmechanik photoelektrischer Prozesse. Ann. Phys. 399, 661–715.
Sugar, J., Corliss, C., 1985. Atomic energy levels of the iron-period elements: potassium through nickel. J. Phys. Chem. Ref. Data 14 (Suppl. 2).
Sugar, J., Musgrove, A., 1990. Energy levels of copper, Cu I through Cu XXIX. J. Phys. Chem. Ref. Data 19, 527–616.
Sugar, J., Musgrove, A., 1995. Energy levels of zinc, Zn I through Zn XXX. J. Phys. Chem. Ref. Data 24, 1803–1872.
TOPbase, Website: ⟨http://cdsweb.u-strasbg.fr/topbase/xsections.html⟩.
Vaghjiani, G.L., 1993. CH_3SH ultraviolet absorption cross sections in the region 192.5–309.5 nm and photodecomposition at 222 and 193 nm and 296 K. J. Chem. Phys. 99, 5938–5943.
Velchev, I., Hogervorst, W., Ubachs, W., 1999. Precision VUV spectroscopy of Ar I at 105 nm. J. Phys. B 32, L511–L516.
Verner, D.A., Yakovlev, D.G., Band, I.M., Trzhaskovskaya, M.B., 1993. Subshell photoionization cross sections and ionization energies of atoms and ions from He to Zn. At. Data Nucl. Data Tables 55, 233–280.
Verner, D.A., Yakovlev, D.G., 1995. Analytic FITS for partial photoionization cross sections. Astron. Astrophys. Suppl. 109, 125–135.
Verner, D.A., Ferland, G.J., Korista, K.T., Yakovlev, D.G., 1996. Atomic data for astrophysics. II. New analytic FITS for photoionization cross sections of atoms and ions. Astrophys. J. 465, 487–498.

Please cite this article as: Huebner, W.F., Mukherjee, J., Photoionization and photodissociation rates in solar and blackbody radiation fields. Planetary and Space Science (2015), http://dx.doi.org/10.1016/j.pss.2014.11.022